NICA Days 2023 and
XII MPD Collaboration Meeting

Belgrade, Serbia
02-06
10.23

Review of QM23 results

Alexey Aparin

Joint Institute for Nuclear Research

Outline:

Introduction
Particle spectra
Femtoscopy
Polarization
Flow
Fluctuations
Hypernuclei
New facilities

Current experimental status

https://github.com/tgalatyuk/interaction_rate_facilities

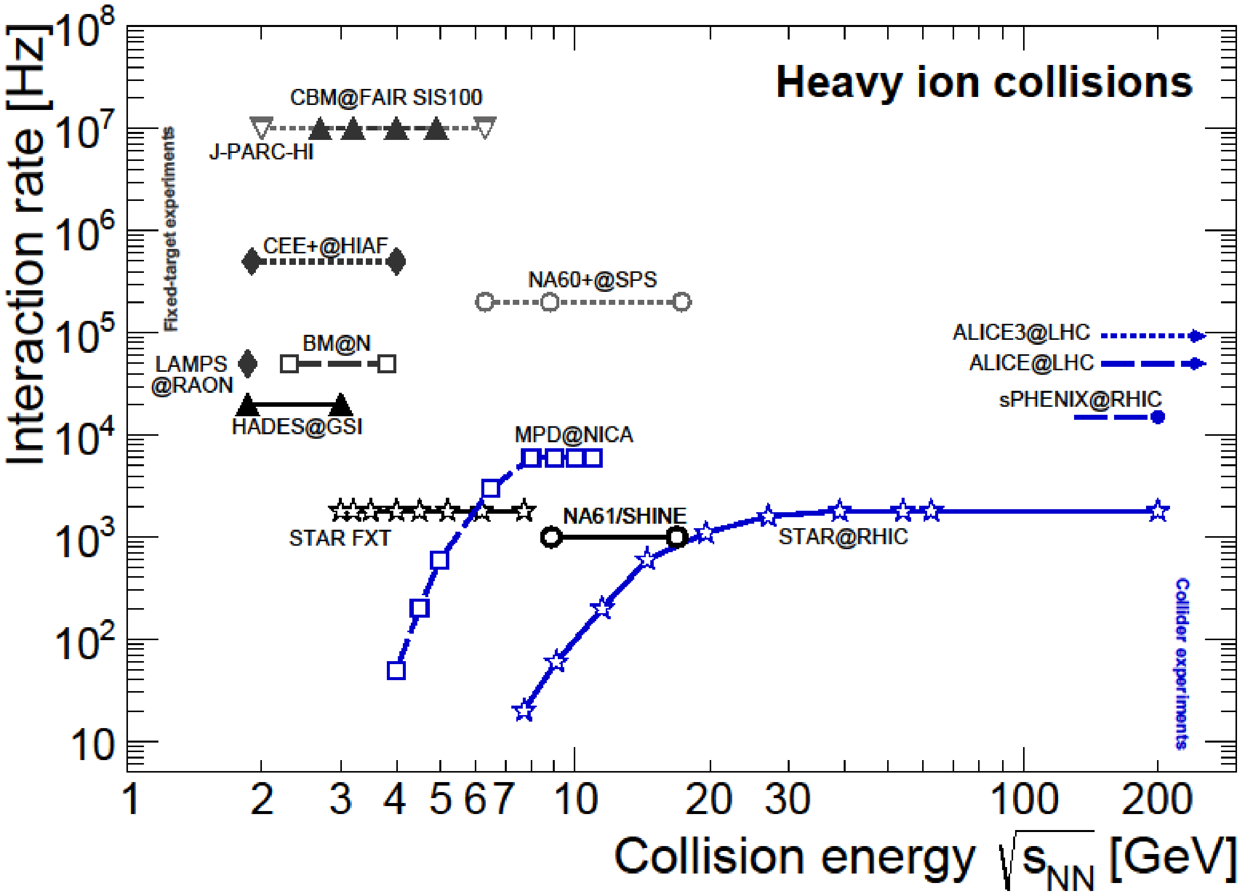

Key observables are rare observables

→ Program needs ever more precise data (statistics!) and sensitivity for rarest signals!

→ Systematic investigation in dependence on energy, size/centrality

HADES; Nature Physics 15 (2019) 10, 1040-1045
T. Galatyuk for HADES, Nucl.Phys.A 967 (2017) 680-683

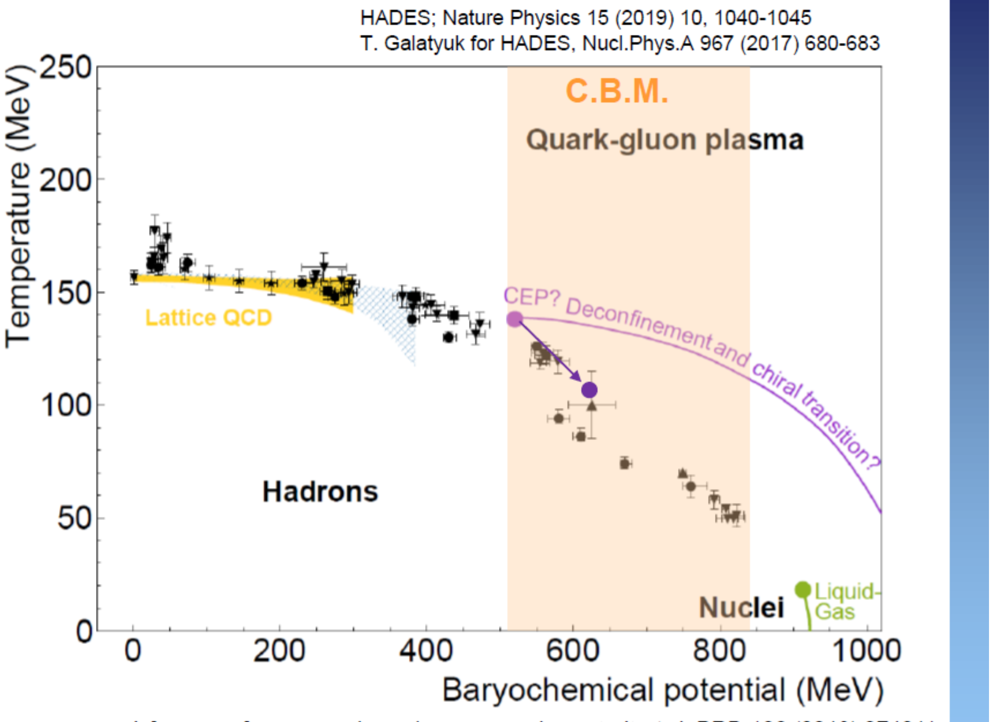

Bazavov *et al.* [HotQCD], PLB 795 (2019) 15-21
Ding *et al.*, [HotQCD], PRL 123 (2019) 6, 062002
Borsanyi *et al.*, PRL 125 (2020) 5, 052001
Isserstedt *et al.* PRD 100 (2019) 074011
Gao, Pawlowski, PLB 820 (2021) 136584
Fu *et al.*, PRD 101 (2020), 054032
Gunkel, Fischer, PRD 104 (2021) 5, 054022

RHIC is an incredibly versatile machine

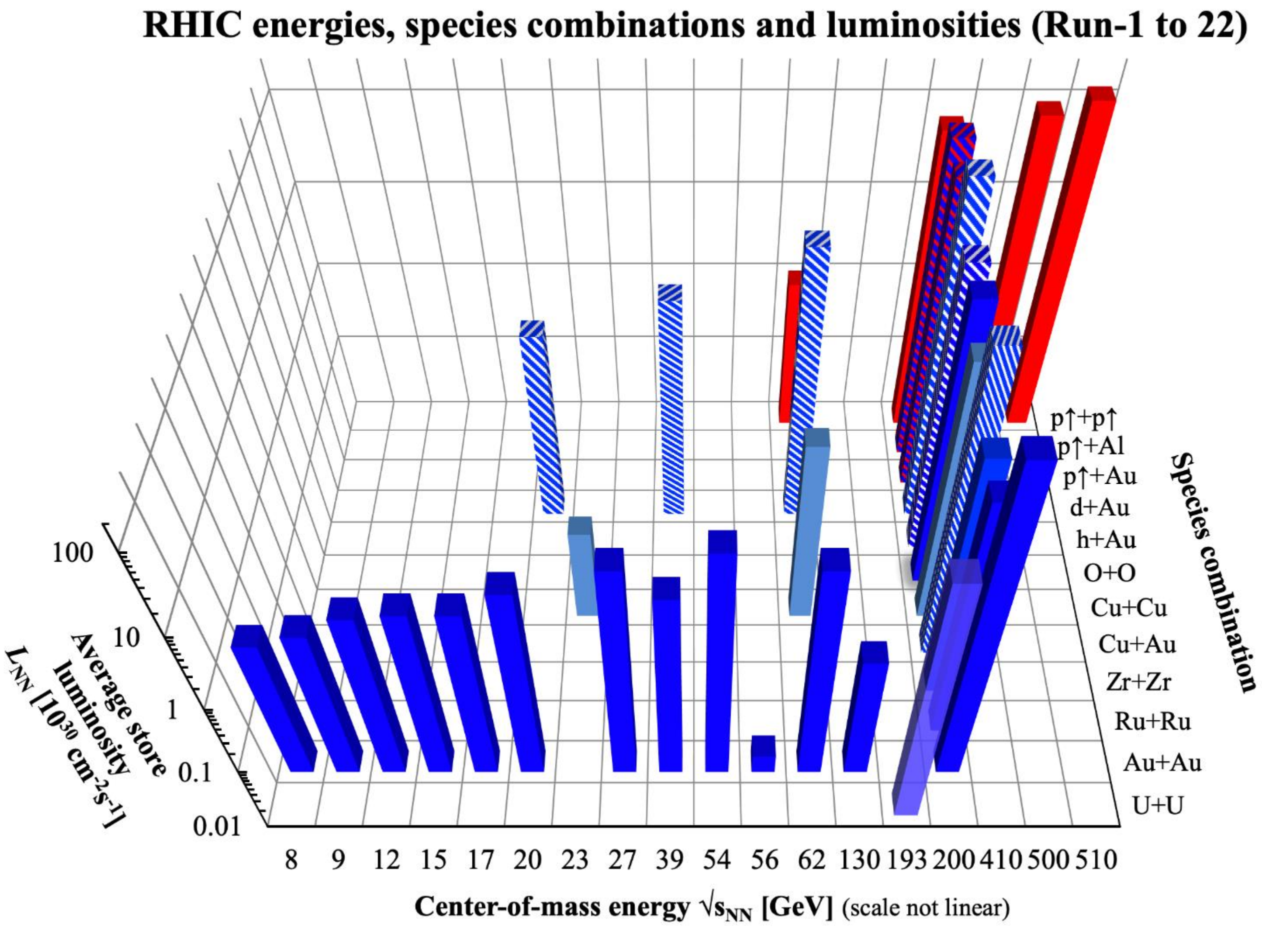

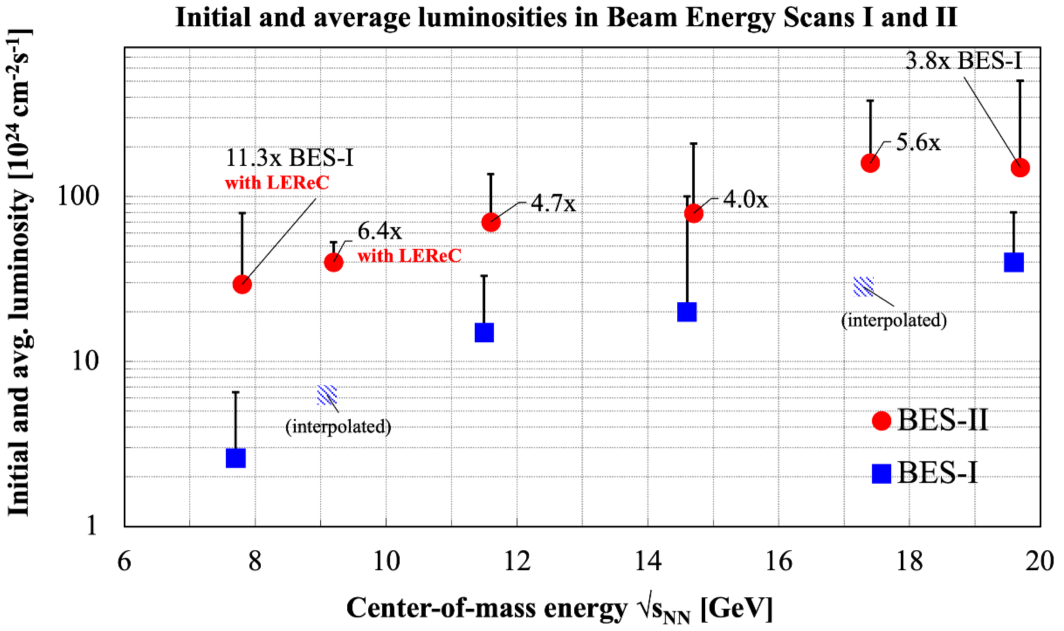

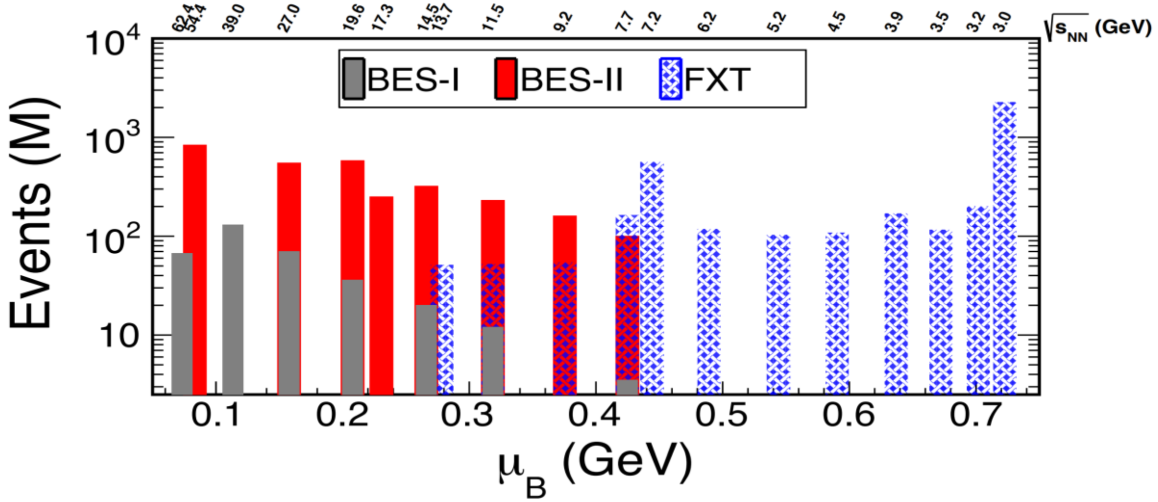

STAR at QM 2023 – 24 Talks, 45 Posters

Recent Data Taking History

(**Will show updates from all systems in red**)

Run 17 – 510 GeV p+p, 54.4 GeV

Run 18 – Isobars (Ru/Zr), 27 GeV, FXT: 3.0, 7.2 GeV

Run 19 – 19.6, 14.6, 200 GeV, FXT 3.2 GeV

Run 20 – 11.5, 9.2, FXT: 3.5, 3.9, 4.5, 5.2, 6.2, 7.7 GeV

Run 21 – 7.7, 17.3, O+O, d+Au, FXT 3.0, 9.2, 11.5, 13.7

Run 22 – 510 GeV p+p (with forward upgrade)

** default system is Au+Au, default energy is 200 GeV

Collider and FXT overlap at: 7.7, 9.2, 11.5 GeV

Motivation

- Onset of deconfinement
- Nature of the phase transition
- Critical Point
- Partonic Matter

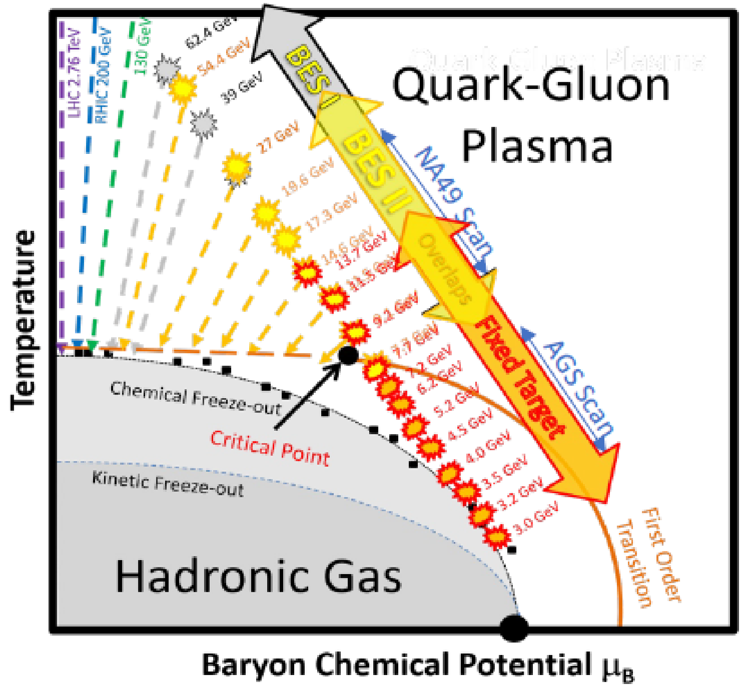

Proton spin

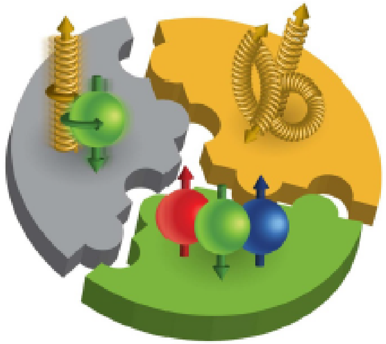

Small Systems

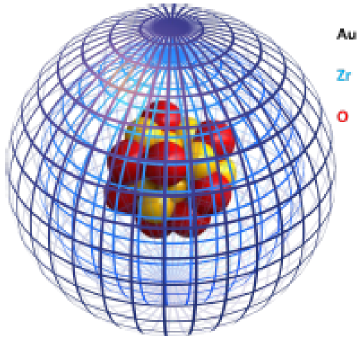

NA61/SHINE physics program

Strong interaction physics:

- study properties of the **onsets of deconfinement and fireball**
- search for the **critical point** of strongly interacting matter
- direct measurements of **open charm**

Neutrino and cosmic ray physics:

- measurements for neutrino programs at J-PARC and Fermilab
- measurements of nuclear fragmentation cross section for cosmic ray physics

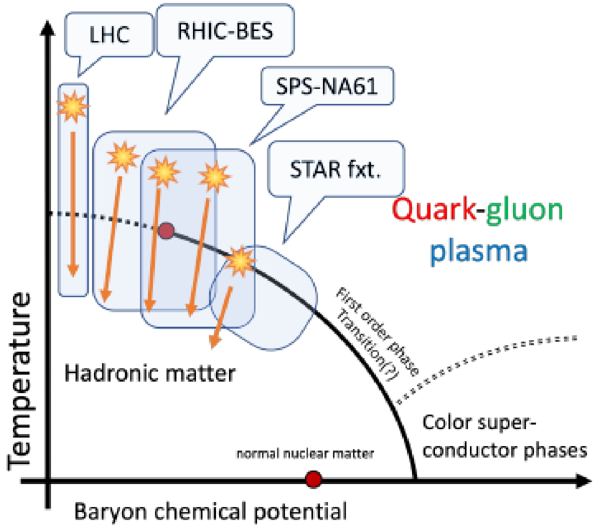

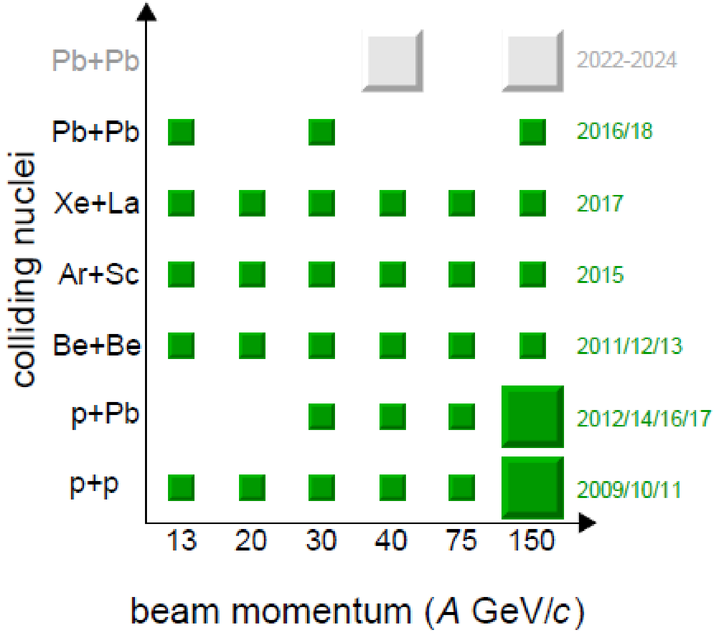

Uniqueness of heavy ion results from NA61/SHINE

theo: Acta Phys.Polon.B 46 (2015) 10, 1991
exp: Phys.Rev.C 77 (2008) 024903

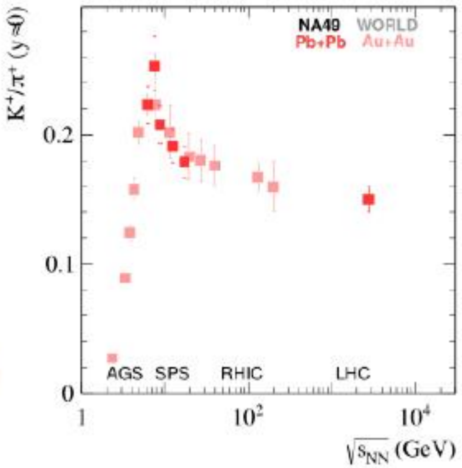

theo: Phys.Part.Nucl. 51 (2020) 3, 337-339
exp: Phys.Rev.C 102 (2020) 011901

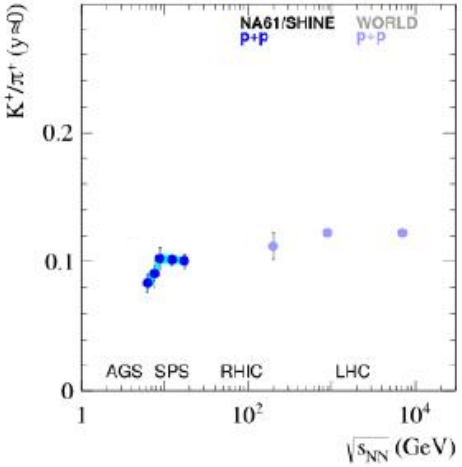

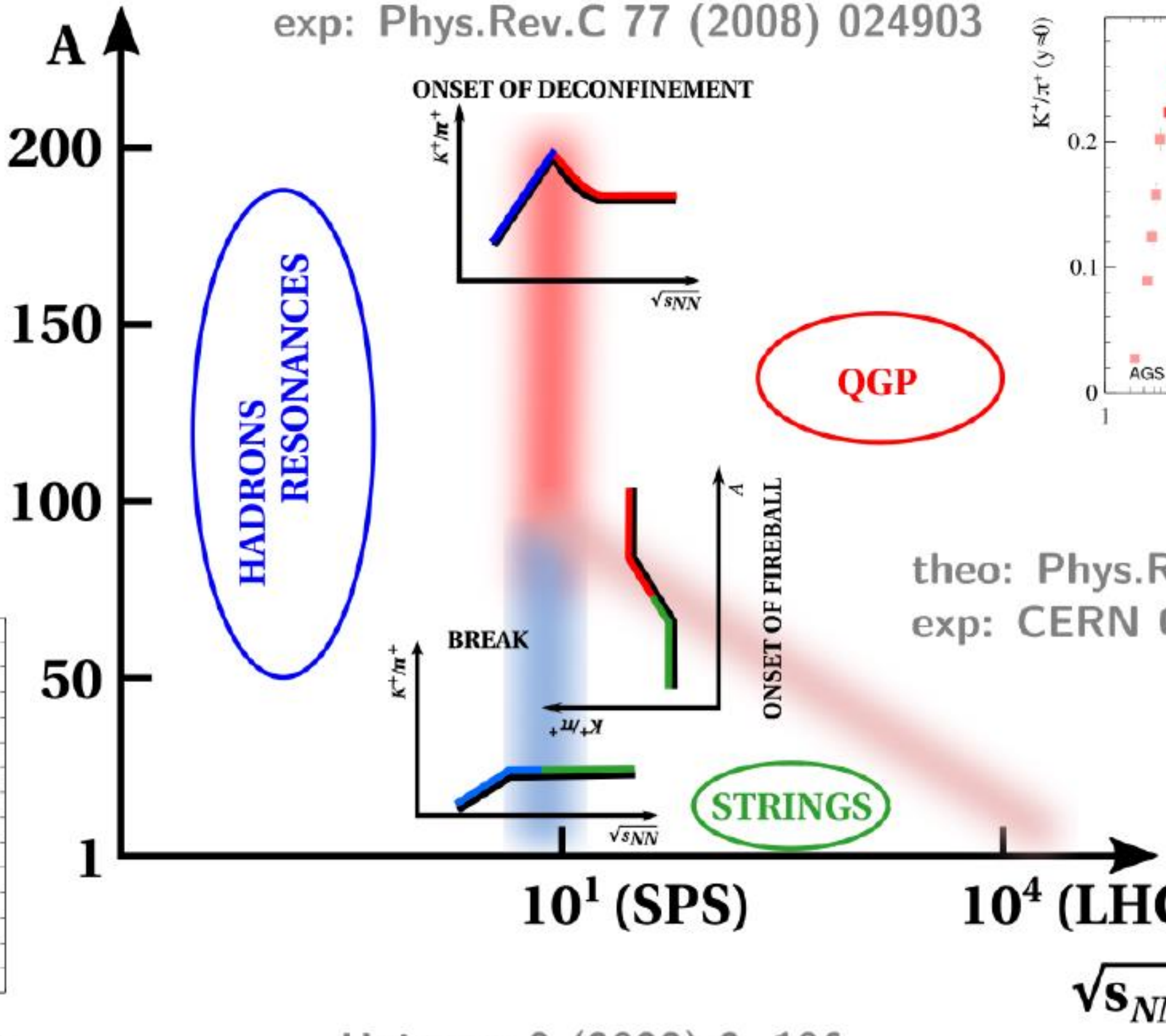

theo: Phys.Rev.D 90 (2014) 025031
exp: CERN Courier, Sep 23^{rd}, 2019

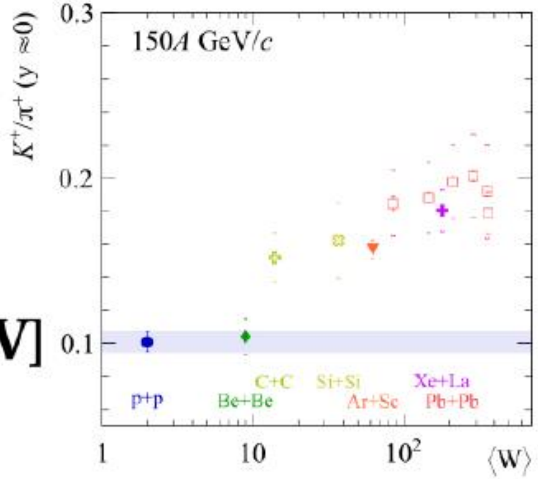

Universe 9 (2023) 2, 106

The HADES Physics Program

(Heavy-)Ion Collisions

- Ar+KCl $\sqrt{s_{NN}}$ = 2.61 GeV, 0.9 bil. evts. (2005)
- Au+Au $\sqrt{s_{NN}}$ = 2.42 GeV, 7.2 bil. evts. (2012)
- Ag+Ag $\sqrt{s_{NN}}$ = 2.55 / 2.42 GeV
  15.2 billion events (2019)

Proton / Pion Beam Experiments

- p+Nb $\sqrt{s_{NN}}$ = 3.2 GeV, 4.2 bil. evts. (2008)
- π+W / π+C / π+PE $\sqrt{s}$ = 1.5 GeV
  1.8 billion events (2014)
- p+p $\sqrt{s}$ = 3.5 GeV, 41.0 billion events (2022)

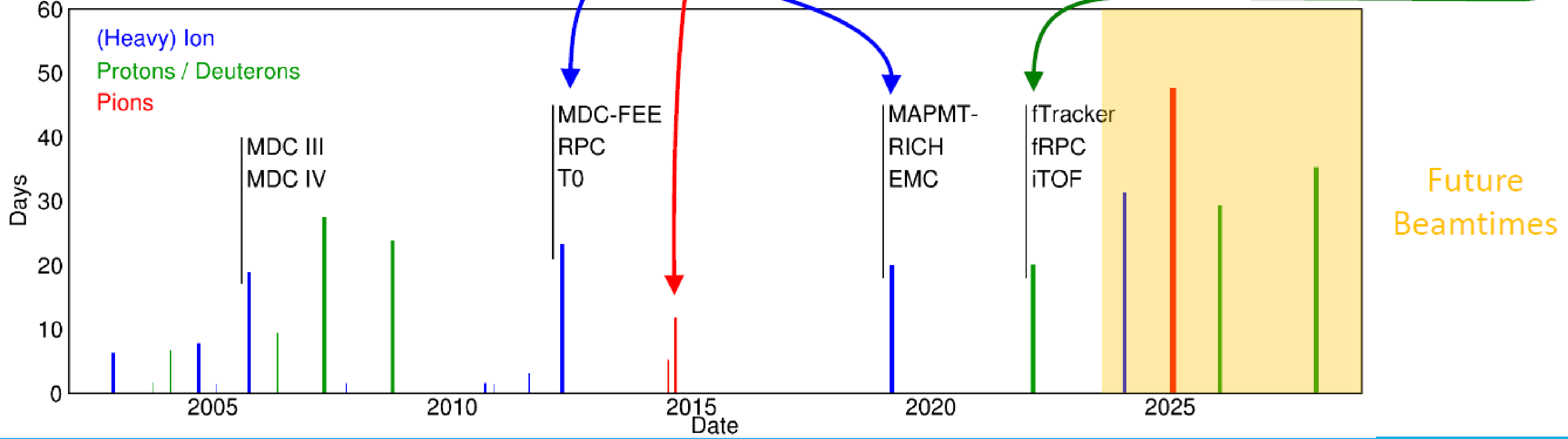

Low collision energies

- Nucleons essentially stopped in collision zone
  - Detected particles predominantly rescattered nucleons
- Slow spectators – $\beta_{CM} \approx 2/3c$
  - Secondary interactions in spectator regions (pole caps)
- Centrality estimation more challenging than at high collision energies

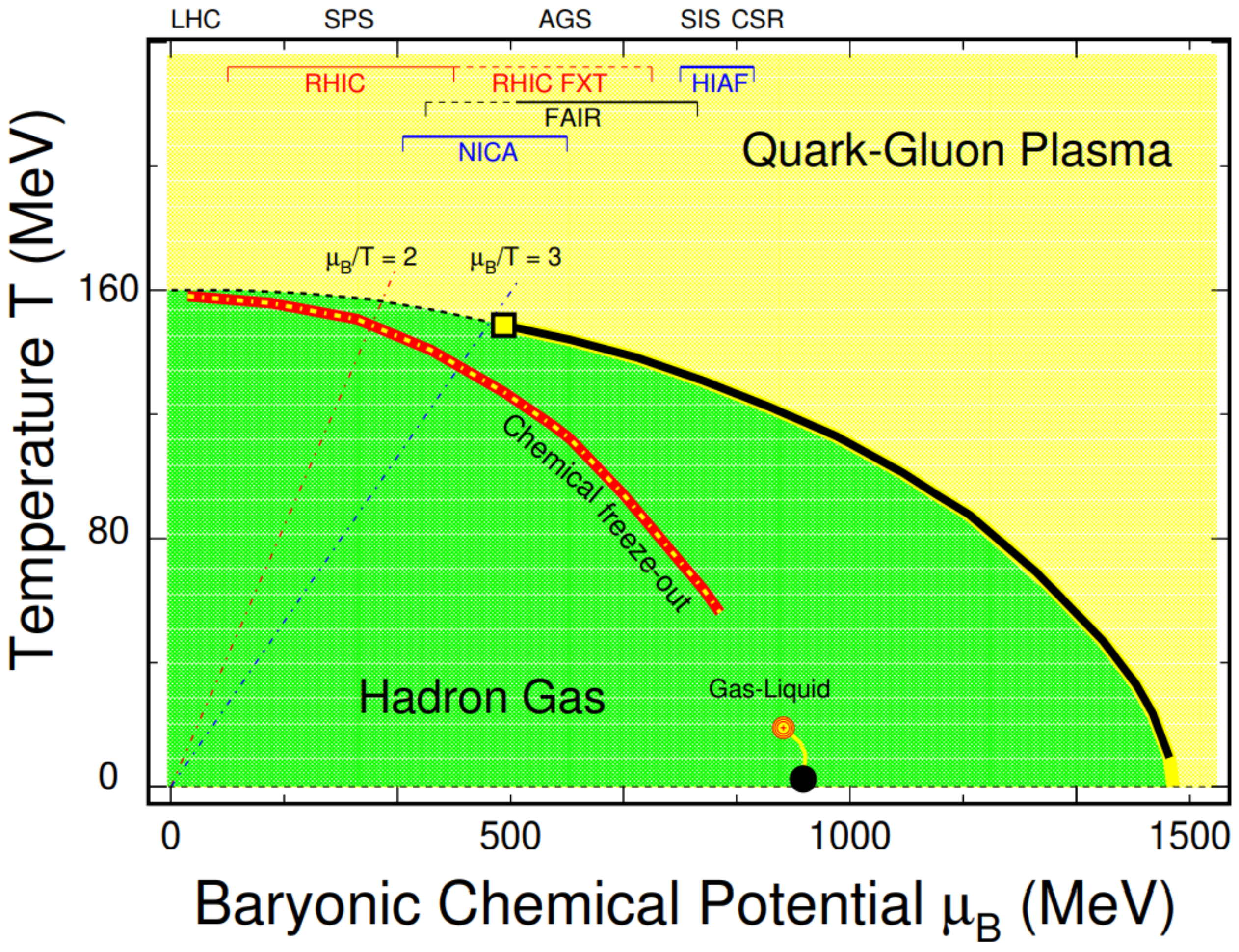

Particle spectra

Mid-Rapidity Yields at 54.4 GeV

Work of Krishan Gopal

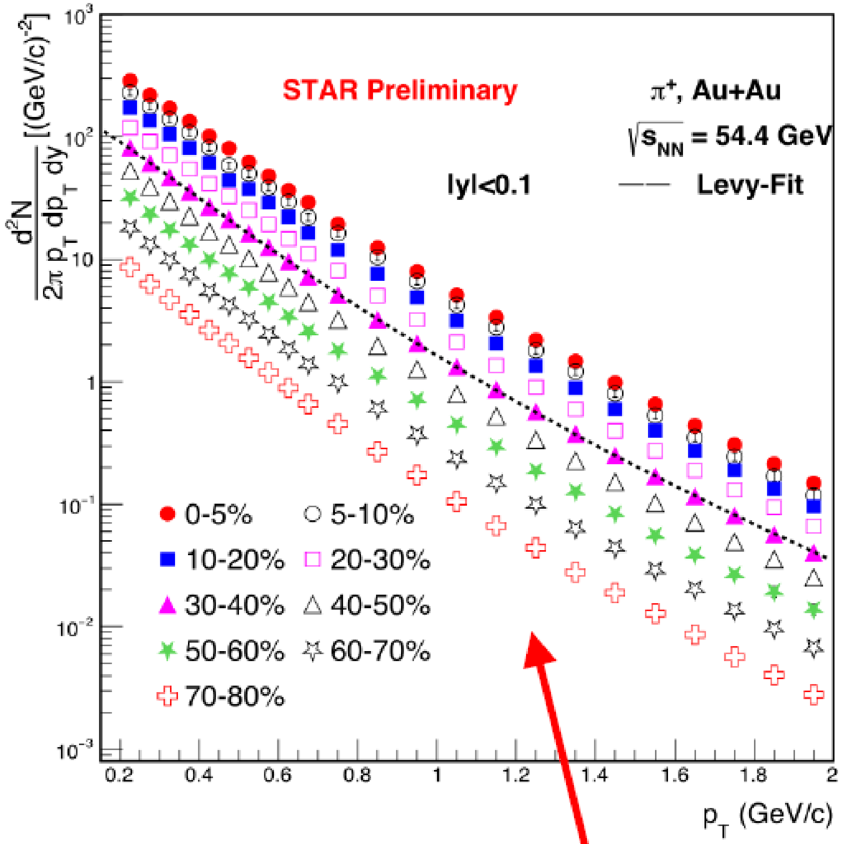

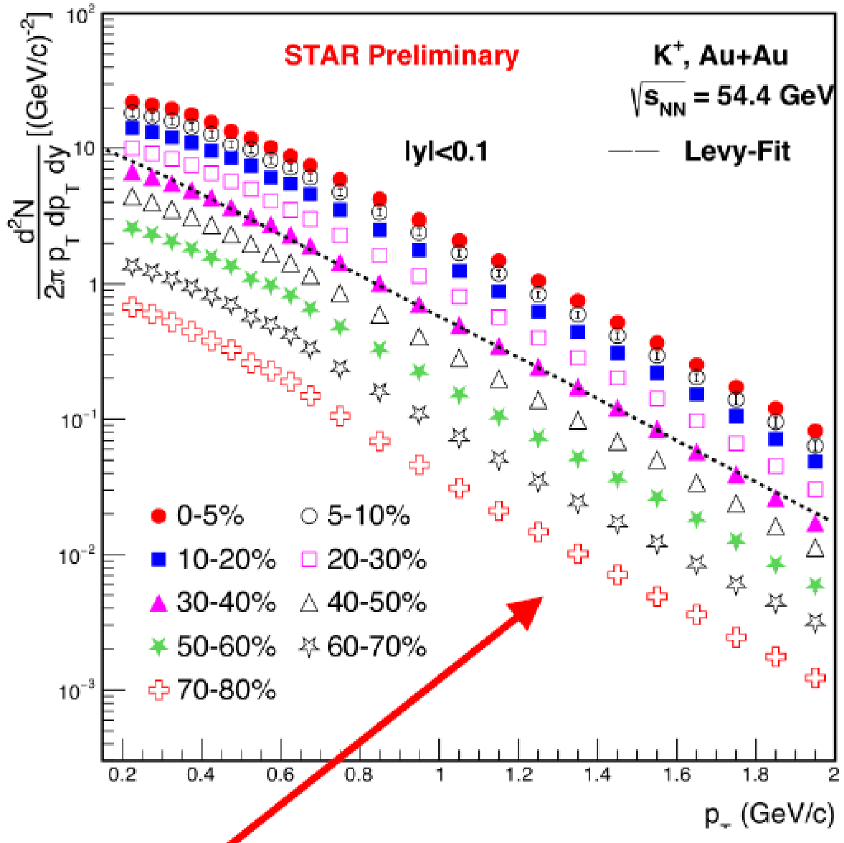

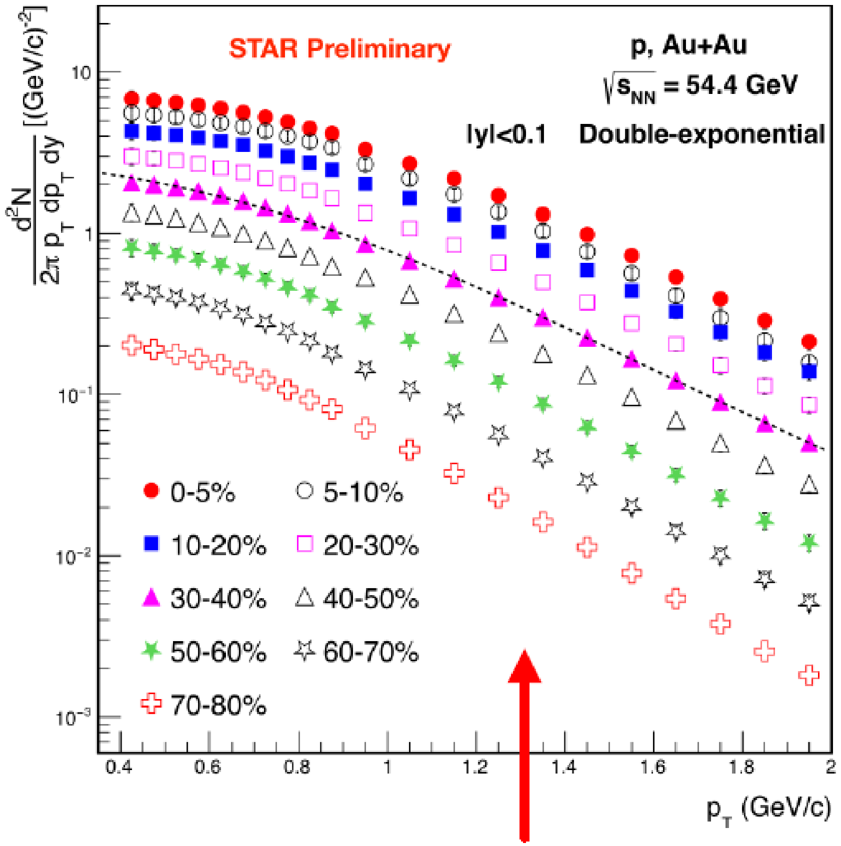

Levy function : $\frac{d^2N}{dy\,dp_T} = \frac{(n-1)(n-2)}{nT[nT+m(n-2)]} \times \frac{dN}{dy} \times p_T \times \left(1+\frac{m_T-m}{nT}\right)^{-n}$

Double exponential : $A_1 e^{-p_T^2/T_1^2} + A_2 e^{-p_T^2/T_2^2}$

- Centrality dependence of yields at y = [-0.1,0.1]

Rapidity Dependent Spectra

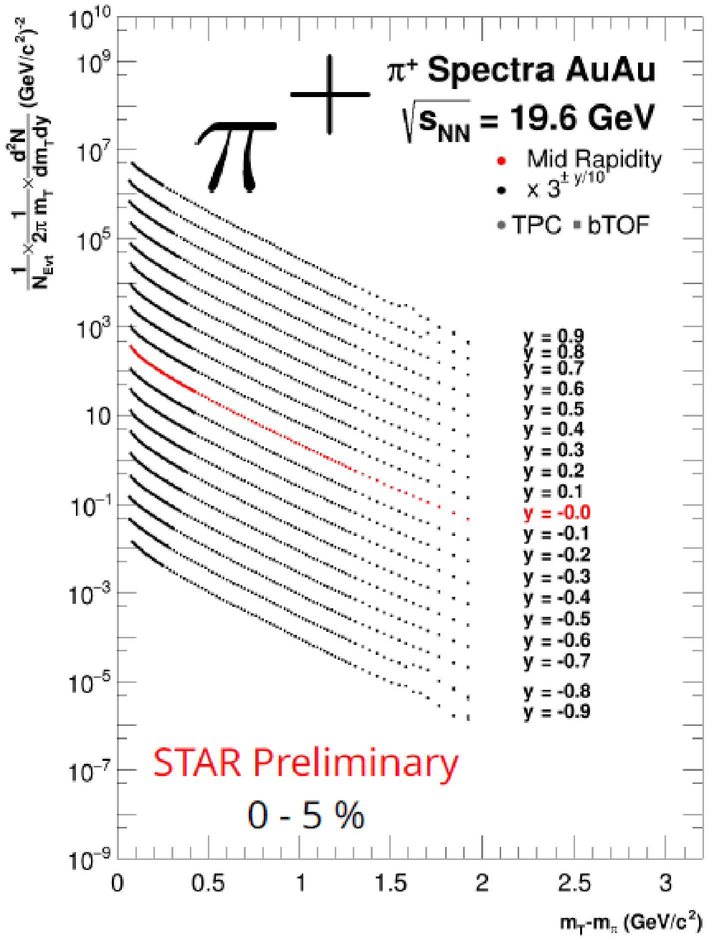

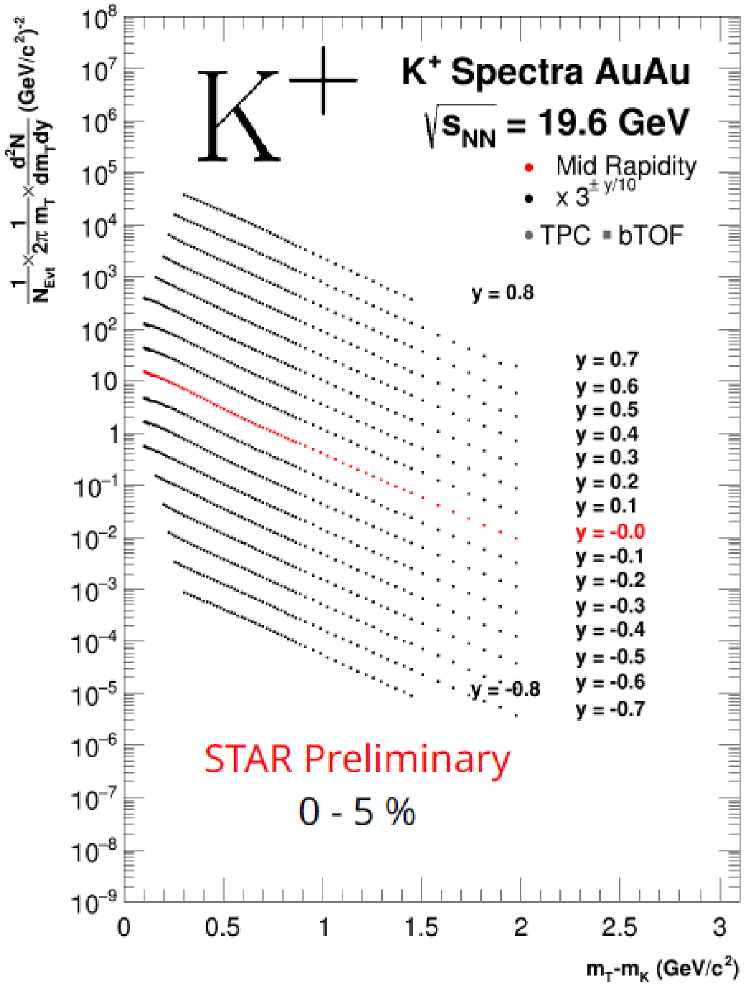

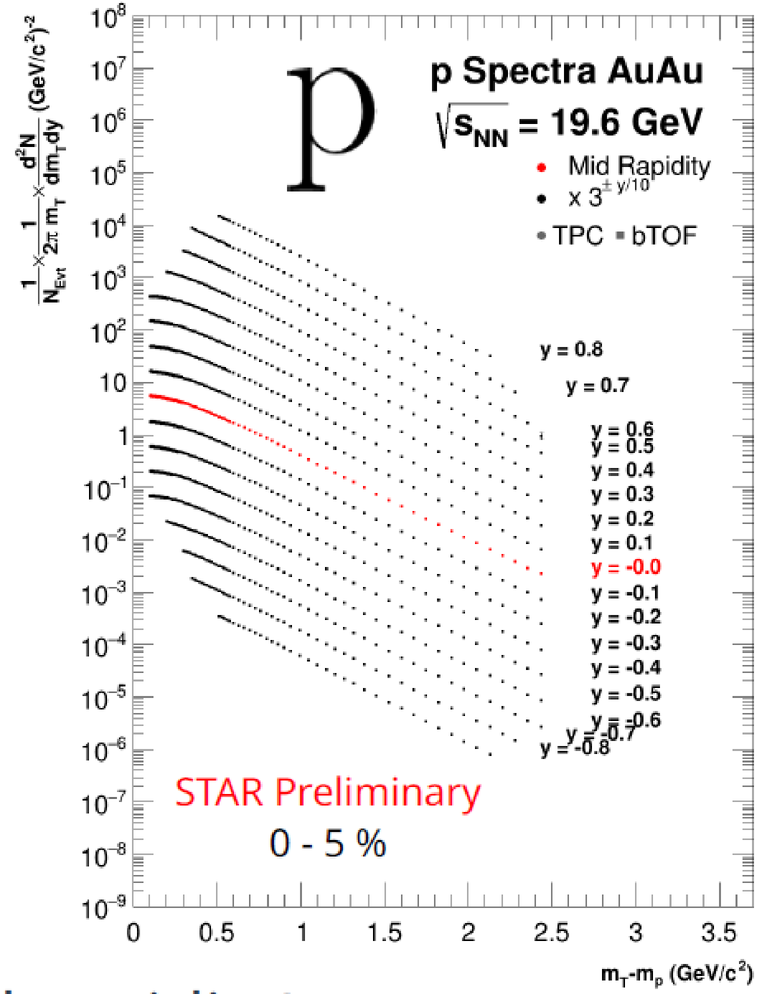

- Wide Rapidity Coverage (BES-I reported mid-rapidity)
- Spectra fit at low pT to extract dN/dy

Particle ratios

- Measure $\pi\pm$, $K\pm$, p, $\bar{p}$ across p_T and rapidity
  - Kinetic & Chemical Freeze-out
  - μ_B and μ_S
  - Associated Production of K+
  - Baryon Stopping
- **Where are we on the QCD phase diagram at kinetic & chemical freeze-out?**

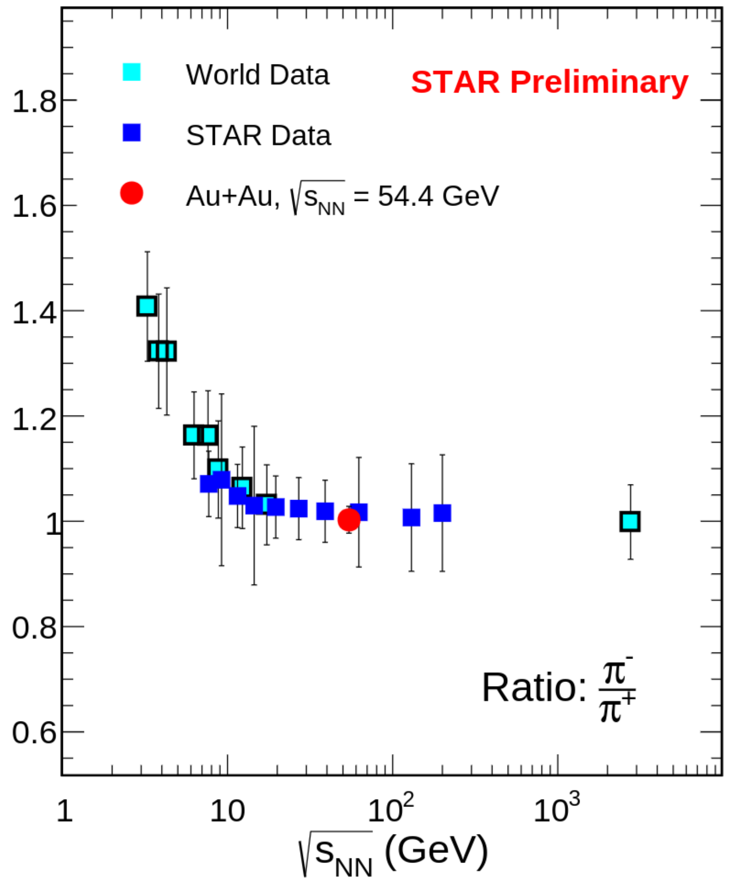

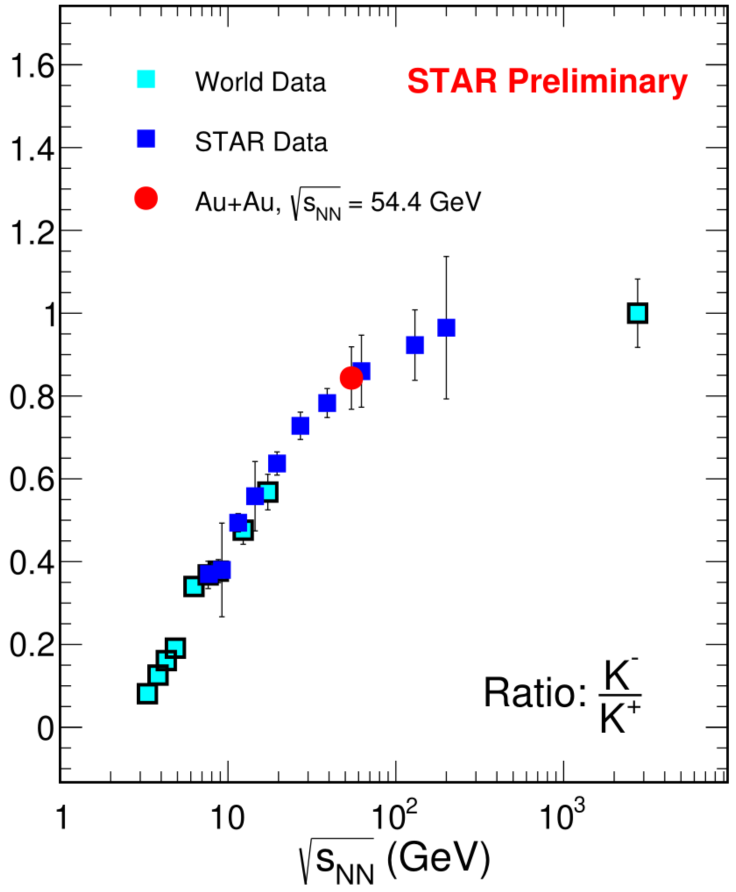

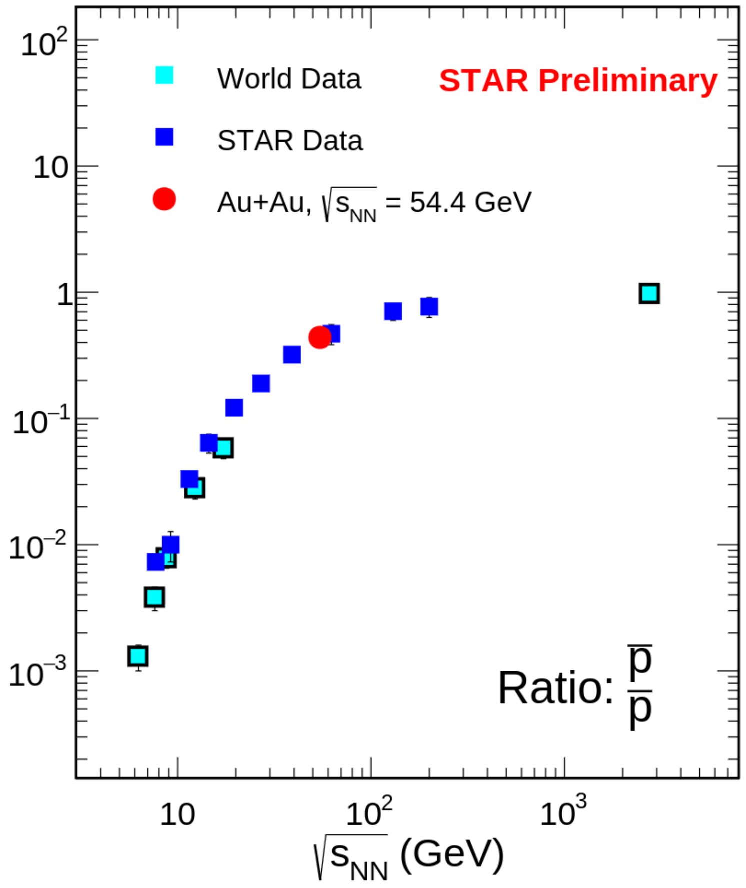

Kinetic Freeze-out at 54.4 GeV

Work of Krishan Gopal

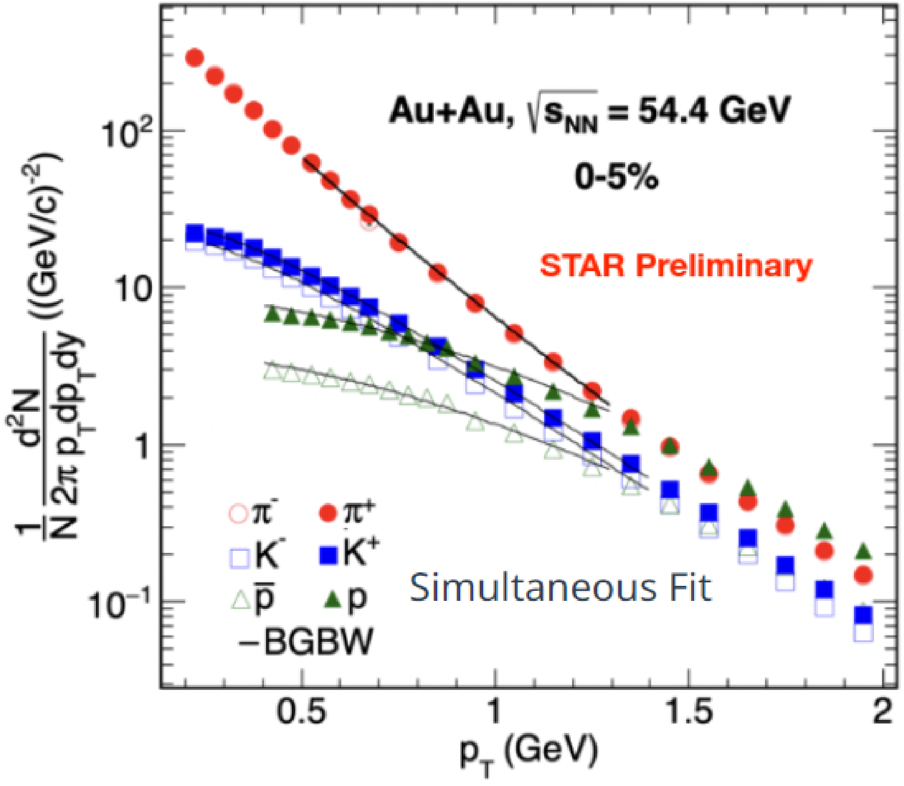

Blast-Wave Model : Hydrodynamic inspired model

$$\frac{dN}{p_T dp_T} \propto \int_0^R r\, dr\, m_T I_0\left(\frac{p_T \sinh\rho(r)}{T_{kin}}\right) \times K_1\left(\frac{m_T \cosh\rho(r)}{T_{kin}}\right)$$

I_0, K_1: Modified Bessel functions
ρ (r) = $\tanh^{-1}\beta$
β = Transverse radial flow velocity
T_{kin}: Kinetic freeze-out temperature

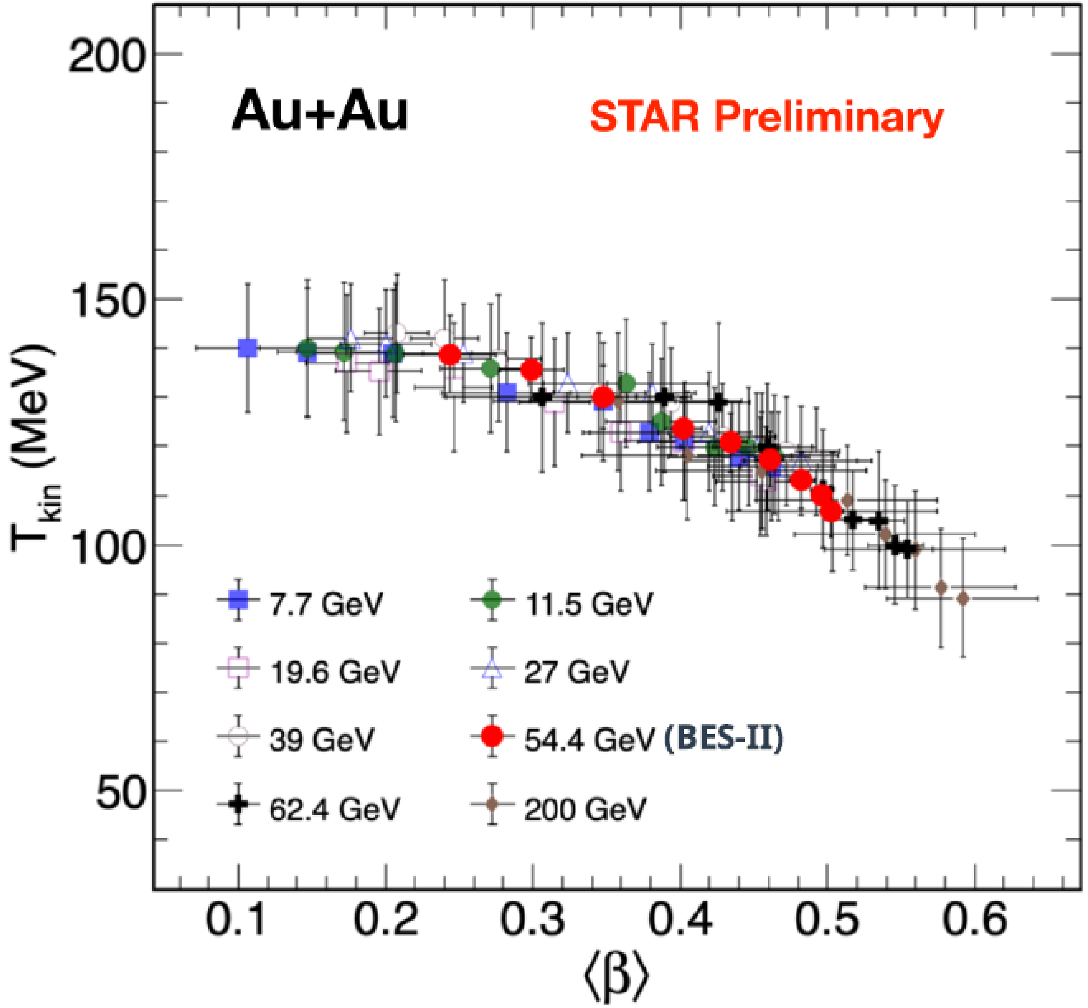

- T_{kin} and <β> show anti-correlated trend, similar to the other BES-I energies

Thermodynamical properties of the medium

Similar rapidity dependence of the T_{chem} and μ_B, μ_S over particle multiplicity

Precise study of the QCD phase diagram location of the interaction at different collision energies

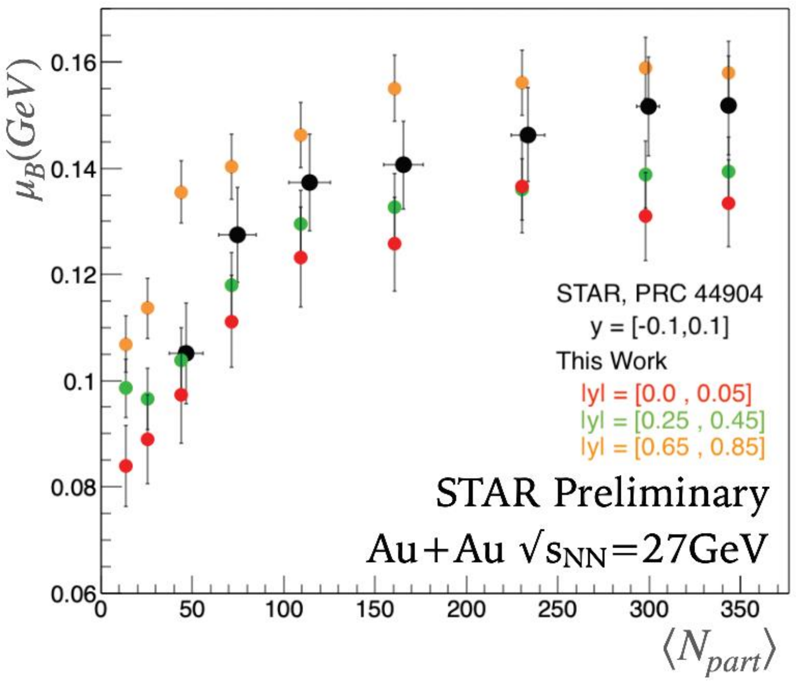

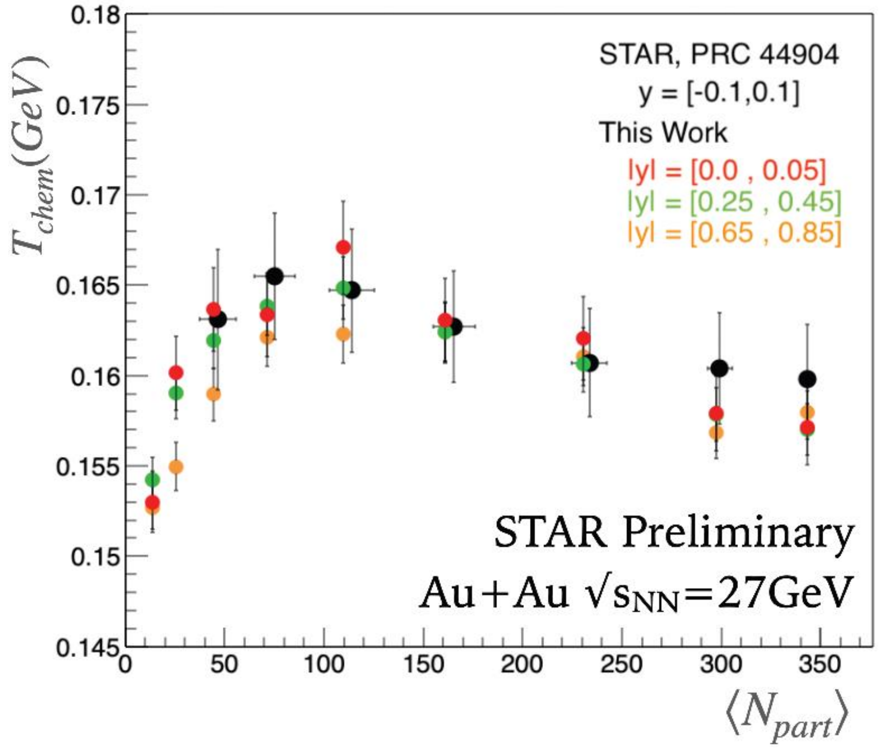

Fits by THERMUS Chemical equilibrium model

$\Delta\mu_B \approx 25$ MeV for $\Delta y = 1$ at 27 GeV

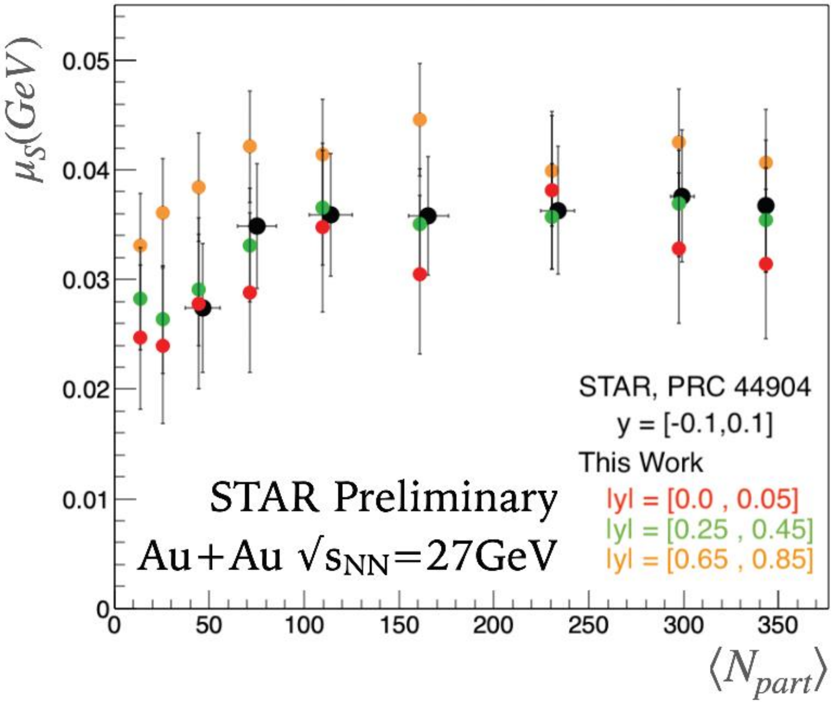

Weak Decay Reconstruction Performance

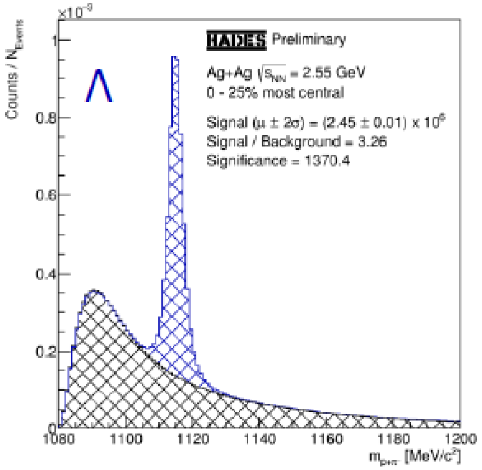

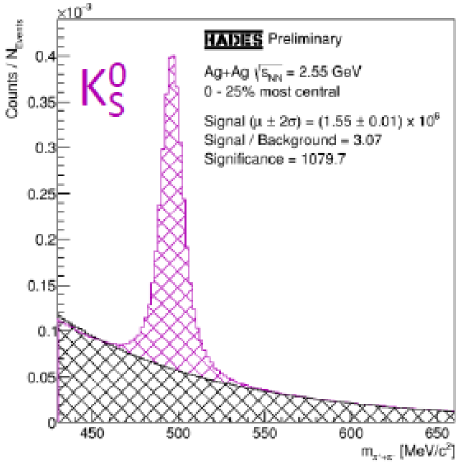

- Large phase space coverage with low statistical errors
- Data points well described by Boltzmann functions
    - ➢ Extrapolation to 4π

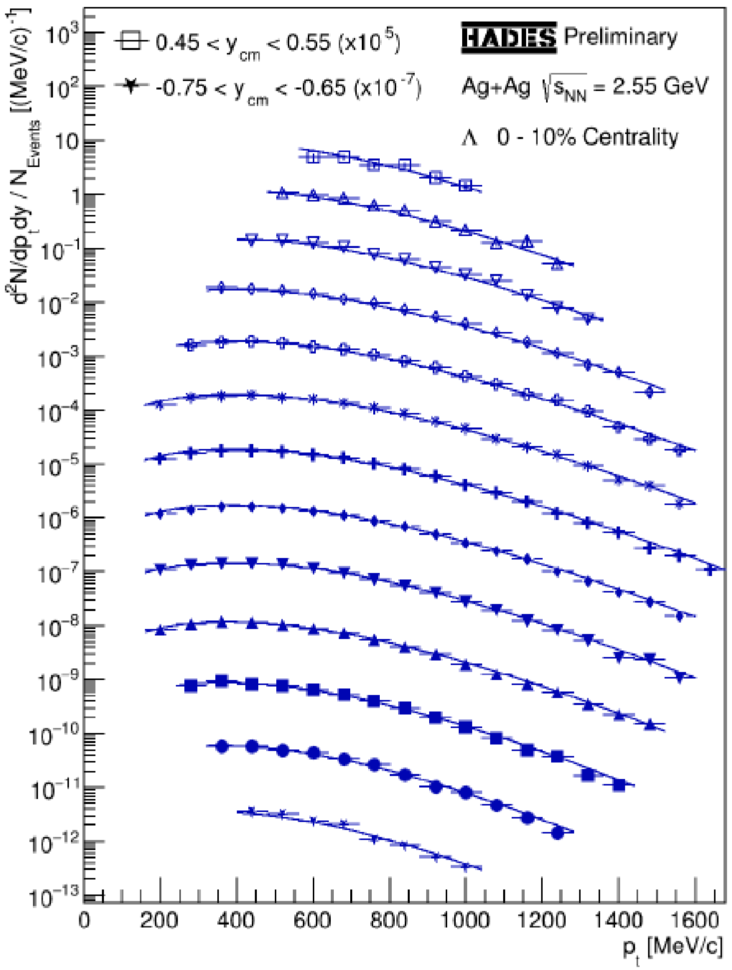

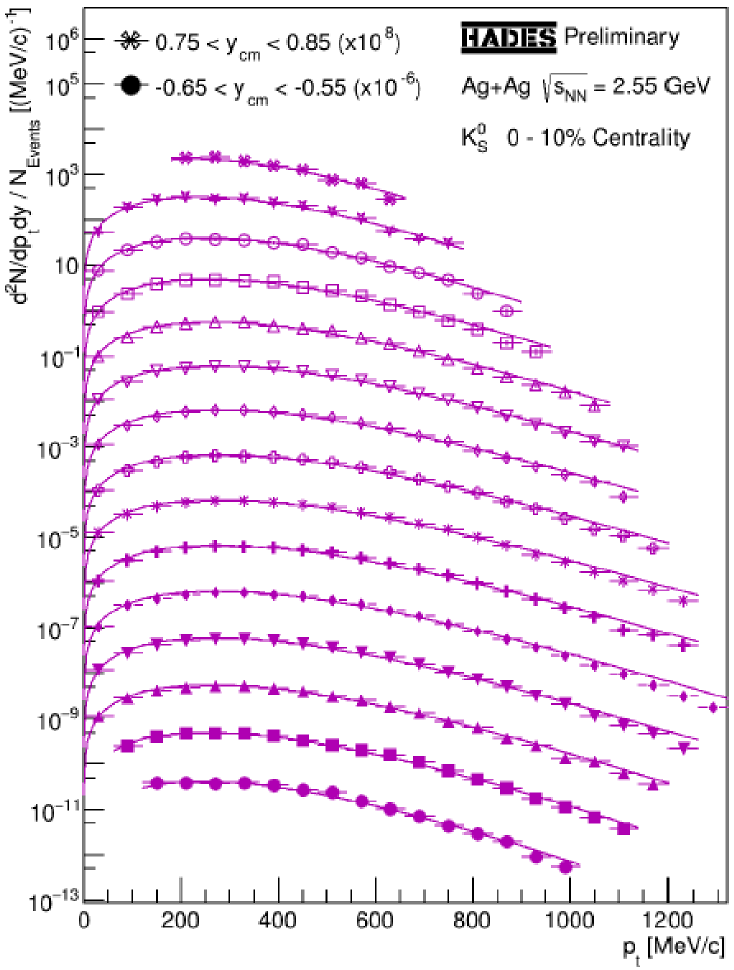

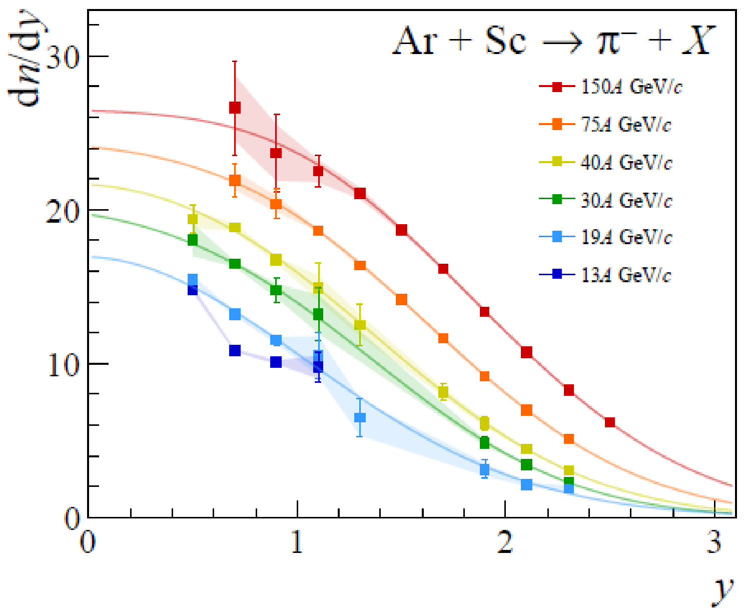

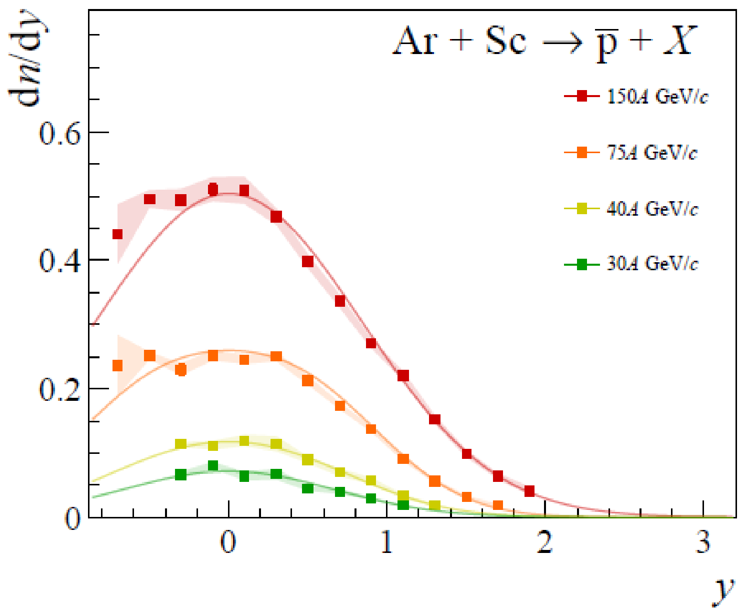

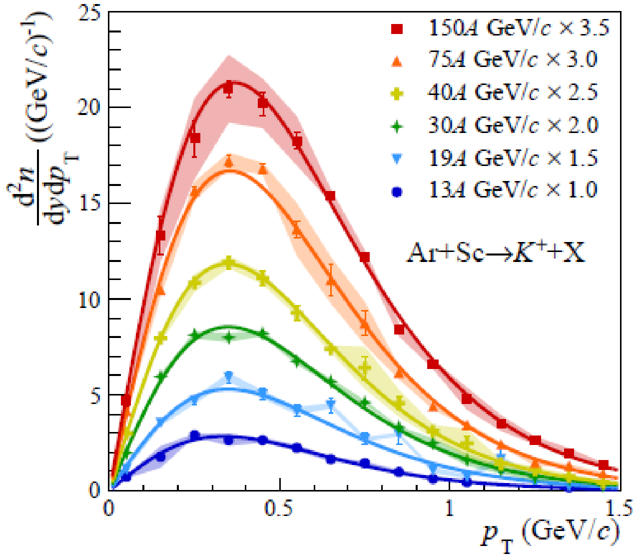

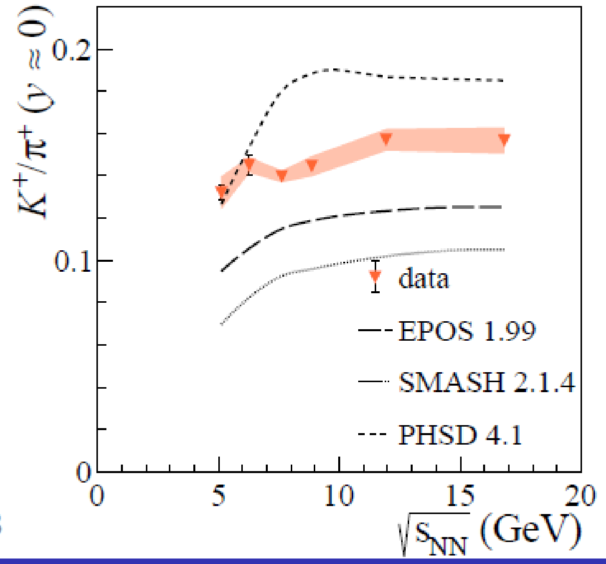

- New final results on $K^{\pm}$, $\pi^{\pm}$, p and $\bar{p}$ in Ar+Sc
- 0-10% of the most central collisions
- Data available at six beam energies in range $\sqrt{s_{NN}} = 5.1 - 16.8$ GeV

arXiv:2308.16683

Spectra of charged particles in Xe+La

See poster by O. Panova

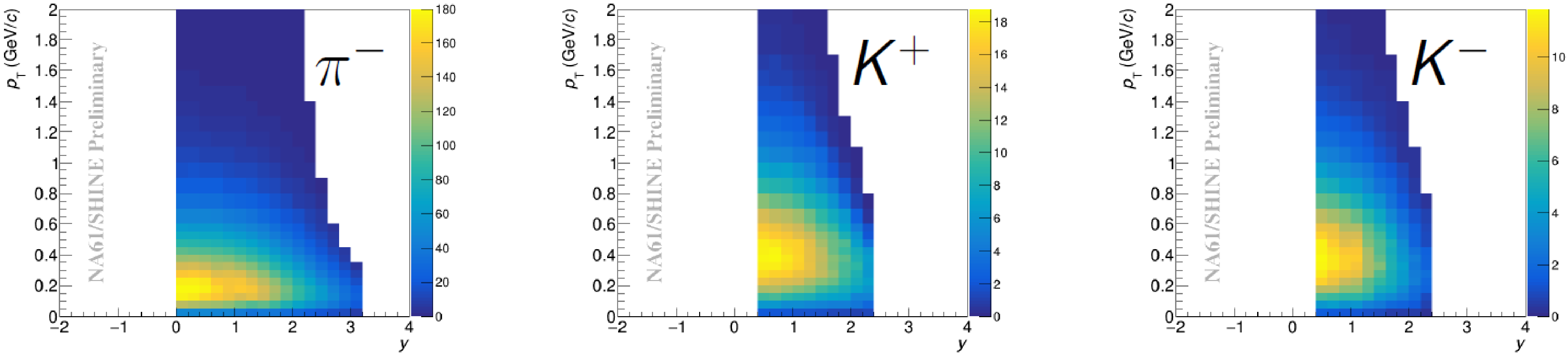

- New preliminary results on $K^{\pm}$ and π^- spectra
- 0-20% of the most central collisions
- Data available at $\sqrt{s_{\mathrm{NN}}} = 16.8$ GeV
- p_T spectra shown for $0.4 < y < 0.6$

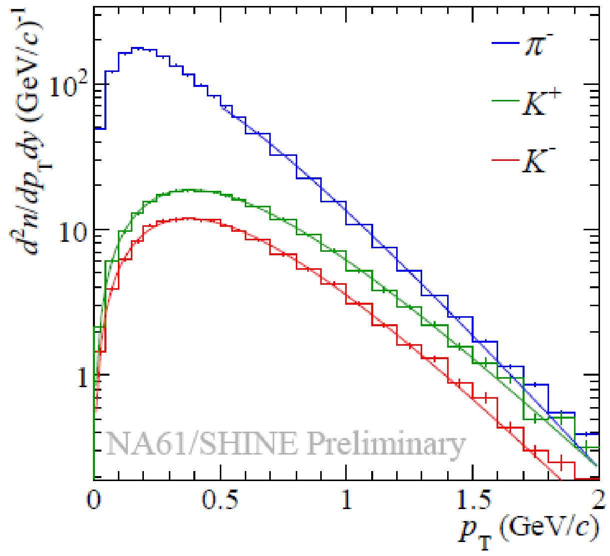

Onset of deconfinement: horn

See poster by O. Panova

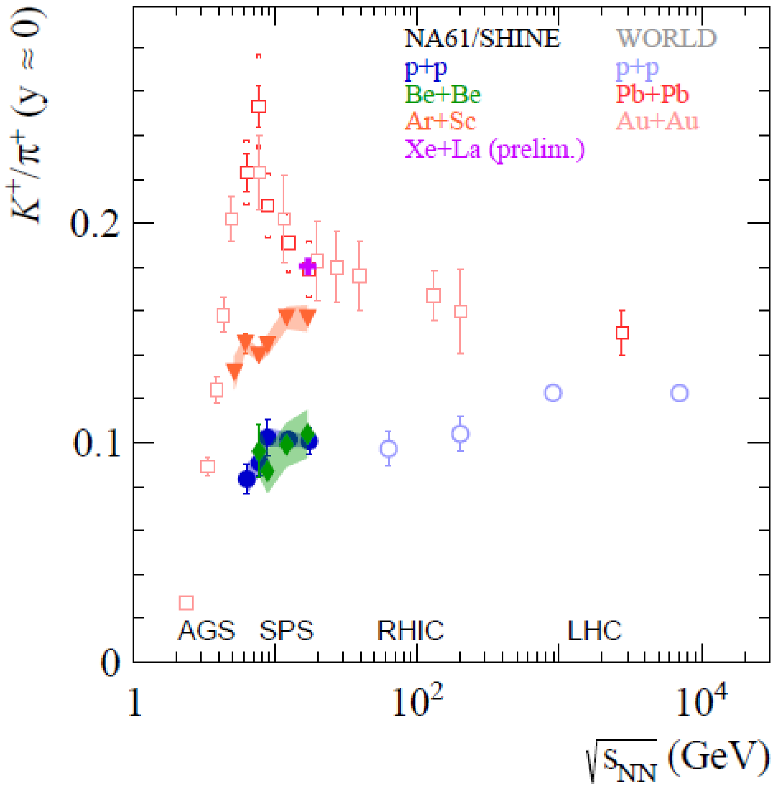

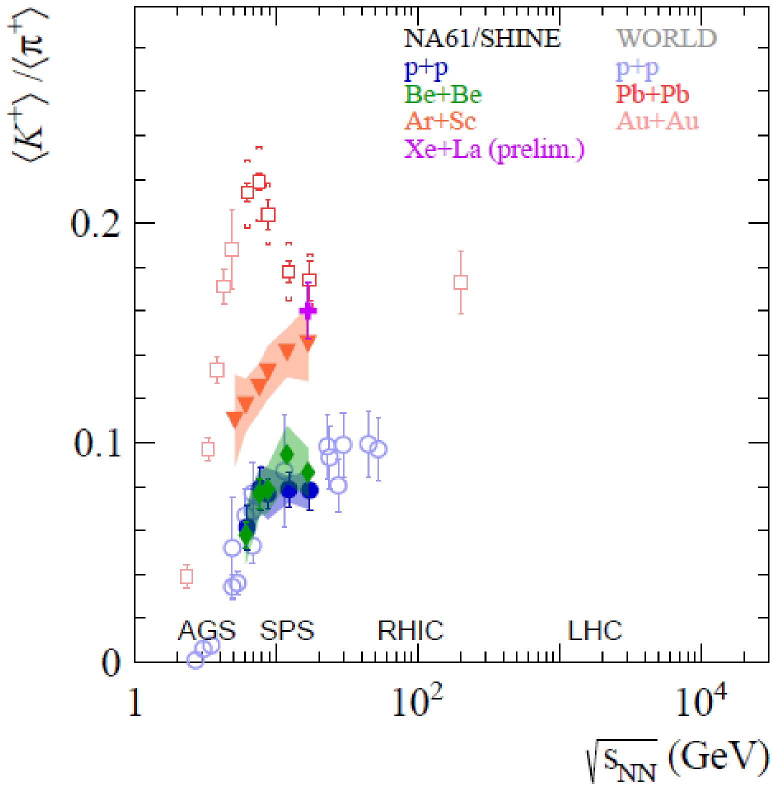

- Rapid change in the energy dependence of K^+/π^+ ratio in Pb+Pb collisions indicated the onset of deconfinement in the SPS energy range, as predicted within SMES
- Plateau-like structure visible in light systems ($p+p$ and Be+Be)
- Ar+Sc systematically higher, Xe+La close to Pb+Pb at $\sqrt{s_{NN}} = 16.8$ GeV

arXiv:2308.16683 (Ar+Sc), Eur.Phys.J.C 81 (2021) 1, 73 (Be+Be), Eur.Phys.J.C 77 (2017) 10, 671 (p+p)

$\bar{\Lambda}/K_s^0$ ratio at 19.6 and 14.6 GeV

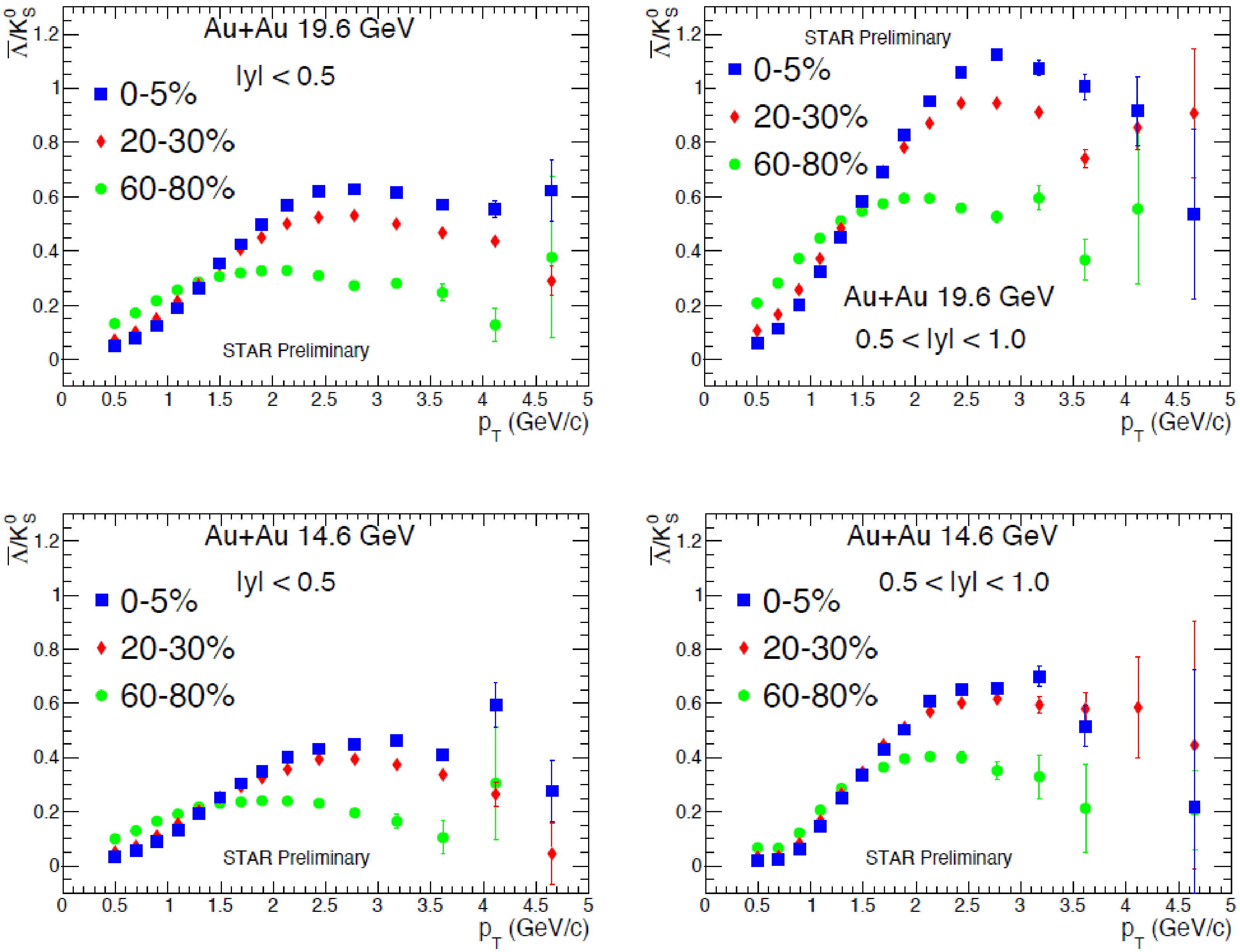

- Clear centrality and rapidity dependence of (anti-)baryon-to-meson ratio at intermediate p_T.
- Baryon enhancement is observed in all measured rapidity regions.

Multiplicity Dependence of Strange Hadron Production in Small Systems

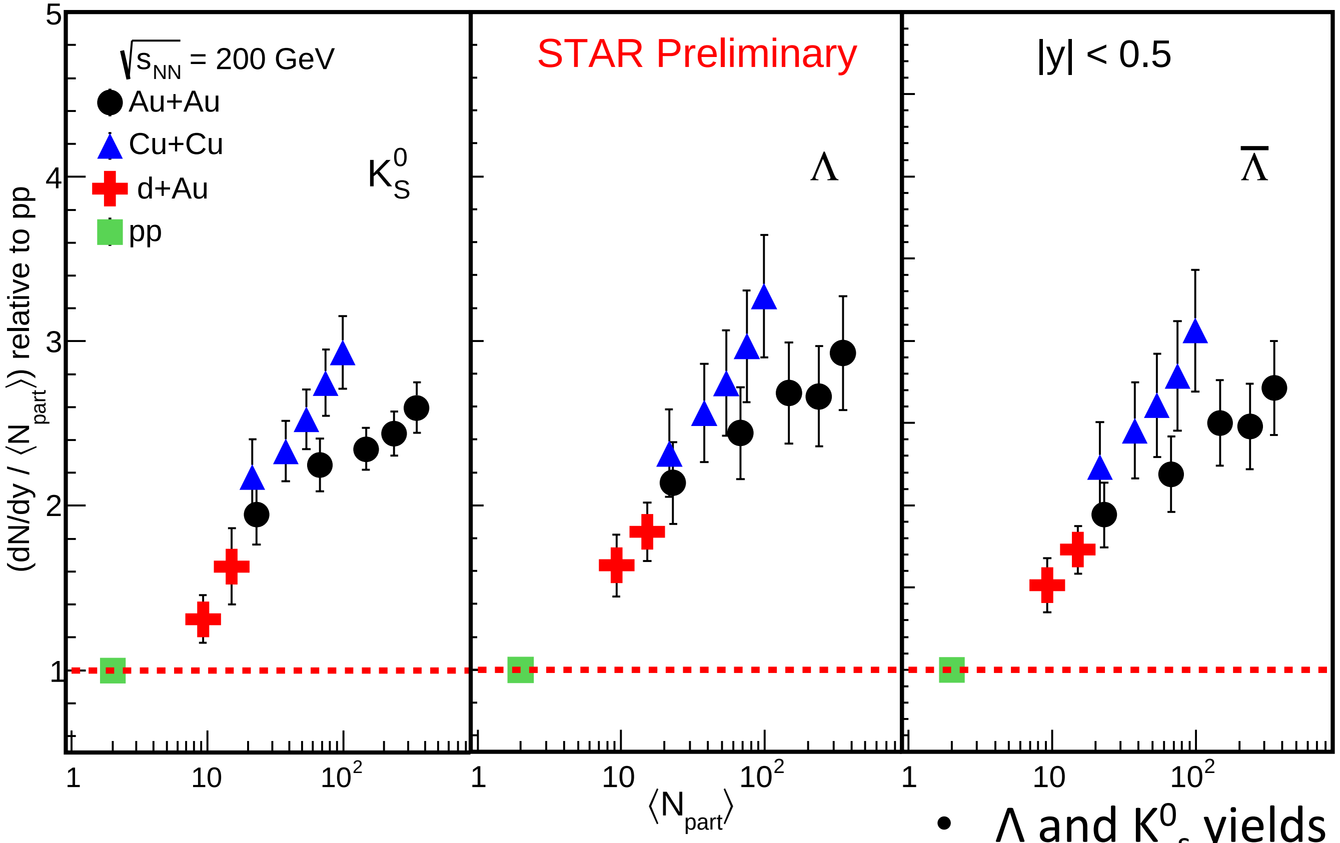

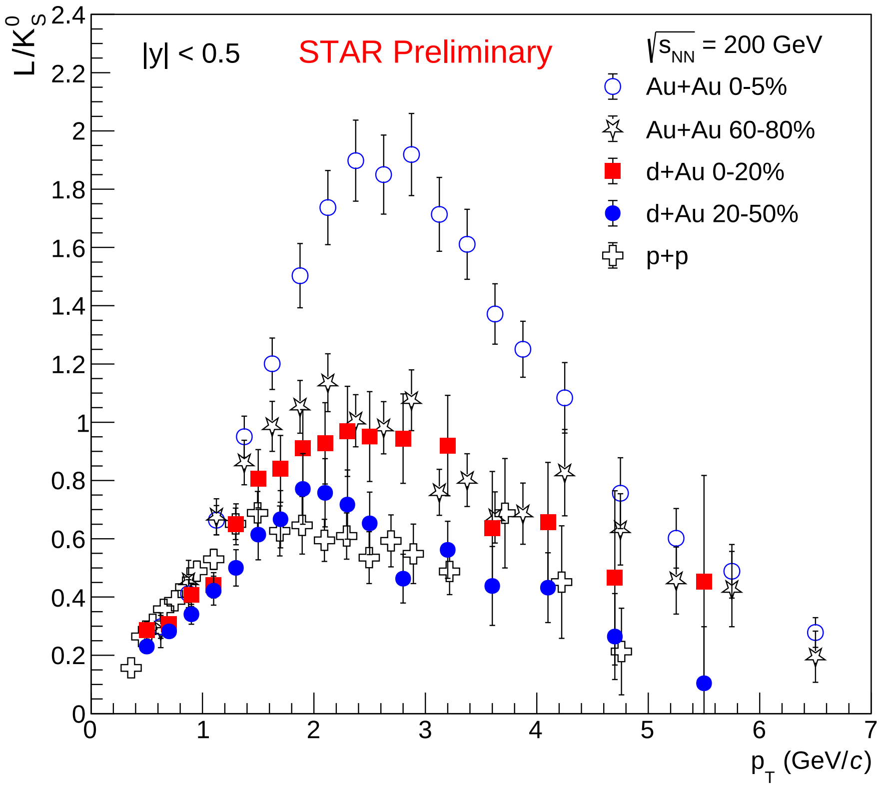

- Λ and K^0_s yields in d+Au at 200 GeV are enhanced
  - Yields connect p+p with peripheral Cu+Cu and Au+Au collisions (yield Cu+Cu > Au+Au)
- Baryon enhancement is observed at intermediate p_T for central d+Au 200 GeV with Λ/K^0_s .

STAR : Phys. Rev. C **75**, 064901 (2007)
STAR : Phys. Rev. Lett. 108, 072301 (2012)
STAR : Phys. Rev. C 79, 034909 (2009)

Energy and centrality dependence of strangeness production

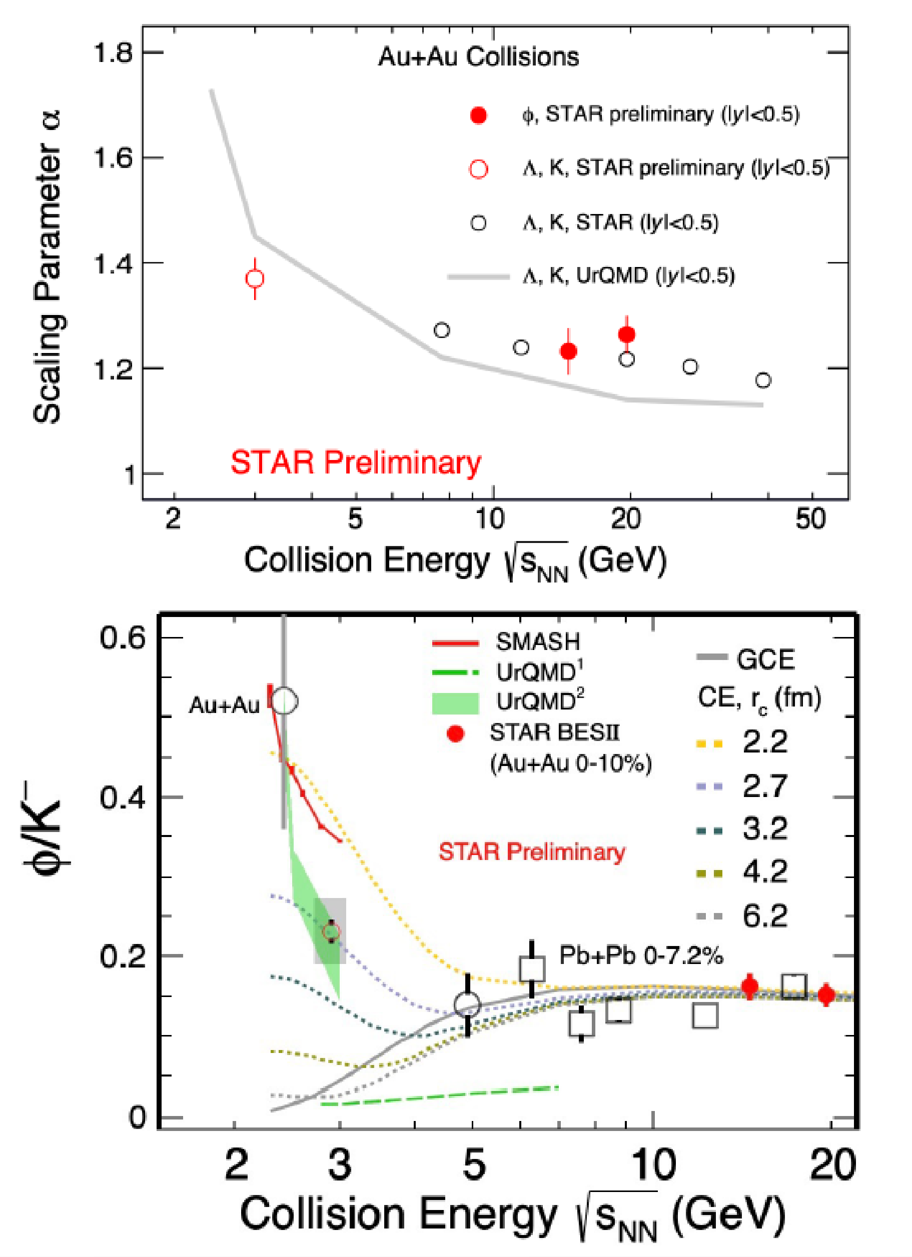

- Fit function: $\frac{dN/dy}{N_{part}/2} = k \times N_{part}^{\alpha-1}$
- Common centrality dependence for ϕ, Λ, K production at 19.6GeV.
- Above 7.7 GeV, data indicates a steeper increase on strangeness yields towards central collisions compared to UrQMD.
  - ✓ Might point to production mechanisms beyond hadronic interactions in this energy range.
- In contrast to 3GeV, ϕ/K^- reach grand canonical ensemble limit at 19.6 and 14.6 GeV.

Weiguang Yuan poster #555

Strange Yields vs. $\langle A_{Part} \rangle$

- Production below (at) free NN-threshold
  - ➢ Missing energy provided by the system
- Centrality dependence compatible with universal scaling assumption:
  Mult $\propto \langle A_{Part} \rangle^{\alpha}$ with $\alpha_{Au+Au} = 1.45 \pm 0.06$
  - ➢ Hierarchy in production thresholds not reflected
  - ➢ Suggests scaling with primary $s\bar{s}$ creation
  - ➢ Hint for quark percolation
    K. Fukushima, T. Kojo, W. Weise, PRD **102**, 096017 (2020)

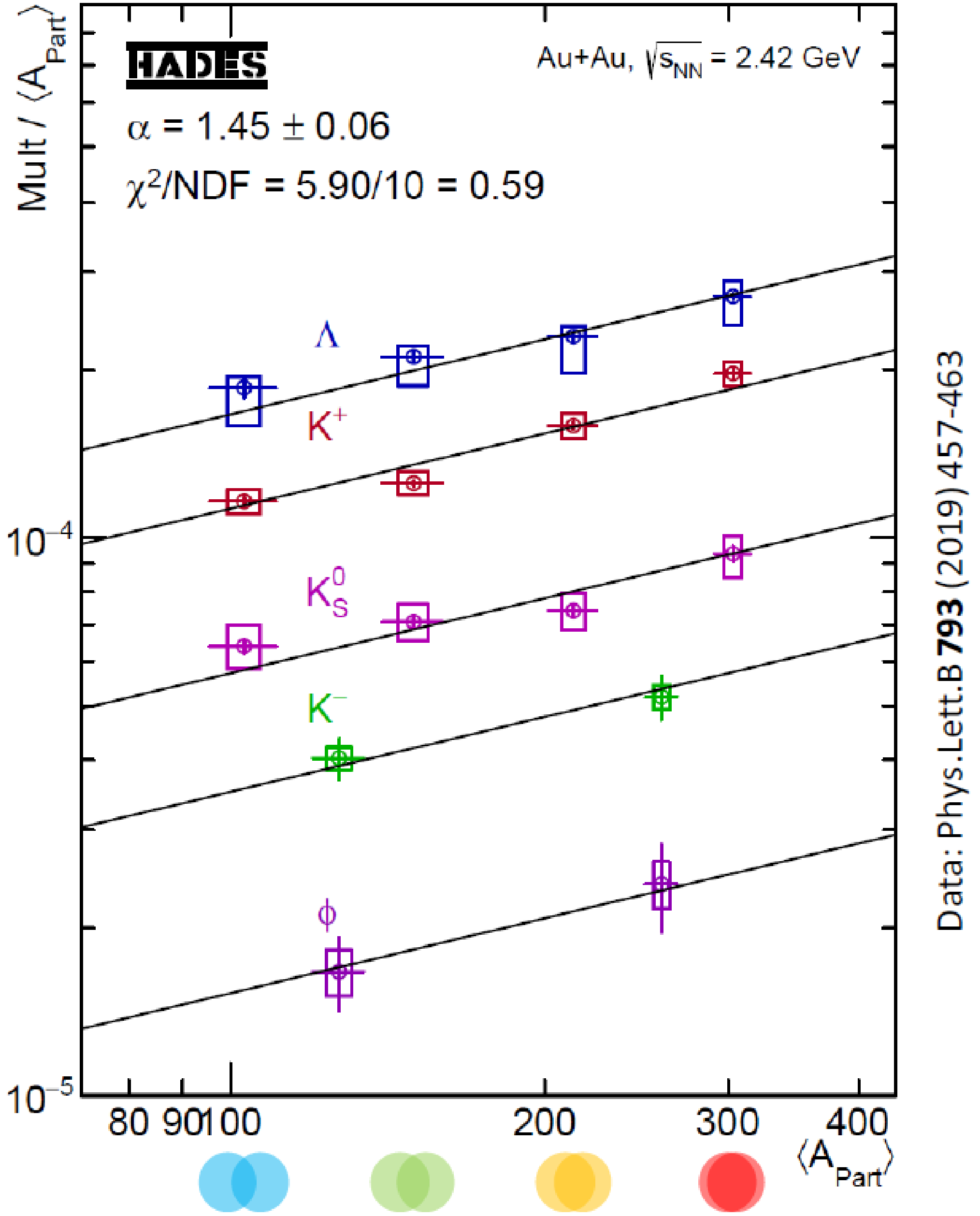

Reconstruction of Σ^0 Hyperons

- Σ^0 Hyperons measured via their two-step electro-weak decay chain: $\Sigma^0 \rightarrow \Lambda + \gamma \rightarrow p + \pi^- + \gamma$
- SHM capable of describing Λ / Σ^0 ratio almost perfectly
- Λ / Σ^0 ratio sensitive to differences between transport models

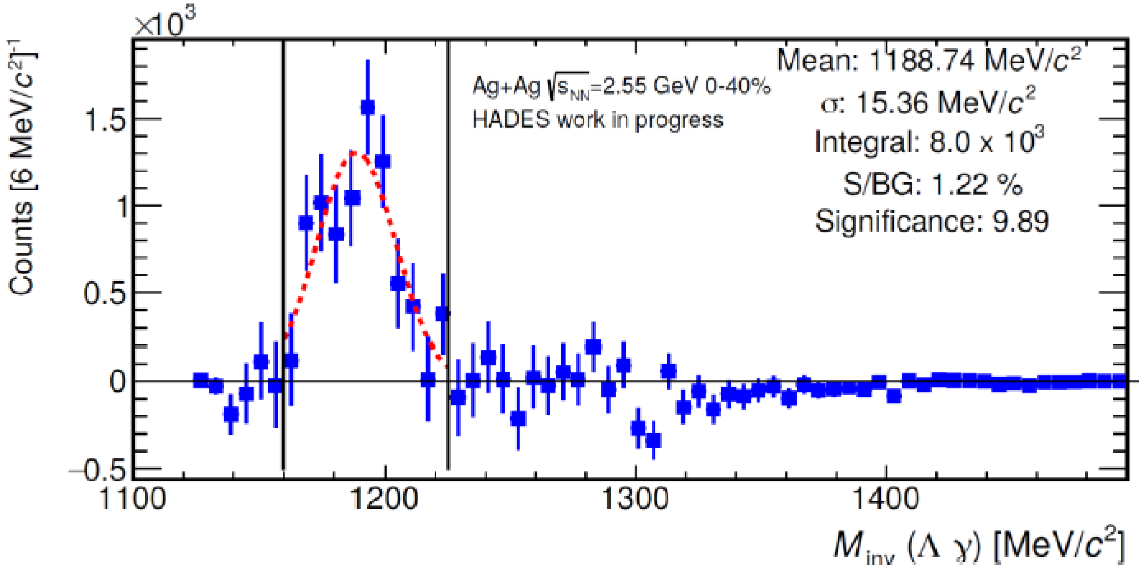

Talk by Marten Becker Wednesday 06.09.2023 10:10

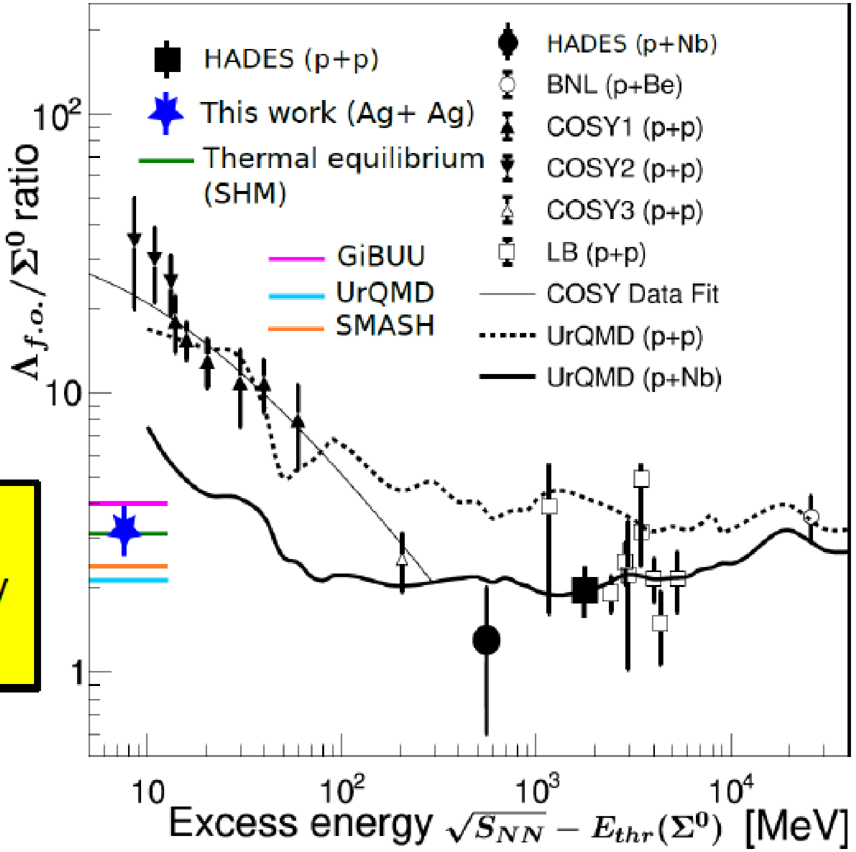

➢ Possibility to investigate differences between various SHM fits and transport models

Strangess & Σ prospects with CBM

- Tracking system allows for precise track and 2ndary vertex reconstruction, Δp=1%
- TOF for hadron ID

→ measure yields, flow, correlations, Λ polarization, …

- **Identification of Σ^+ and Σ^- via their decay topology**: search for kink!

$\Sigma^+ \rightarrow p\pi^0$	$\bar{\Sigma}^+ \rightarrow \bar{p}\pi^0$	BR = 51.6%
$\Sigma^+ \rightarrow n\pi^+$	$\bar{\Sigma}^+ \rightarrow \bar{n}\pi^-$	BR = 48.3%
$\Sigma^- \rightarrow n\pi^-$	$\bar{\Sigma}^- \rightarrow \bar{n}\pi^-$	BR = 99.8%

→ (p/n) like ratios! → access to isospin dependence?

→ Σ^-/Σ^+ ratio is expected to carry $E_{sym}(\rho)$ information (stiff/soft)

Find tracks of Σ and its charged daughter in STS and MVD

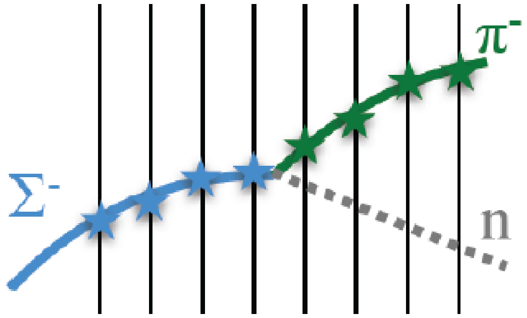

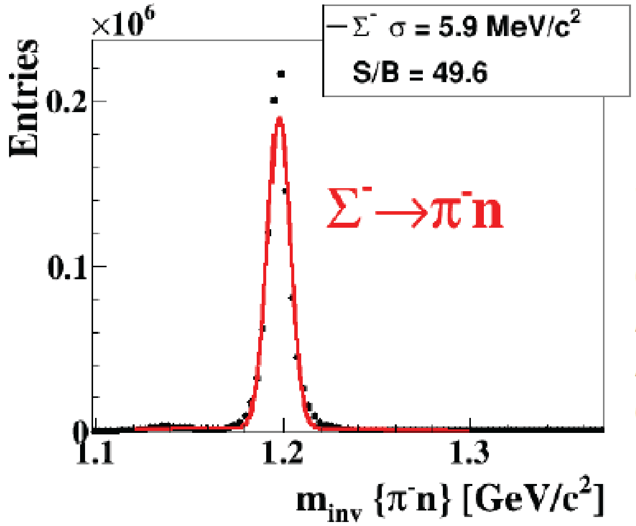

Simulations: UrQMD, 5M central collisions Au+Au, 10 AGeV beam energy

G.C. Yong et al, *Phys.Rev.C* 106 (2022) 2, 024902

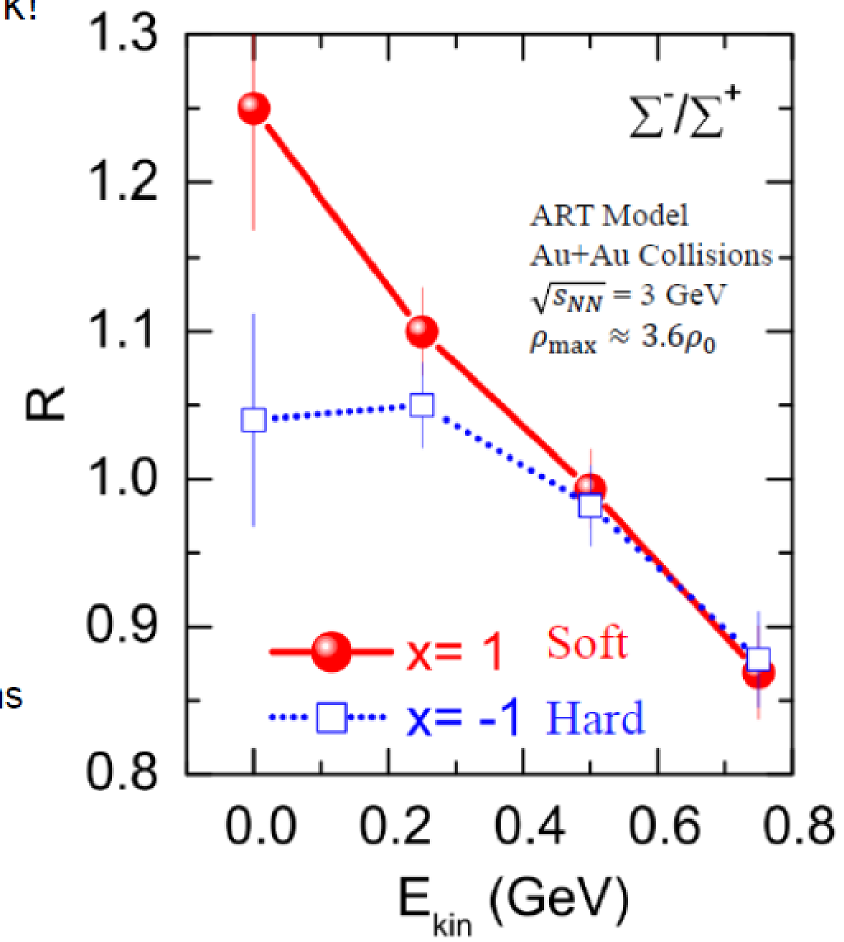

Femtoskopy

Femtoscopy

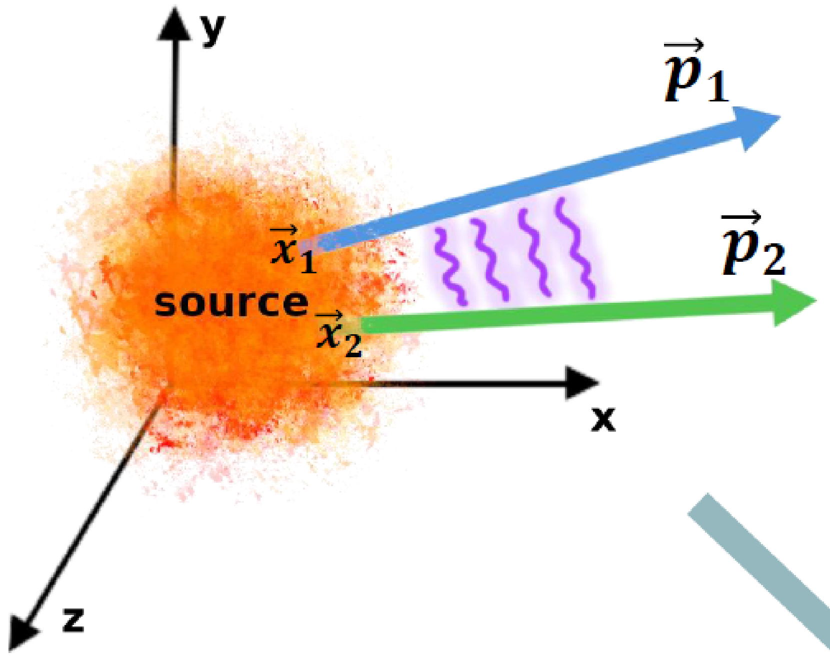

$q = |\vec{p}_1 - \vec{p}_2|$: momentum difference

$r = |\vec{x}_1 - \vec{x}_2|$: relative distance

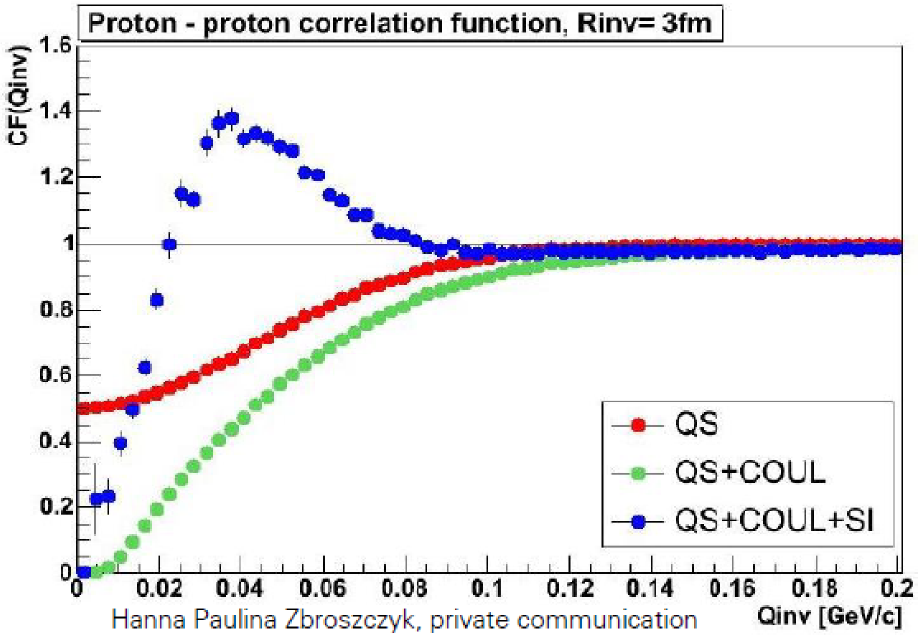

Effects and interactions:

- QS – quantum statistics (Bose-Einstein or Fermi-Dirac), identical particles
- Coul – Coulomb interactions, charged particles
- SI – strong interactions, hadrons

$CF < 1$: repulsion

$CF = 1$: no correlation

$CF > 1$: attraction

$$CF(r,q) = \int S(r)|\Psi(r,q)|^2 d^3r$$

Determine the geometry and dynamic properties (traditional femtoscopy)

Determine the interactions (non-traditional femtoscopy)

Proton-nuclei interactions

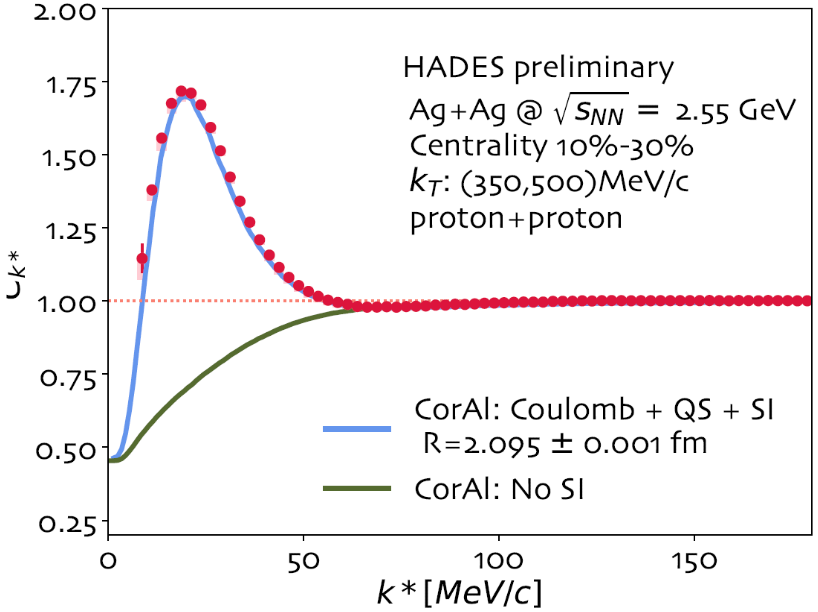

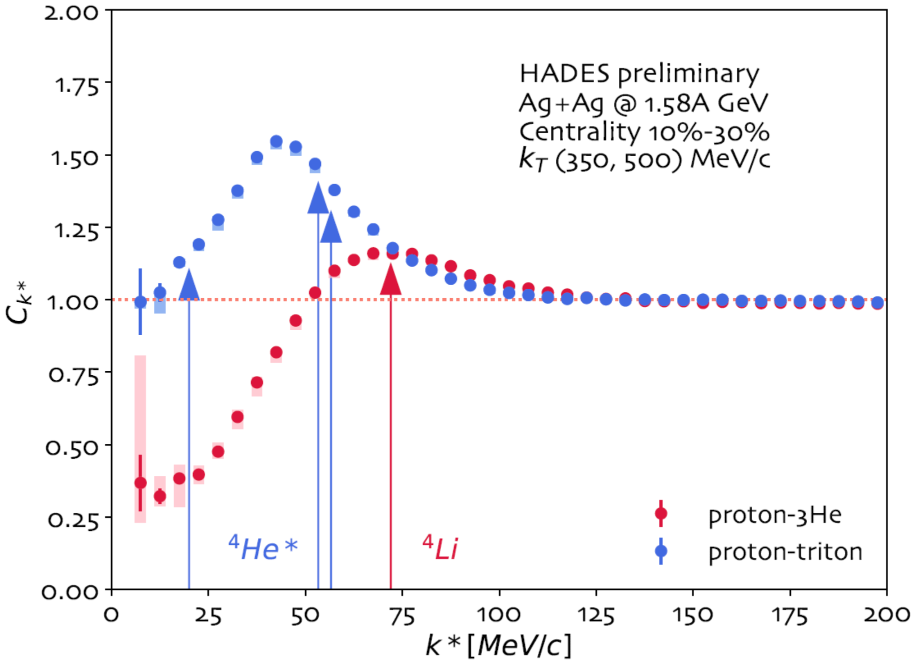

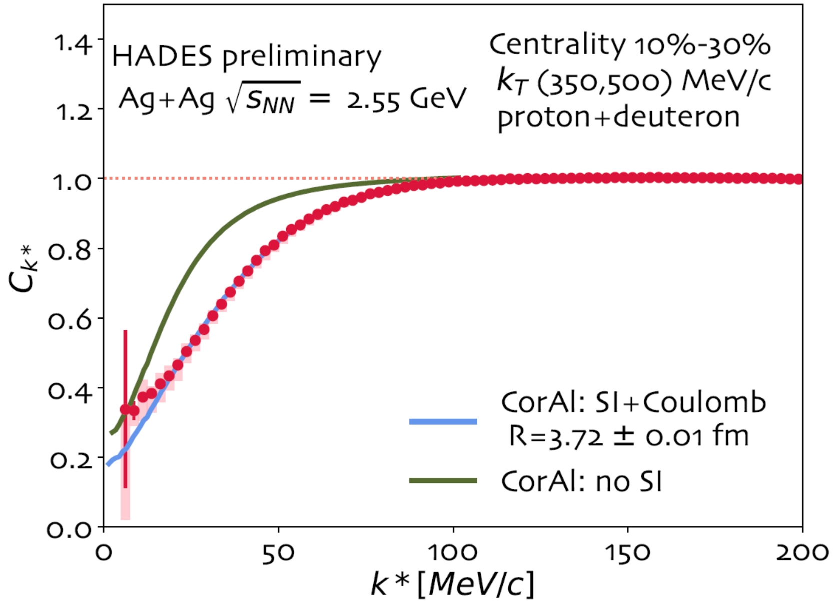

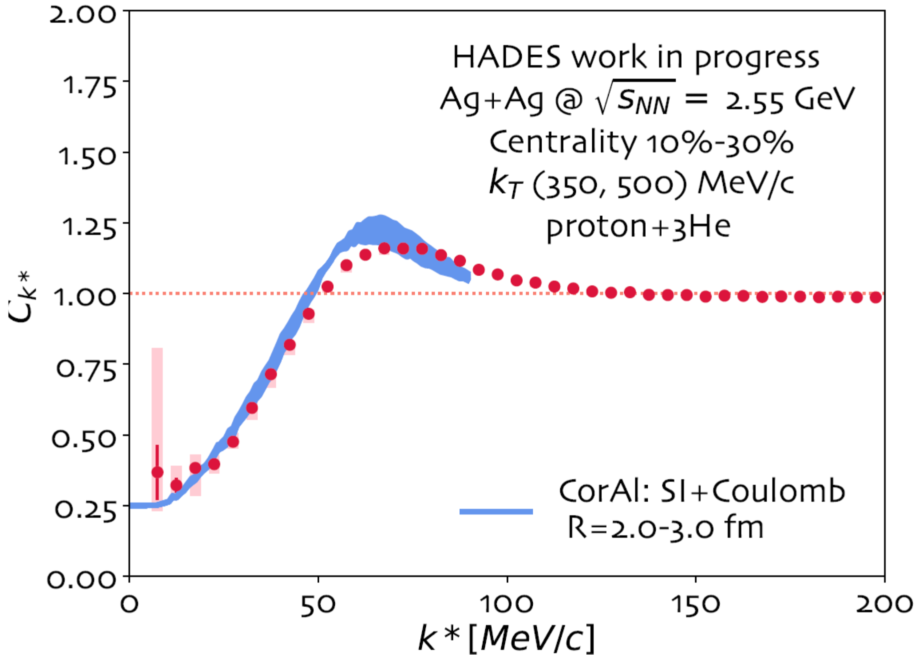

Proton-lambda correlation functions, Ag+Ag at 2.55 GeV

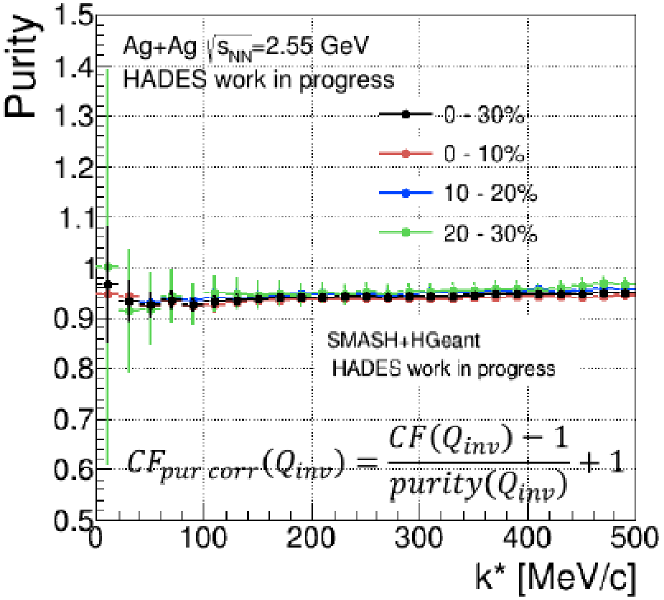

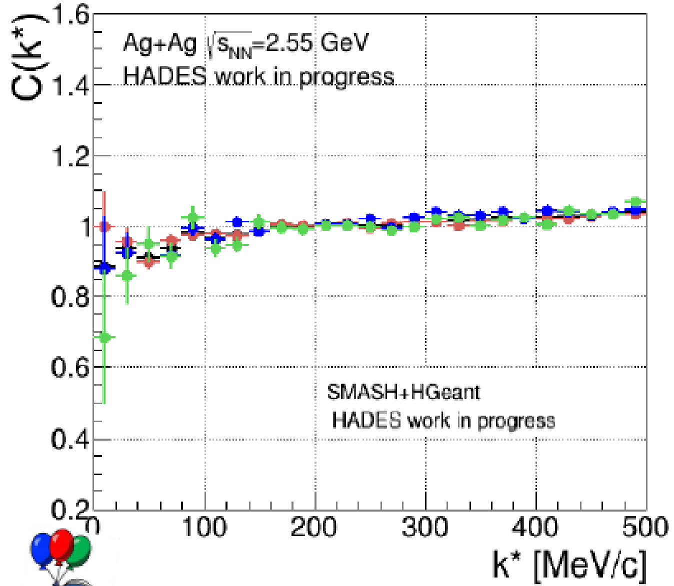

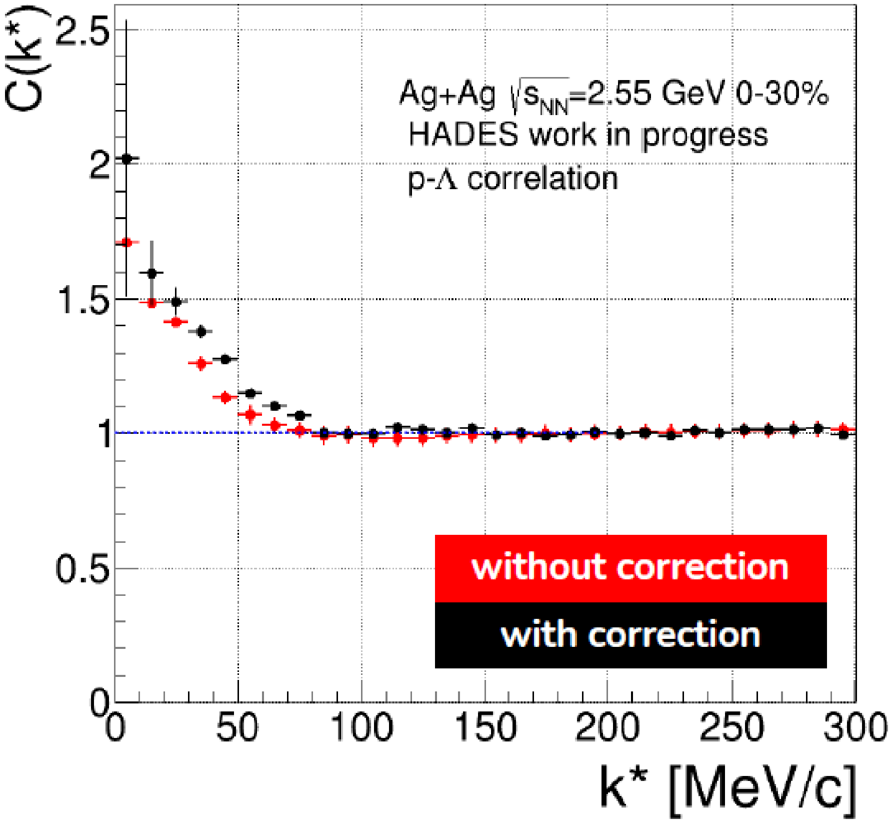

Quality correlation function achieved

$$k^* = \frac{|\vec{p}_1 - \vec{p}_2|}{2} \text{ in PRF}$$

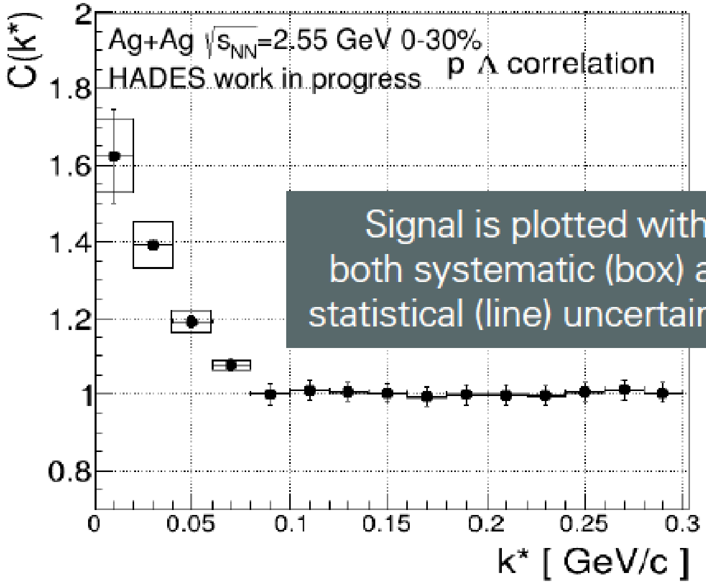

Signal is plotted with both systematic (box) and statistical (line) uncertainties

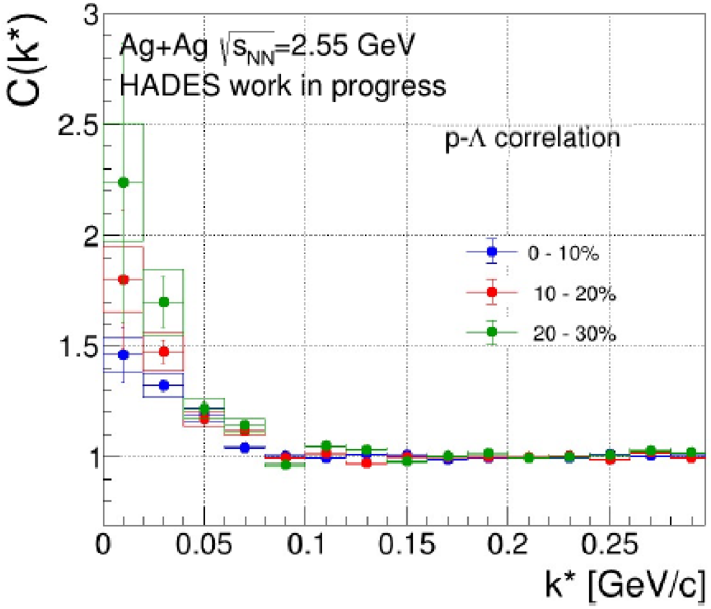

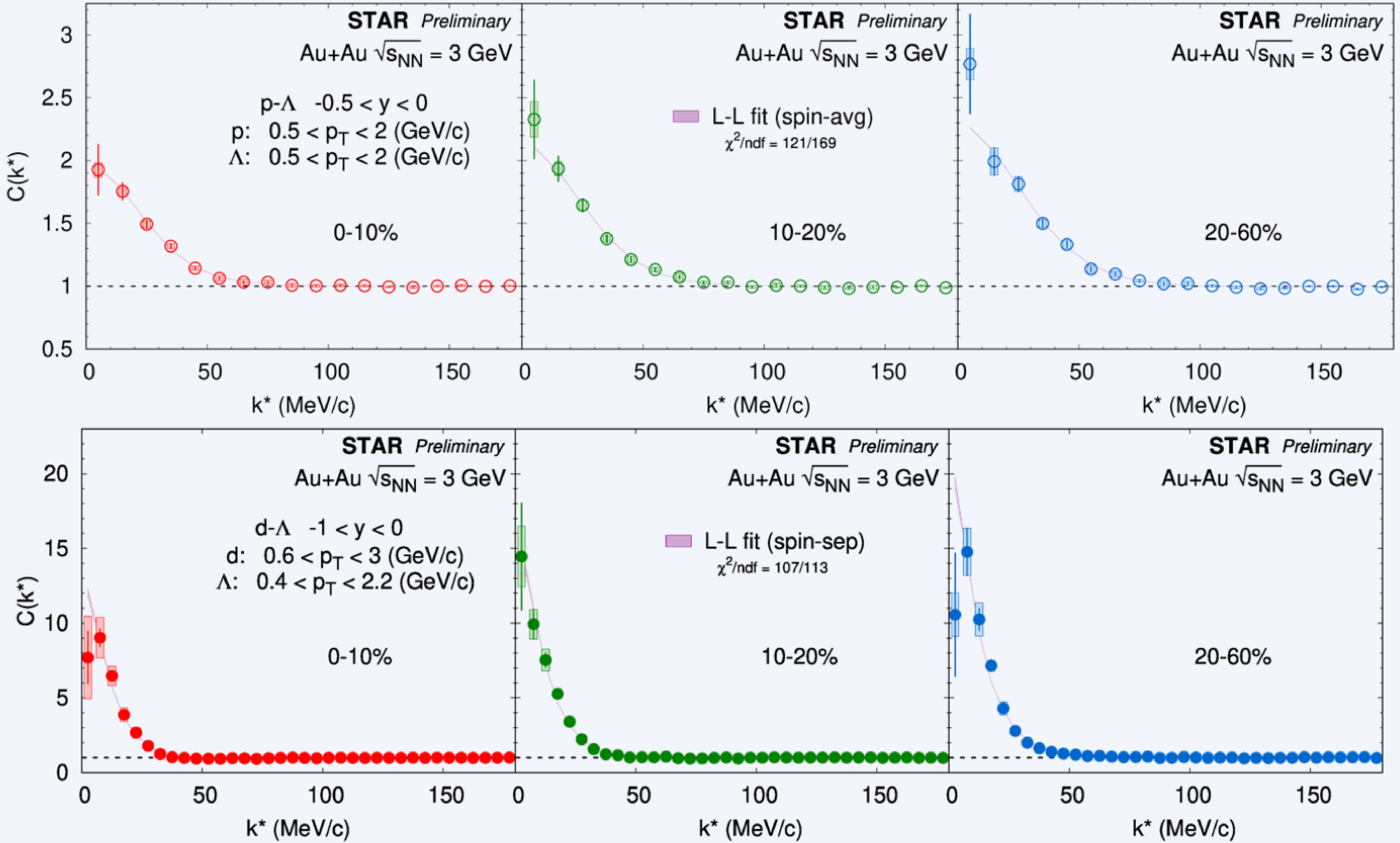

STAR Preliminary
Au+Au √sNN = 3 GeV
p-Λ -0.5 < y < 0
p: 0.5 < pT < 2 (GeV/c)
Λ: 0.5 < pT < 2 (GeV/c)
0-10%
10-20%
20-60%
L-L fit (spin-avg)
χ2/ndf = 121/169
C(k*)
k* (MeV/c)
d-Λ -1 < y < 0
d: 0.6 < pT < 3 (GeV/c)
Λ: 0.4 < pT < 2.2 (GeV/c)
L-L fit (spin-sep)
χ2/ndf = 107/113

Correlation Function & Spin States

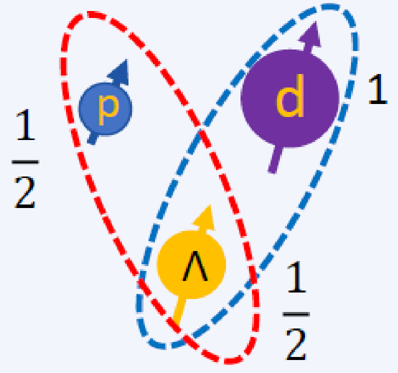

Singlet State	$^1S_0$	(S)
Triplet State	$^3S_1$	(T)

Doublet State	$^2S_{1/2}$	(D)
Quartet State	$^4S_{3/2}$	(Q)

p-Λ: $|\psi(r,k)|^2 \rightarrow \frac{1}{4}|\psi_0(r,k)|^2 + \frac{3}{4}|\psi_1(r,k)|^2$

d-Λ: $|\psi(r,k)|^2 \rightarrow \frac{1}{3}\left|\psi_{1/2}(r,k)\right|^2 + \frac{2}{3}\left|\psi_{3/2}(r,k)\right|^2$

- Different spin states with different f_0 and d_0 parameters
- **p-Λ correlation:** current statistics is not enough to separate two spin states → spin-averaged fit
- **d-Λ correlation:** very different f_0 for (D) and (Q) are predicted → **Spin-separated fit**

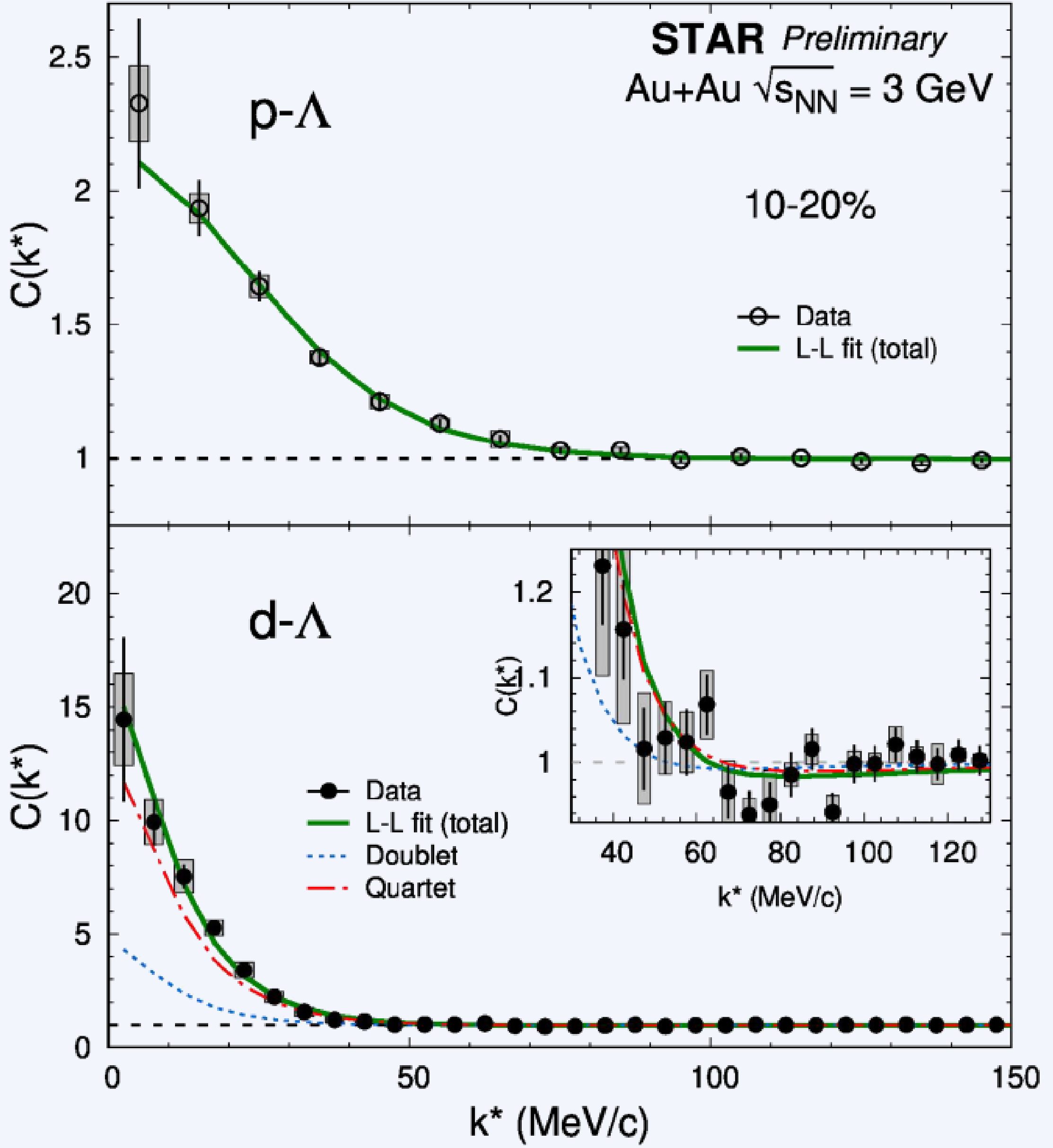

Scatterings Length (f_0) and Effective Range (d_0)

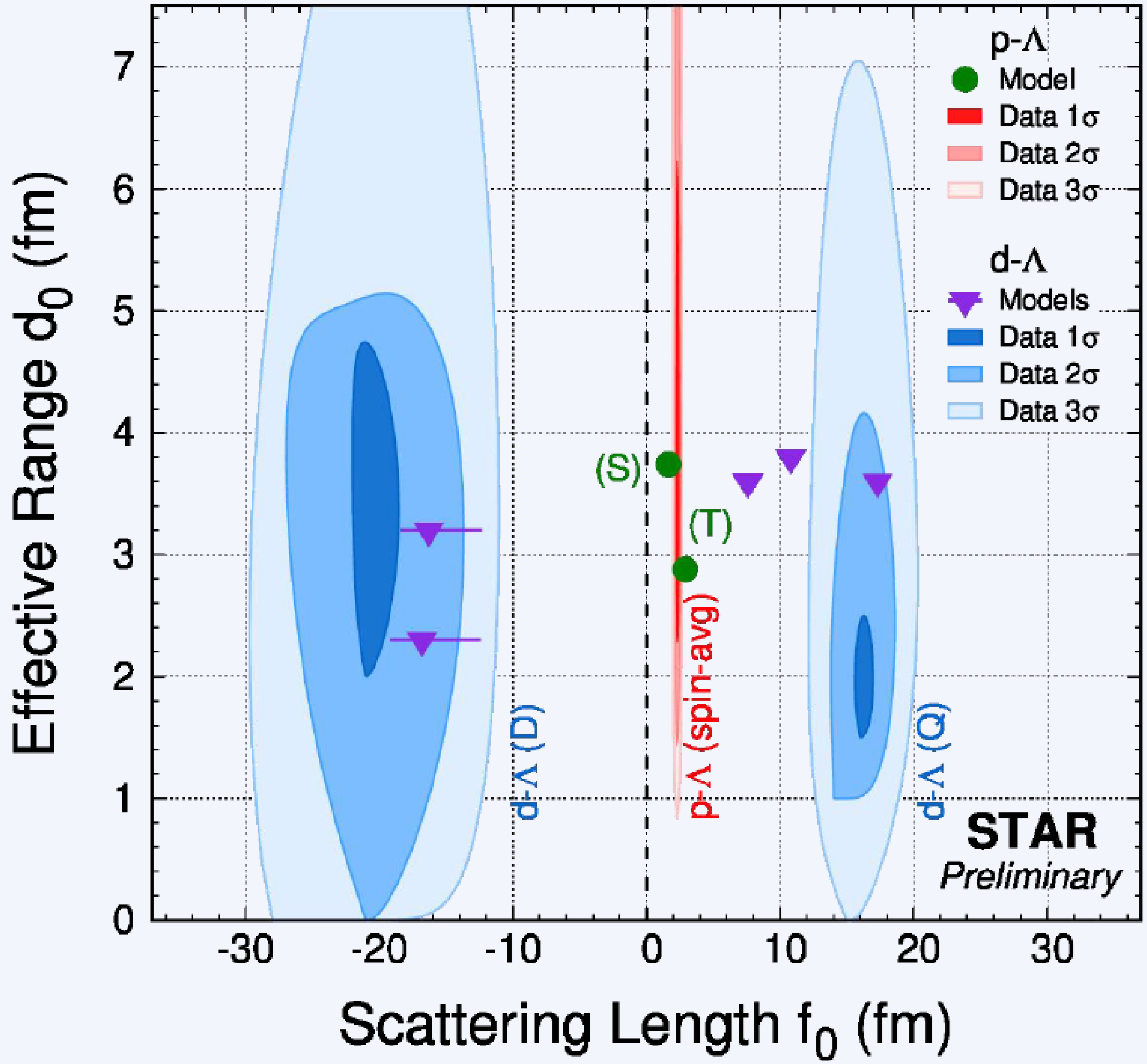

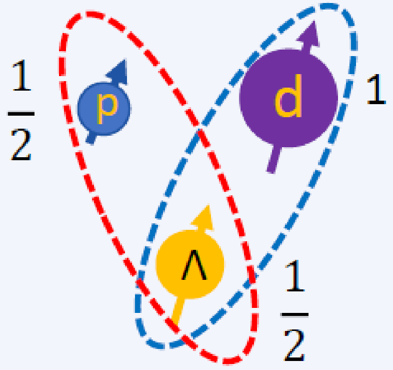

$$\frac{1}{f(k)} \approx \frac{1}{f_0} + \frac{d_0 k^2}{2} - ik$$

- The constraint of the effective range (d_0) is weaker

- The measurement is done at freeze-out
- Spin-avg for f_0 & d_0 p-Λ system

  $f_0 = 2.32^{+0.12}_{-0.11}$ fm $d_0 = 3.5^{+2.7}_{-1.3}$ fm
- Successfully separate two spin states in d-Λ

  $f_0(D) = -20^{+3}_{-3}$ fm $d_0(D) = 3^{+2}_{-1}$ fm

  $f_0(Q) = 16^{+2}_{-1}$ fm $d_0(Q) = 2^{+1}_{-1}$ fm

*Edge of d-Λ contours are shown with Bezier smooth to improve the visibility

H. W. Hammer, Nucl. Phys. A 705 (2002) 173
F. Wang, et al. Phys.Rev.Lett. 83 (1999) 3138
M. Schäfer, et al. Phys.Lett.B 808 (2020) 135614
A. Cobis, et al. J. Phys. G 23 (1997) 401
G. Alexander, et al. Phys. Rev. 173 (1968) 1452
J. Haidenbauer, Phys.Rev.C 102 (2020) 3, 034001
J. Haidenbauer, et al. Nucl. Phys. A 915 (2013) 24

Polarization

Λ Global Polarization

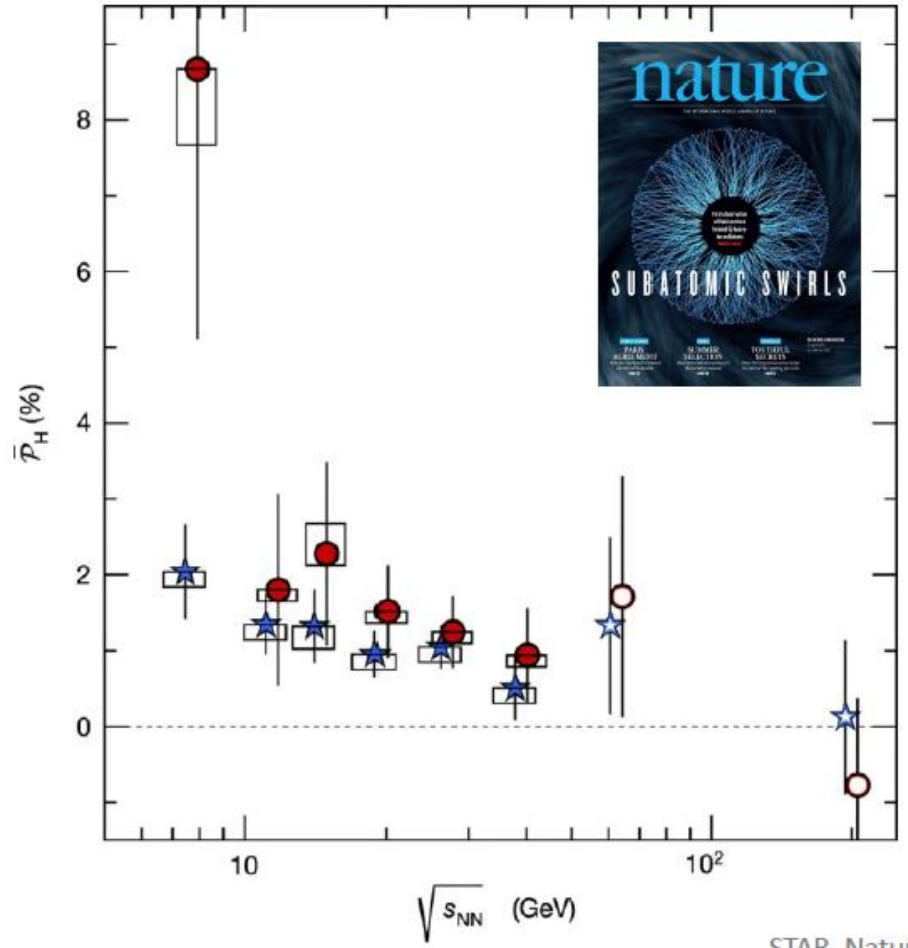

STAR, Nature 548 62 (2017)

$$S^{\mu}_{\varpi}(p) = -\frac{1}{8m}\epsilon^{\mu\rho\sigma\tau}p_{\tau}\frac{\int_{\Sigma} d\Sigma \cdot p n_F(1-n_F)\varpi_{\rho\sigma}}{\int_{\Sigma} d\Sigma \cdot p n_F}$$

$$\varpi_{\mu\nu} = -\frac{1}{2}(\partial_{\mu}\beta_{\nu} - \partial_{\nu}\beta_{\mu})$$

$$s = \frac{1}{2}P \approx \frac{1}{4}\frac{\omega}{T}$$

$$P_{\Lambda} \approx \frac{1}{2}\frac{\omega}{T} + \frac{\mu_{\Lambda}B}{T} \quad P_{\bar{\Lambda}} \approx \frac{1}{2}\frac{\omega}{T} - \frac{\mu_{\Lambda}B}{T}$$

$$\omega = (P_{\Lambda} + P_{\bar{\Lambda}})k_B T/\hbar \sim 10^{22}s^{-1}$$

Most vortical fluid

Hyperon polarization in heavy ion collisions

Acta Phys. Sin. Vol. 72, No. 7(2023) 072401

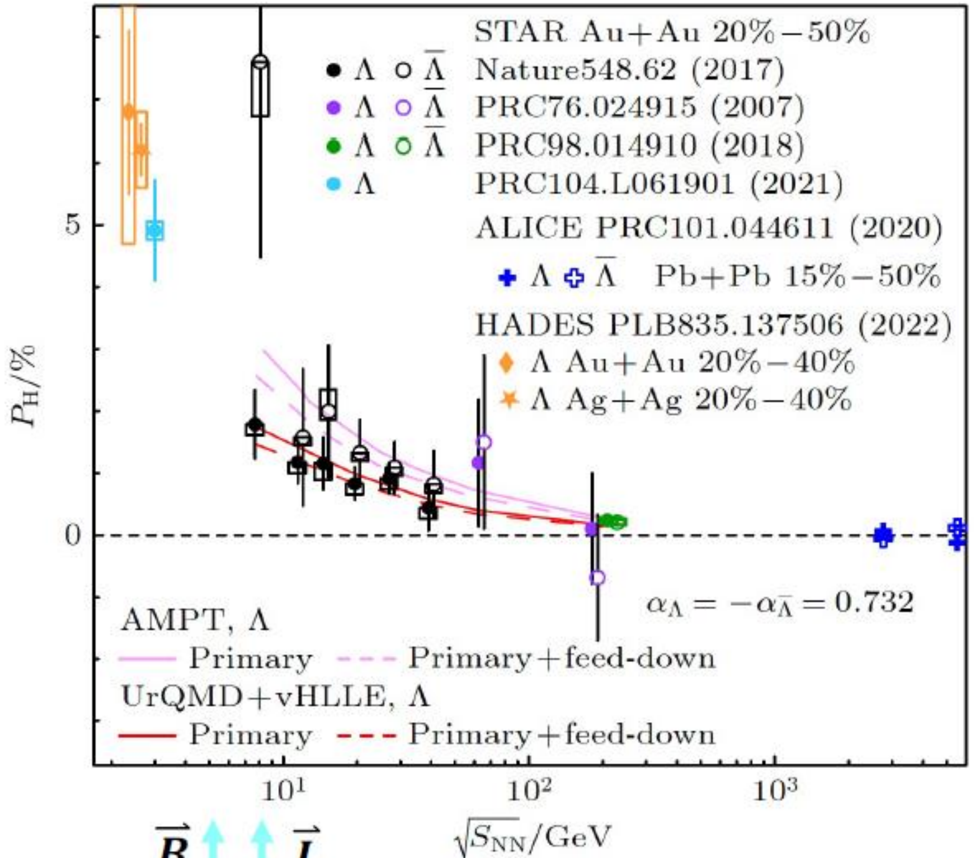

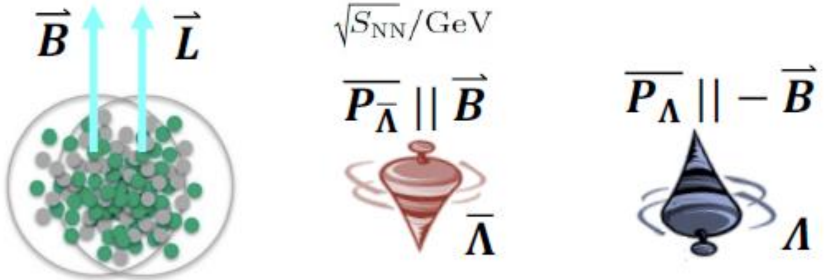

S. Alzhrani et al., PRC 106.014905

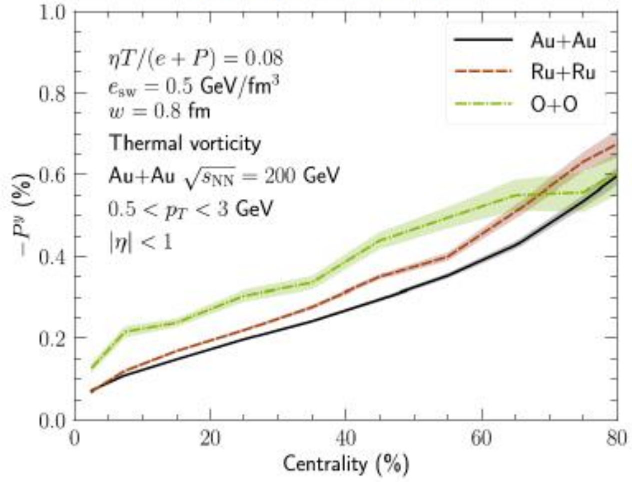

S.Z, Shi, K.L. Li, J.F. Liao, PLB 788 (2019) 409–413

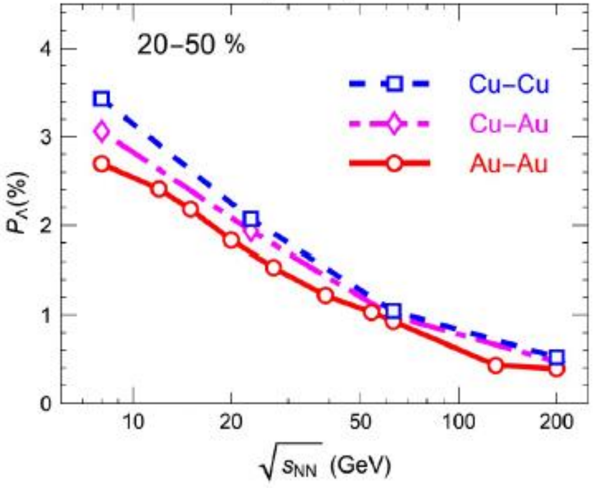

- Λ / $\bar{\Lambda}$ global polarization splitting with BES-II data?
- **Global polarization collision system size dependence**

$${}^{197}_{79}Au > {}^{96}_{44}Ru, {}^{96}_{40}Zr > {}^{63}_{29}Cu > {}^{16}_{8}O$$

? → $P_\Lambda^{Au} < P_\Lambda^{Ru} \approx P_\Lambda^{Zr} < P_\Lambda^{Cu} < P_\Lambda^{O}$

- Local polarization in isobar collisions

Global polarization in Au+Au with BES-II data (19.6, 27 GeV)

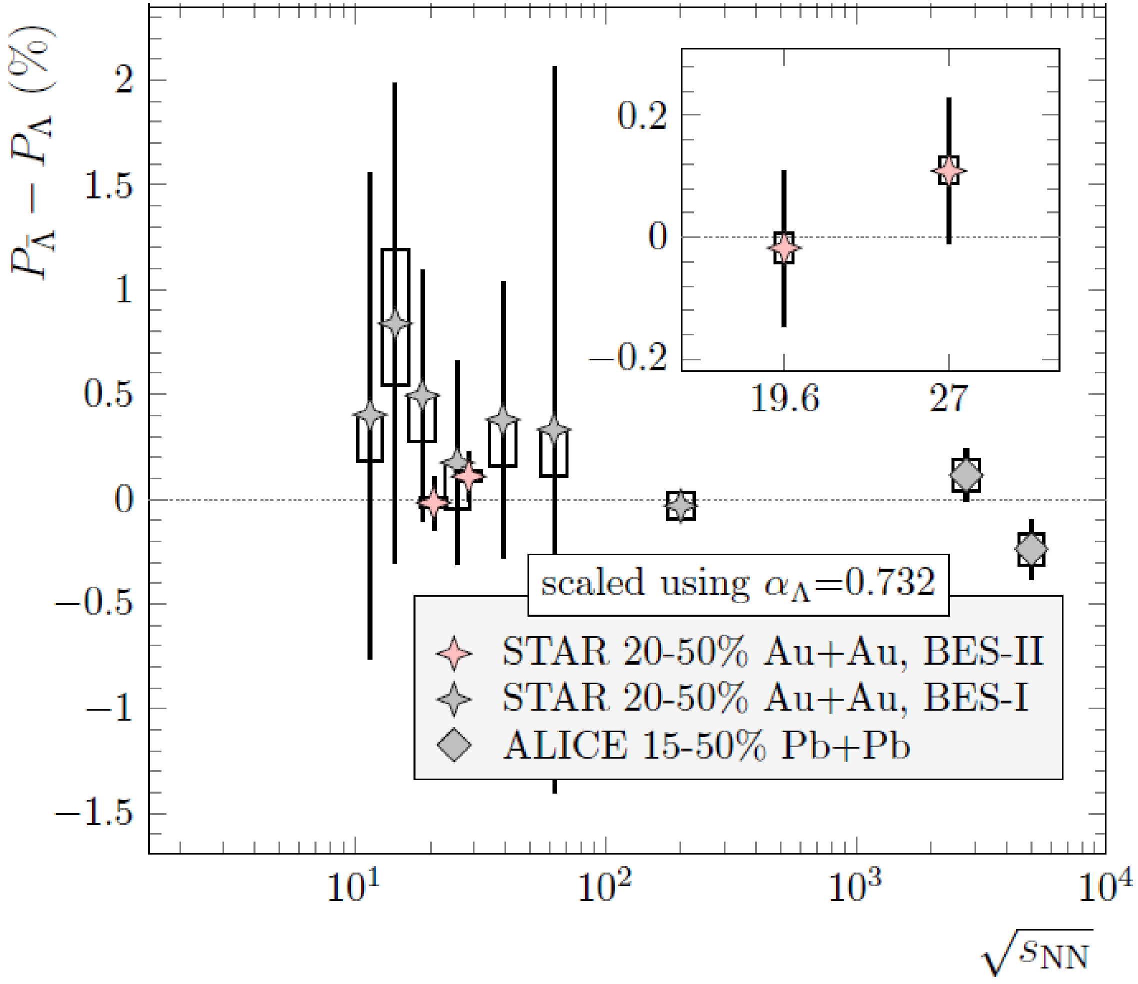

- No splitting of Λ / $\bar{\Lambda}$ observed

Au+Au	19.6 GeV	27 GeV
$P_{\bar{\Lambda}} - P_{\Lambda}$ (%)	-0.018 $\pm 0.127(stat.)$ $\pm 0.024(sys.)$	0.109 $\pm 0.118(stat.)$ $\pm 0.022(sys.)$

- $|B| \approx \frac{T_s|P_{\bar{\Lambda}} - P_{\Lambda}|}{2|\mu_\Lambda|}$, using hydrodynamics

  T_s =150 MeV : the temperature of the emitting source
  $\mu_\Lambda = -1.93\times10^{-14}$ MeV/T : the magnetic moment of the Λ hyperon

- Upper limit on late stage magnetic field
  - 95% confidence level
  - $B < 9.4\times10^{12}\ T$ at 19.6 GeV
  - $B < 1.4\times10^{13}\ T$ at 27 GeV

STAR, PRC 108, 014910 (2023)

Centrality dependence of local polarization

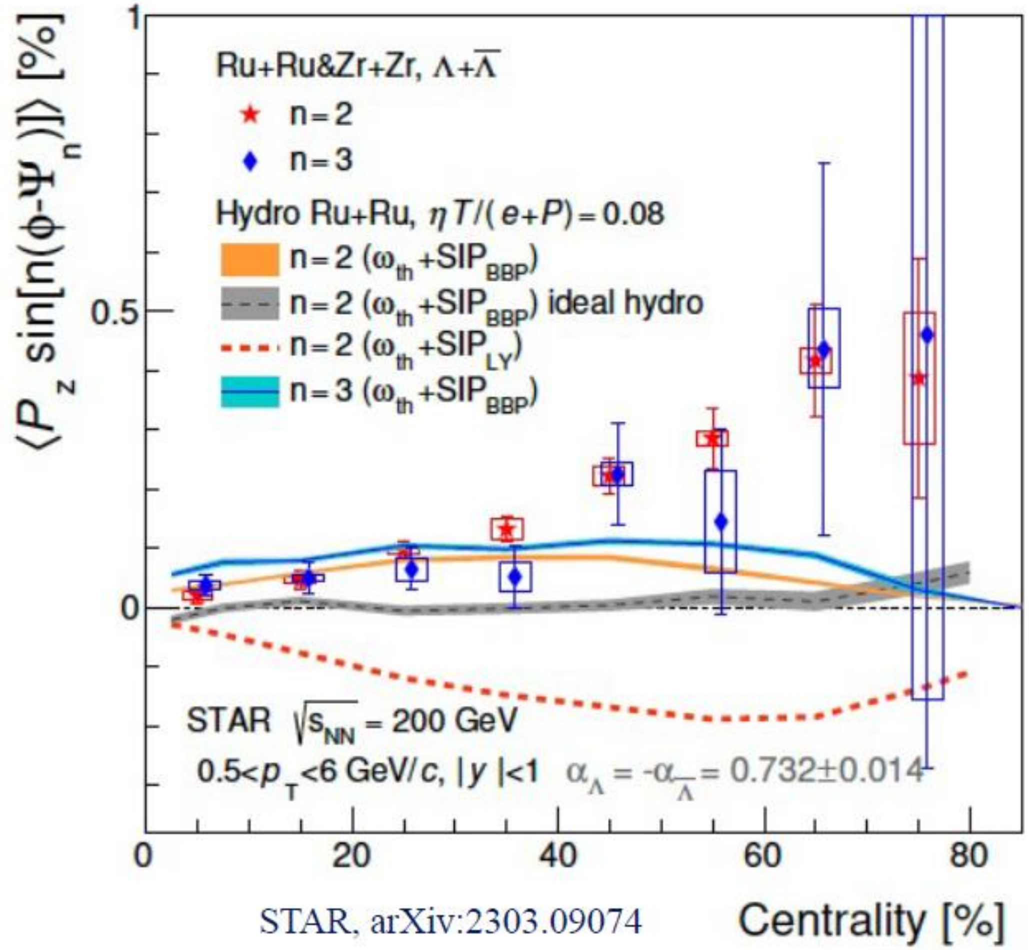

STAR, arXiv:2303.09074

- Local polarization w.r.t second-order event plane increases with centrality
- Significant local polarization w.r.t third-order event plane
- Comparable local polarization w.r.t second and third order event plane
- Hydrodynamic models with shear term reasonably describe the data for central collisions, but not for peripheral

S. Alzhrani et al., PRC 106.014905

The Sign Puzzle

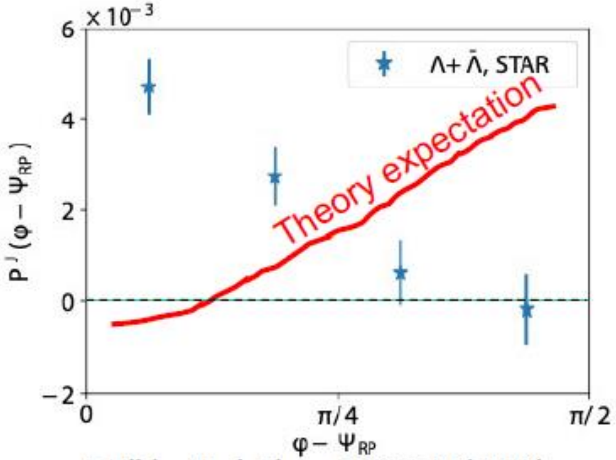

T. Niida, Nucl. Phys. A 982 511 (2019)

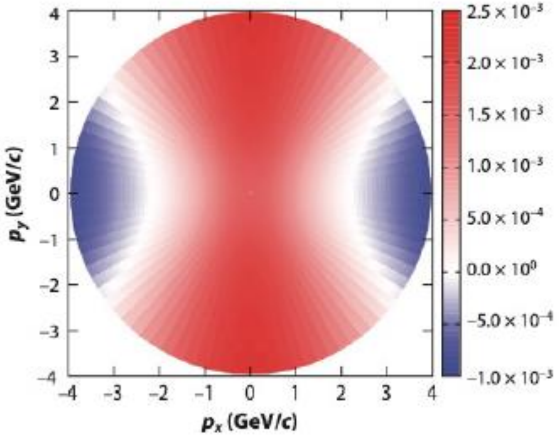

F. Becattini, L. Csernai and D. J. Wang, PRC 88 034905 (2013)
F. Becattini, et al. Eur. Phys. J. C 75 406 (2015)
W.T. Deng and X.G. Huang, PRC 93 064907 (2016)
Y.L.Xie et al., PRC 94 054907 (2016)
I.Karpenkon and F. Becattini, Eur.Phys.J. C 77 213 (2017)
Y.Xie, D.Wang and L.P.Csernai, PRC 95 031901 (2017)
H.Li et al., NPA 967 772 (2017)
B.Fu, K.Xu, X.G.Huang and H.Song, PRC 103 024903 (2021)

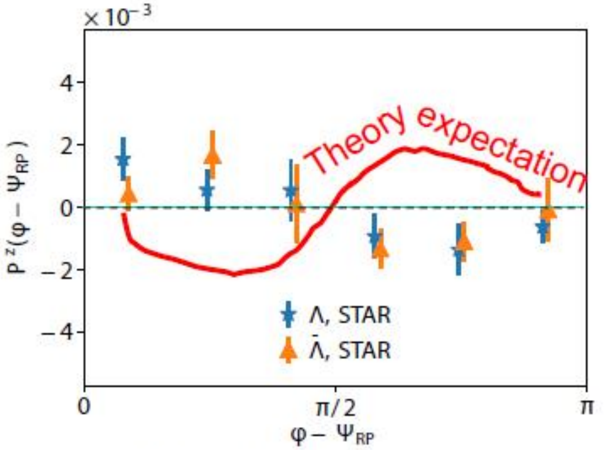

STAR, PRL 123 132301 (2019)

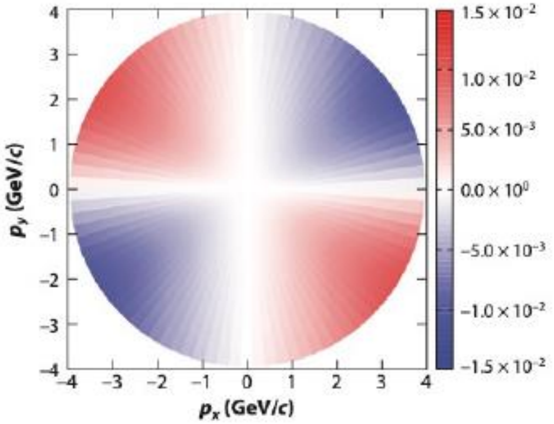

F. Becattini, et al. Eur. Phys. J. C 75 406 (2015)
F. Becattini and Iu. Karpenko, PRL 120 012302 (2018)
X.L. Xia et al. PRC 98 024905 (2018)
D.X. Wei, W.T. Deng and X.G. Huang, PRC 99 014905 (2019)
Y. Sun and K.M. Ko, PRC 99 011903 (2019), [Explains the sign but non magnitude.]
Y.F. Liu, Y.Sun and C.M. Ko PRL 125 062301 (2020). [explains the sign, sort of].
B.Fu, K.Xu, X.G.Huang and H.Song, PRC 103 024903 (2021)

The Sign Puzzle

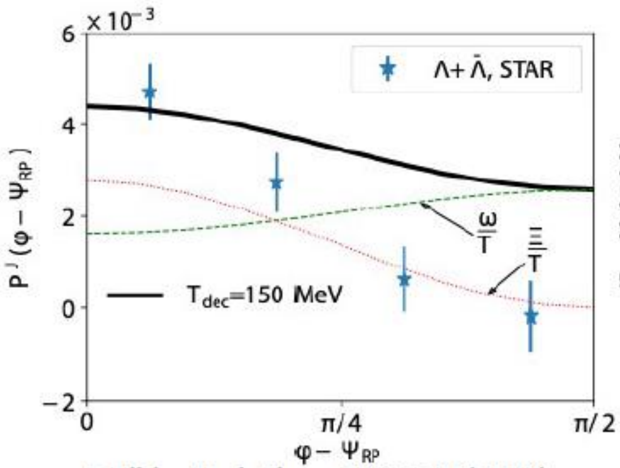

T. Niida, Nucl. Phys. A 982 511 (2019)
F. Becattini et al., PRL 127 272302 (2021)

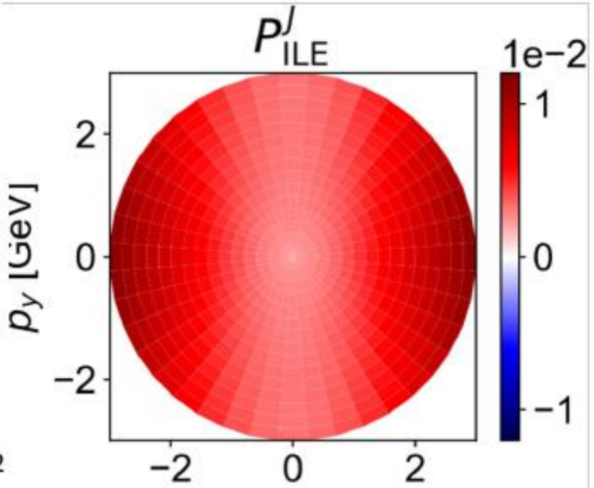

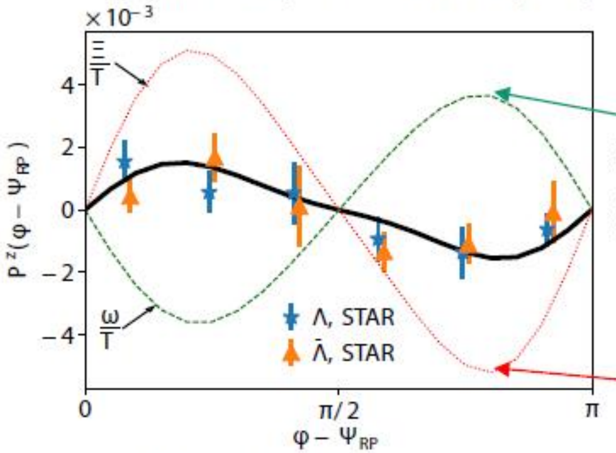

STAR, PRL 123 132301 (2019)
F. Becattini et al., PRL 127 272302 (2021)

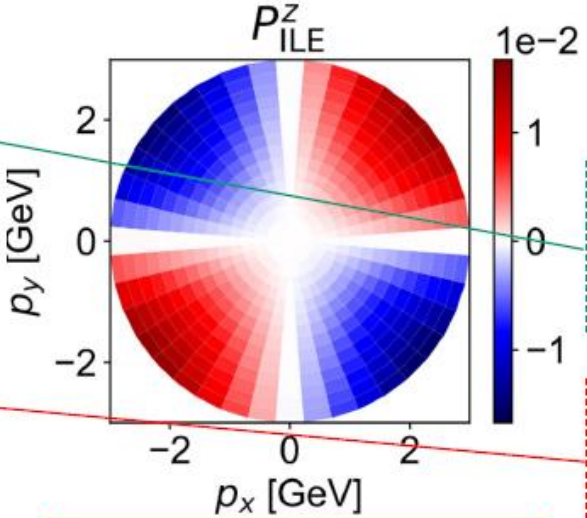

Thermal shear vorticity can give right signs.

Models with thermal shear :
F.Becattini, M.Buzzzegoli and A. Palermo, PLB 820 136519 (2021)
S.Liu and Y. Yin, JHEP 07 188 (2021)
B. Fu et al., PRL 127 142301 (2021)
F. Becattini et al., PRL 127 272302 (2021)
C.Yi, S.Pu and D.L. Yang, PRC 104 064901 (2021)
W. Florkowski et al., PRC 105 064901 (2022)

Other phenomenology models :
H.Z. Wu, L.G. Pang, X.G. Huang and Q. Wang, Phys.Rev.Research 1 033058 (2019)
Y.Xie, D.Wang and L.P. Csernai, EPJ C 80 39 (2020)
Y.F. Liu, Y. Sun and C.M. Ko, PRL 125 062301 (2020)
H.Z. Wu, L.G. Pang, X.G Huang and Q. Wang, NPA 1005 121831 (2021)

$$S^\mu_\varpi(p) = -\frac{1}{8m}\epsilon^{\mu\rho\sigma\tau}p_\tau \frac{\int_\Sigma d\Sigma\cdot p n_F(1-n_F)\varpi_{\rho\sigma}}{\int_\Sigma d\Sigma\cdot p n_F}$$

$$\varpi_{\mu\nu} = -\frac{1}{2}(\partial_\mu\beta_\nu - \partial_\nu\beta_\mu)$$

Thermal vorticity

$$S^\mu_\xi(p) = -\frac{1}{4m}\epsilon^{\mu\rho\sigma\tau}\frac{p_\tau p^\lambda}{\varepsilon}\frac{\int_\Sigma d\Sigma\cdot p n_F(1-n_F)\hat{t}_\rho\xi_{\sigma\lambda}}{\int_\Sigma d\Sigma\cdot p n_F}$$

$$\xi_{\mu\nu} = \frac{1}{2}(\partial_\mu\beta_\nu + \partial_\nu\beta_\mu)$$

Thermal shear

Shear induced polarization

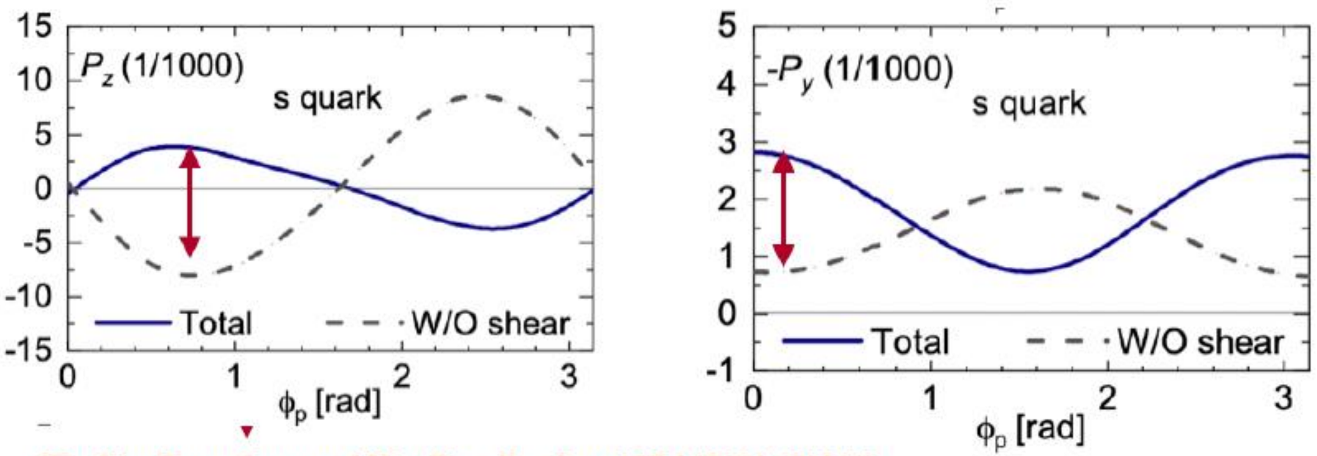

[Fu, Liu,,Pang, Song and Yin, Phys.Rev.Lett.127.142301 (2021)]

- ✓ Thermal vorticity
- ✓ Shear induced vorticity
- ✓ s quark scenario

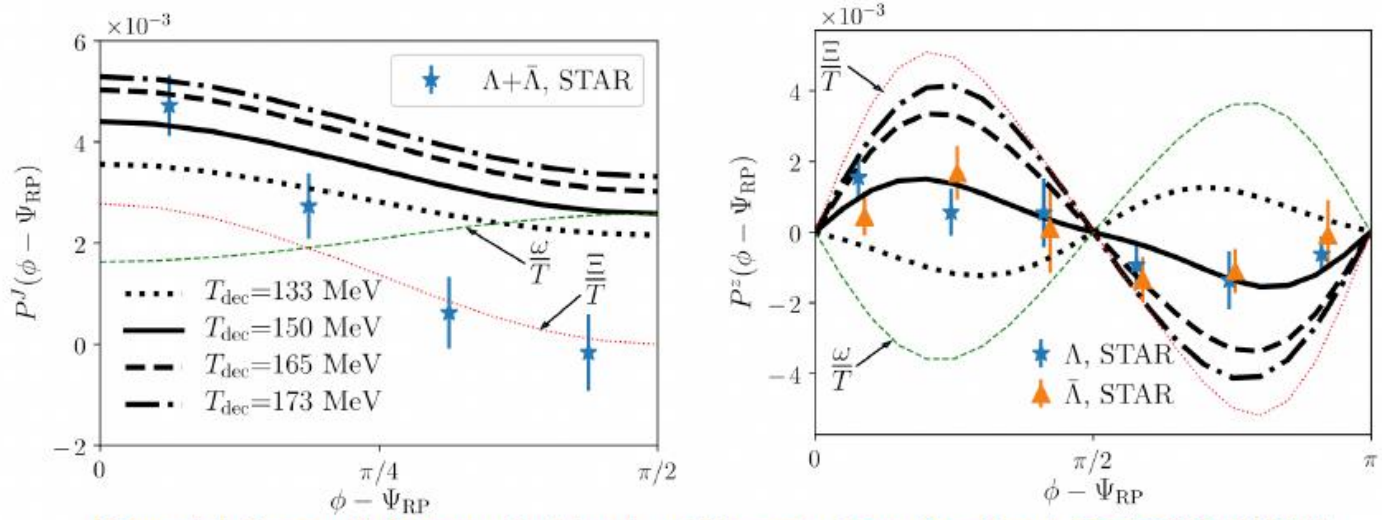

[Becattini, Buzzegoli, Palermo, Inghirami and Karpenko, Phys. Rev. Lett.1 27. 272302 (2021)]

- ✓ Kinetic vorticity
- ✓ Shear induced vorticity
- ✓ Isothermal equilibrium

Theoretical uncertainty:
SHE?
Initial condition?
Transport properties?

Global Spin Alignment

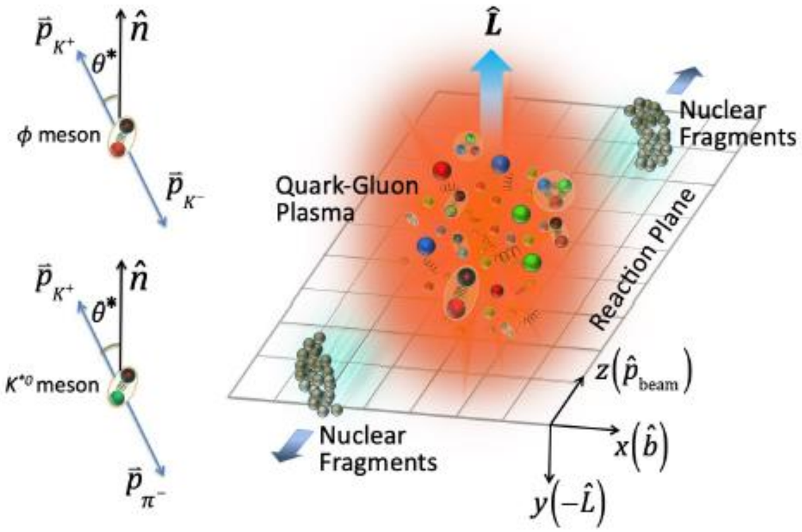

The spin state of a vector meson can be described by a 3x3 spin density matrix.

The diagonal element ρ_{00} corresponds to the probability of finding a vector meson in spin state 0 out of 3 possible spin states of -1, 0 and 1.

$$\frac{dN}{d(\cos\theta^*)} = N_0 \times \left[(1-\rho_{00}) + (3\rho_{00}-1)\cos^2\theta^* \right]$$

A deviation of ρ_{00} from 1/3 would indicate a non-zero spin alignment.

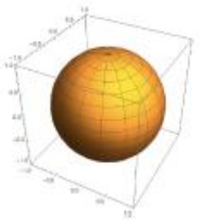

$\rho_{00} = \frac{1}{3}$

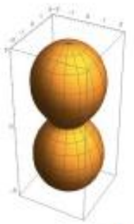

$\rho_{00} > \frac{1}{3}$

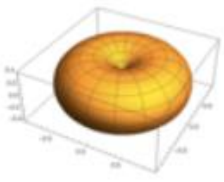

$\rho_{00} < \frac{1}{3}$

From quark combination :

$$\rho_{00}^{V} = \frac{1-\langle P_q P_{\bar{q}} \rangle}{3+\langle P_q P_{\bar{q}} \rangle} \approx \frac{1}{3} - \frac{4}{9}\langle P_q P_{\bar{q}} \rangle$$

The large ρ_{00} puzzle

$$\rho_{00} \approx \frac{1}{3} + C_\Lambda + C_\varepsilon + C_E + C_F + C_L + C_A + C_\varphi + C_g$$

Physics Mechanisms	(ρ_{00})
c_Λ: Quark coalescence vorticity & magnetic field[1]	< 1/3 (Negative ~ 10^{-5})
c_ε: E-comp. of Vorticity tensor[1]	< 1/3 (Negative ~ 10^{-4})
c_E: Electric field[2]	> 1/3 (Positive ~ 10^{-5})
c_F: Fragmentation[3]	> or, < 1/3 (~ 10^{-5})
c_L: Local spin alignments[4]	< 1/3
c_A: Turbulent color field[5]	< 1/3
c_φ: Vector meson strong force field[6]	> 1/3 (Can accommodate large positive signal)
c_g: Glasma fields + effective potential	could be significant

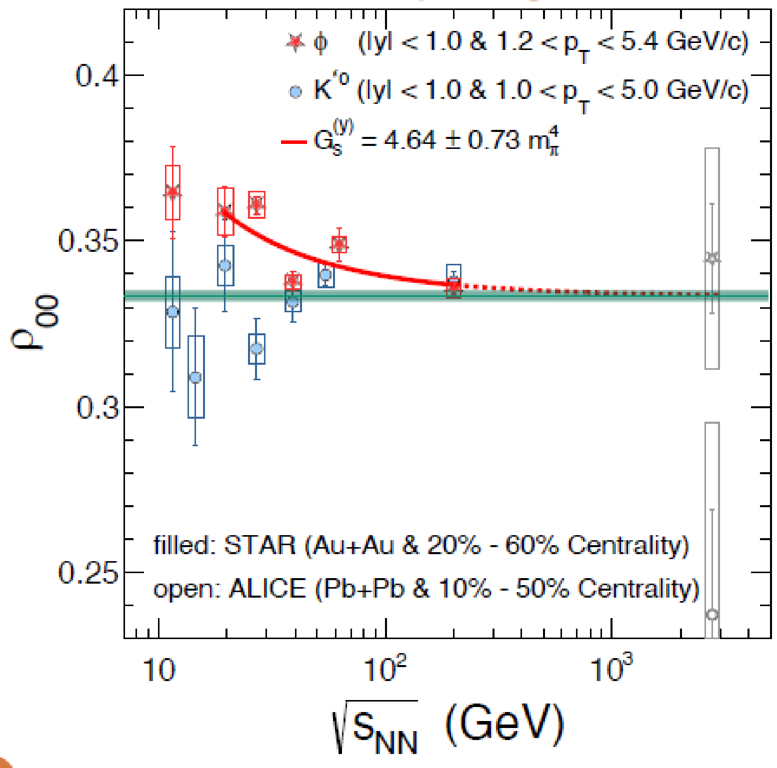

STAR, Nature 614 244 (2023)

strong force

ϕ exhibits surprisingly large global spin alignment while K* displays little.

Sign Change in $\Delta(dv_1/dy)$

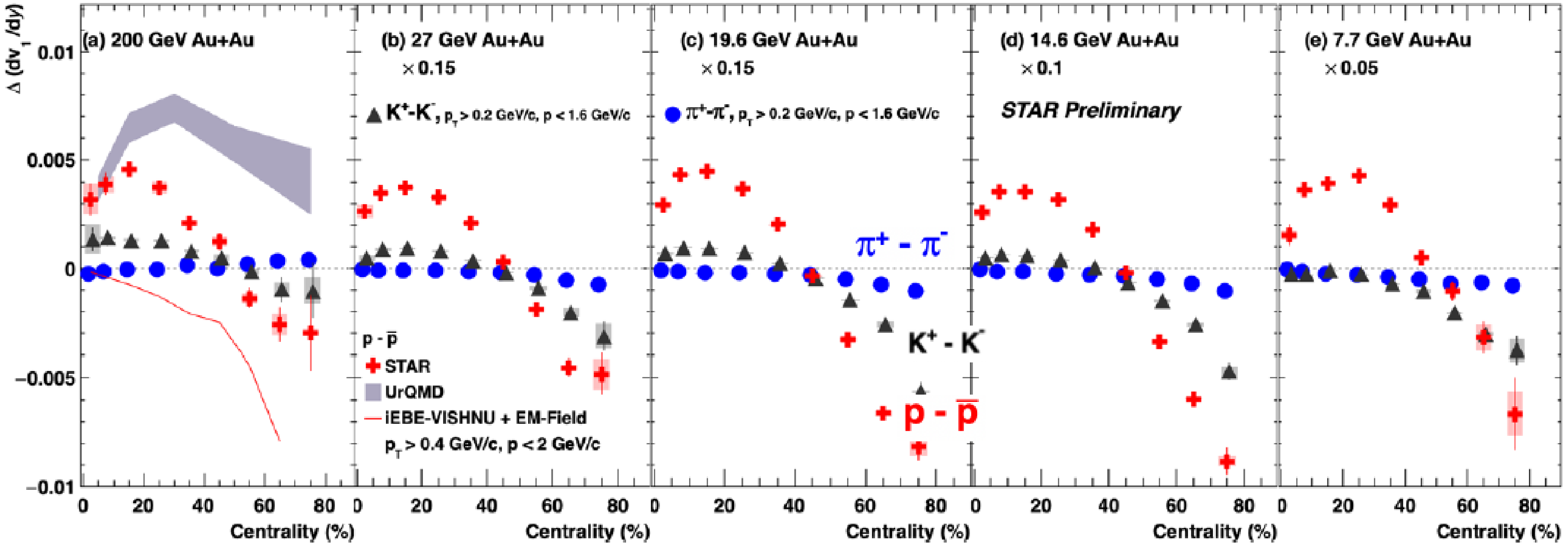

STAR, arXiv:2304.03430 (2023)
Aditya P. Dash for STAR, QM 2023
#347 WED 17:10

Feature consistent with EM field effects.
Can we utilize the information to quantify EM field ?

Chiral Magnetic Effect : Where Are We ?

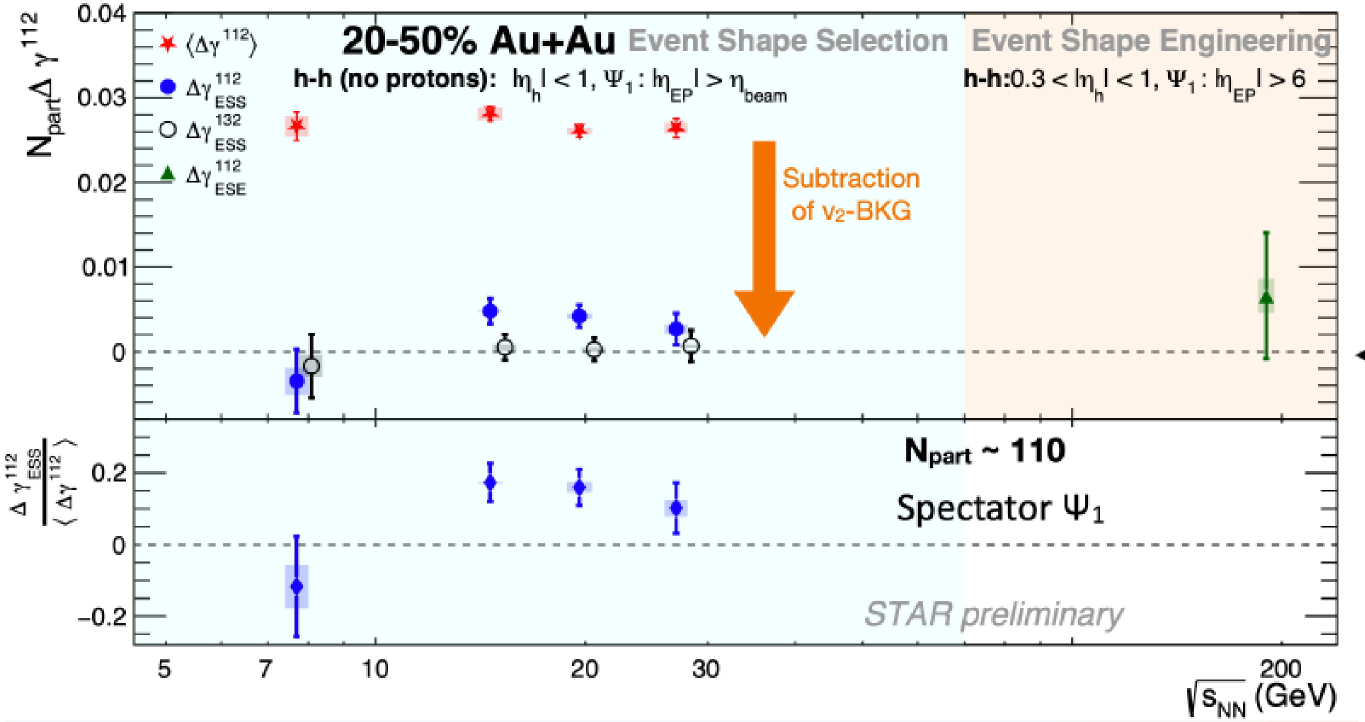

Zero CME line

Z. Xu for STAR, QM 2023
#868 TUES 10:10

Hint of excess beyond background.

Chiral Vortical Effect

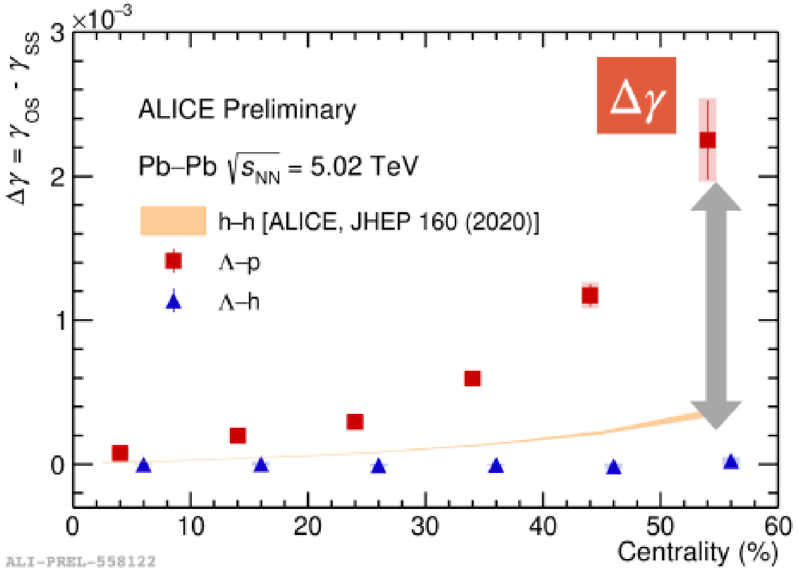

C. Wang for ALICE, QM 2023
#456 TUES 8:50

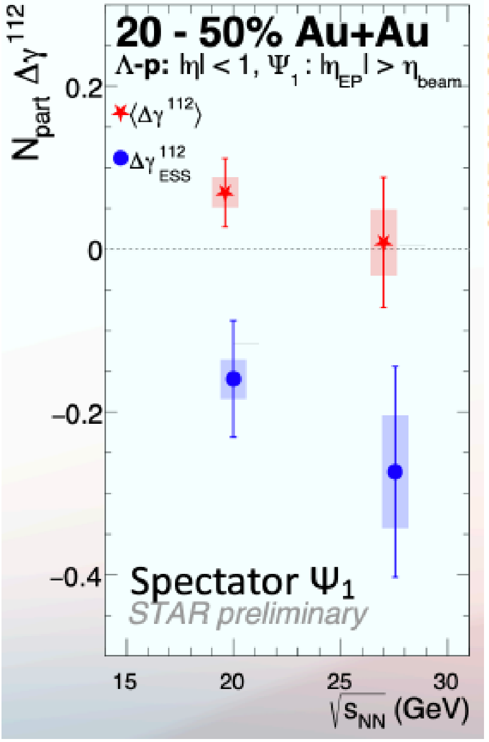

Z. Xu for STAR, QM 2023
#868 TUES 10:10

B

ω

Chiral Magnetic Effect	vs	**Chiral Vortical Effect**
Chirality Imbalance (μ_A)	--	Chirality Imbalance (μ_A)
Magnetic Field ($\omega\mu_e$)	--	Fluid Vorticity ($\omega\mu_B$)
Electric Charge (j_e)	--	Baryon Number (j_B)

Electric Charge Separation

Baryonic Charge Separation

Expectation :
CVE@LHC < CVE@RHIC

Measurement before background subtraction are comparable.

Flow

Elliptic and triangular flow of light nuclei

Tues 1120
R. Sharma
ID 631

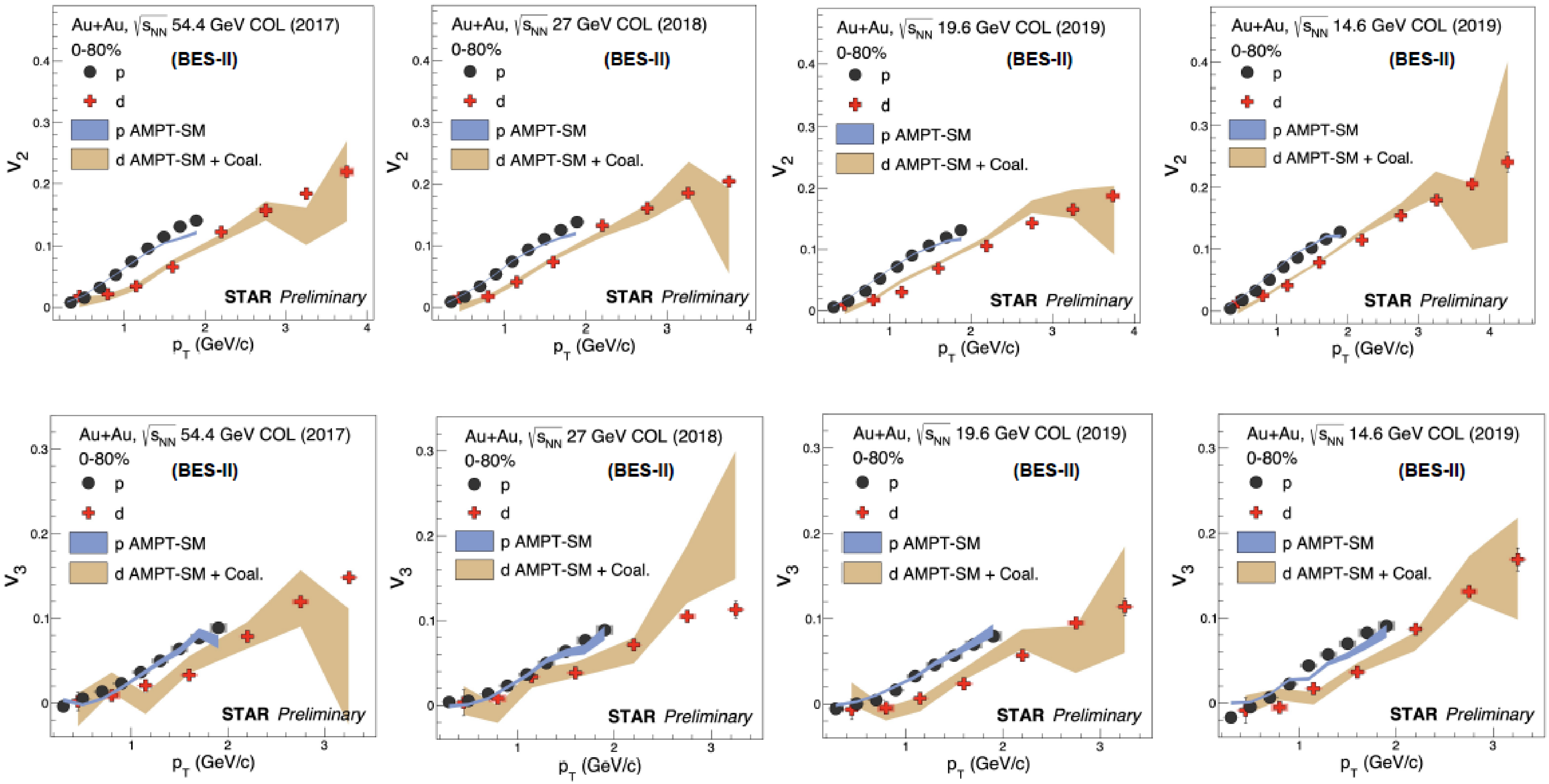

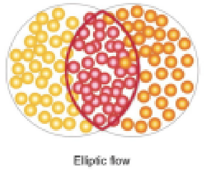

PRC 72, 064901 (2005) Nucl. Phys. A 729 (2003) 809–834
Proton v2: Phys. Rev. C 93, 014907 (2016); Phys. Rev. C 88, 014902 (2013); Phys. Lett. B 827, 137003 (2022)

- Light nuclei production → **thermal** model or **coalescence**
- AMPT+Coal. describes deuteron v_2 and v_3
- $V_2(p_T)$ - Deviation of ~20-30% from mass number scaling
- $v_3(p_T)$ - mass number scaling within ~10%

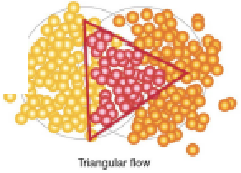

PRC 72, 064901 (2005)
Nucl. Phys. A 729 (2003) 809–834

Flow in small systems

He+Au(2014) d+Au(2016) p+Au(2015)

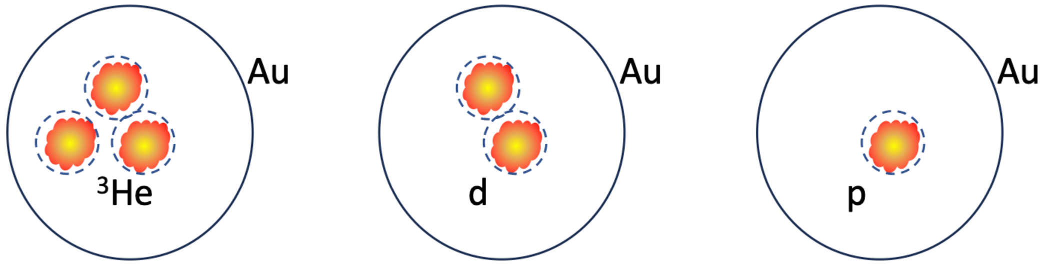

	Nucleon Glauber $\varepsilon_2(\varepsilon_3)$	Sub-Nucleon Glauber $\varepsilon_2(\varepsilon_3)$
0-5% pAu	0.23(0.16)	0.38(0.30)
0-5% dAu	0.54(0.18)	0.51(0.31)
0-5% ^{3}He+Au	0.50(0.28)	0.52(0.35)

Nucleon Glauber: J. L. Nagle, et. al., PRL 113 (2014) 112301
Sub-nucleon: K. Welsh, et. al., PRC 94 (2016) 024919

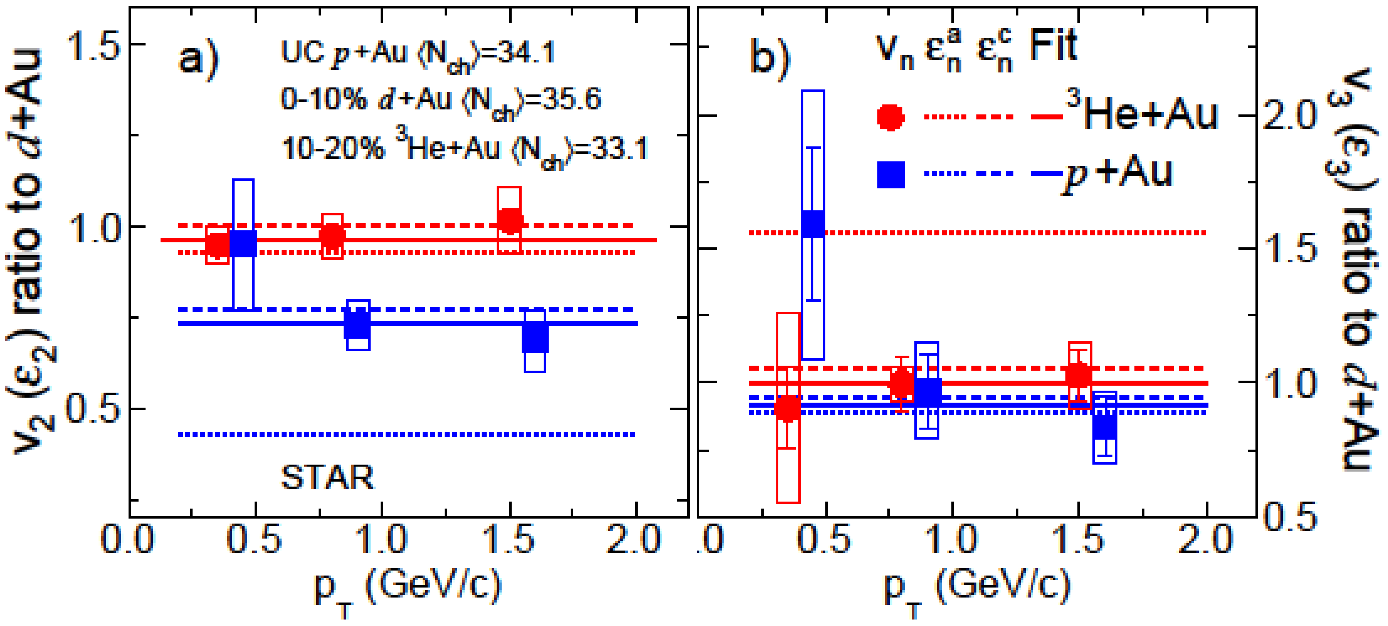

- Data at midrapidity
  - $v_2^{\mathrm{He+Au}} \sim v_2^{\mathrm{d+Au}} > v_2^{\mathrm{p+Au}}$
  - $v_3^{\mathrm{He+Au}} \sim v_3^{\mathrm{d+Au}} \sim v_3^{\mathrm{p+Au}}$
- Suggests significant influence of sub-nucleonic fluctuations
  - Need to study pre-flow

STAR, PRL 130 (2023) 242301

Anti-flow of Kaon

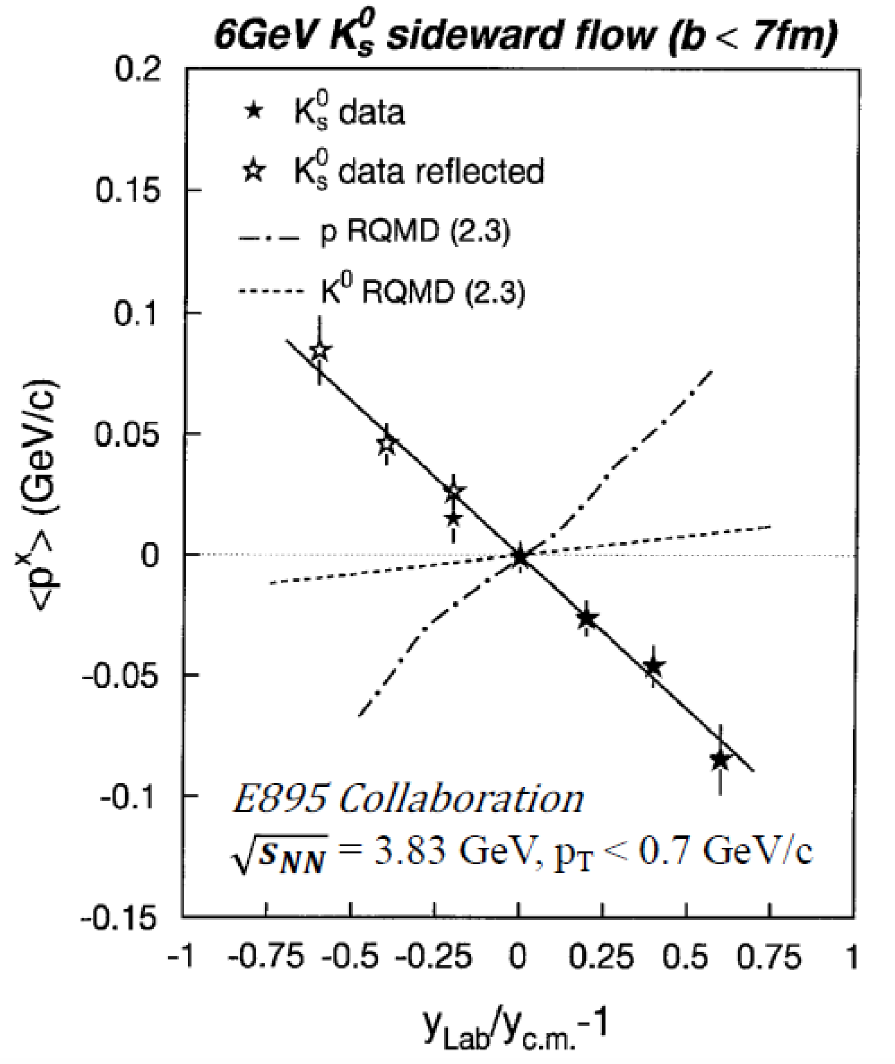

P. Chung et al. (E895 Collaboration), Phys. Rev. Lett. 85, 940(2000).

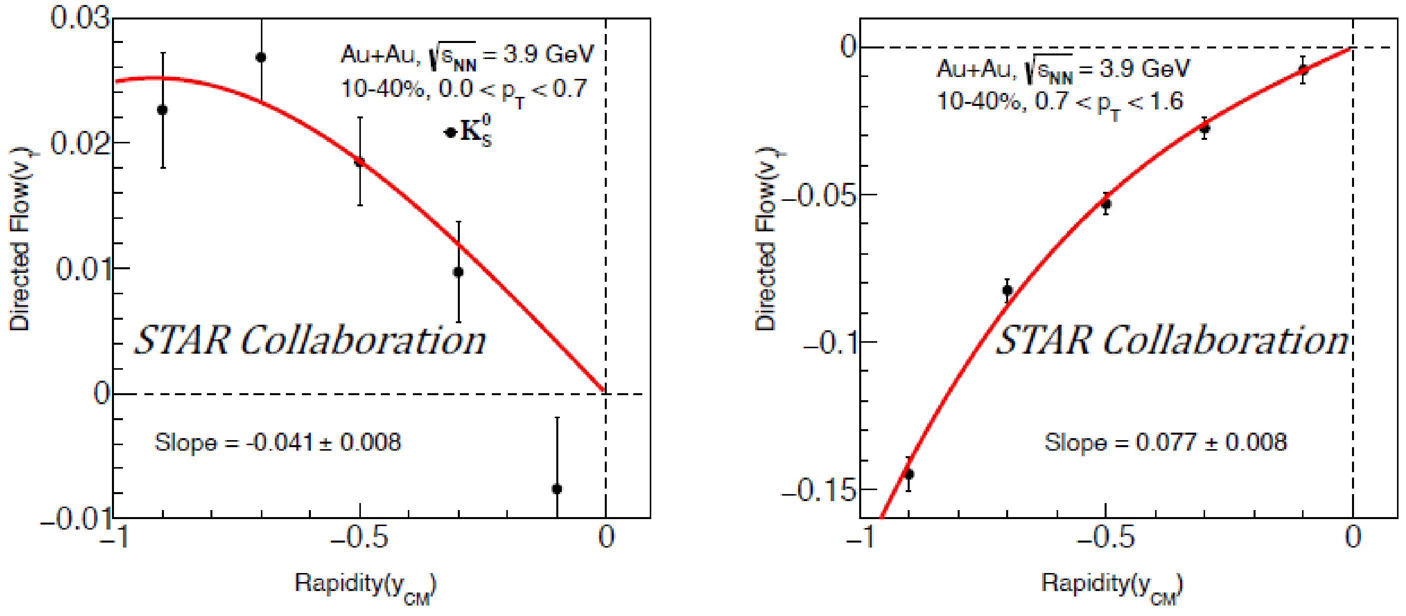

- Anti-flow observed for K_S^0 at 3.9 GeV with p_T < 0.7 GeV/c.
- Normal flow of K_S^0 with p_T > 0.7 GeV/c.
  → Strong p_T dependence of K_S^0 v_1 slope

Note: fitting function: $v_1 = p_0 * y + p_1 * y^3$
fitting range: $-1 < y_{CM} < 0$

Anti-flow of Mesons

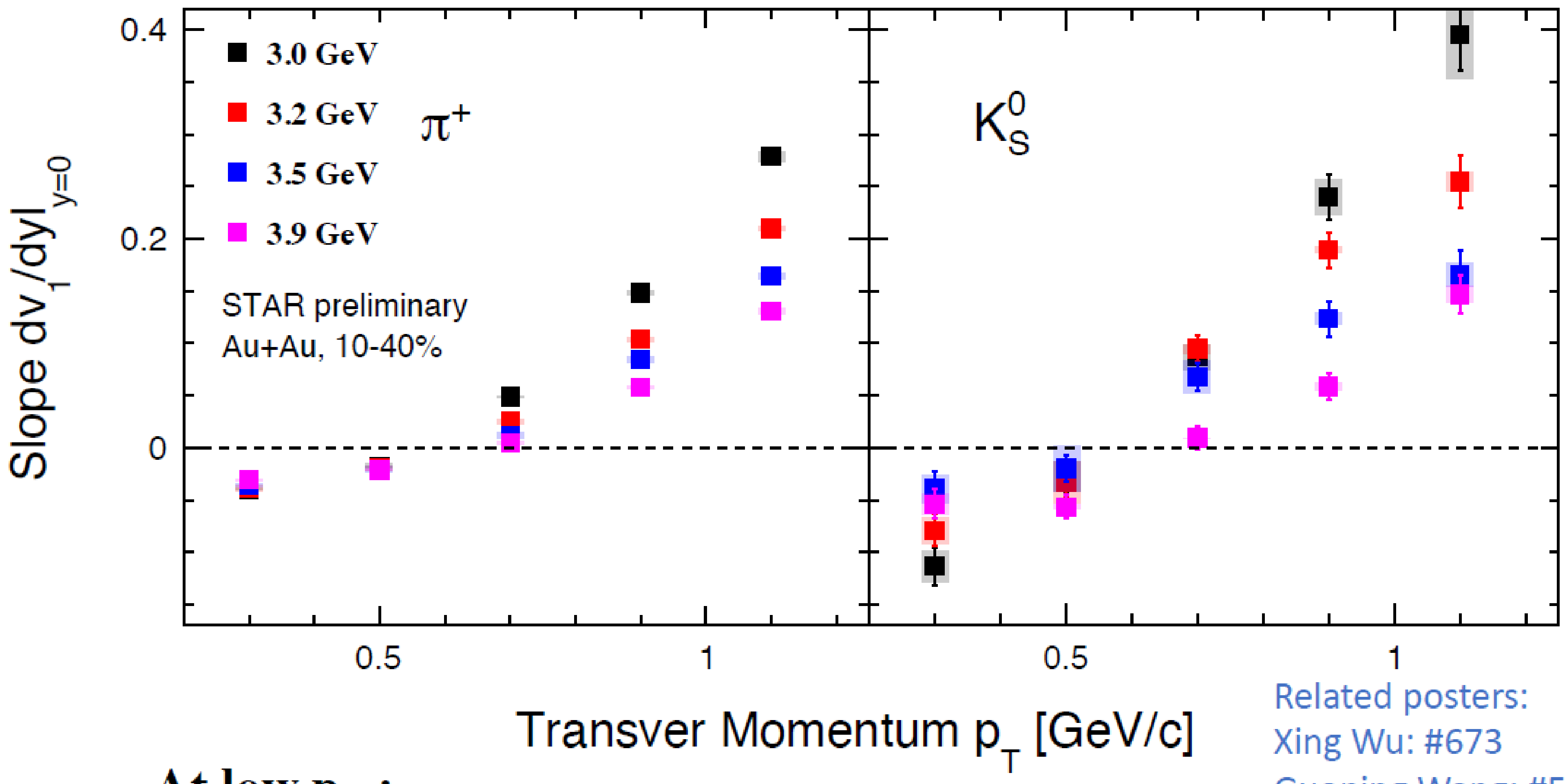

Related posters:
Xing Wu: #673
Guoping Wang: #551

At low p_T :

- $\pi^+(u\bar{d})$ and $K_S^0(d\bar{s})$ show negative v_1 slope.
- Anti-flow observed at 3 – 3.9 GeV.

Note: fitting function: $v_1 = p_0*y + p_1*y^3$
fitting range: $-1 < y_{CM} < 0$

Energy Dependence of v_1, v_2

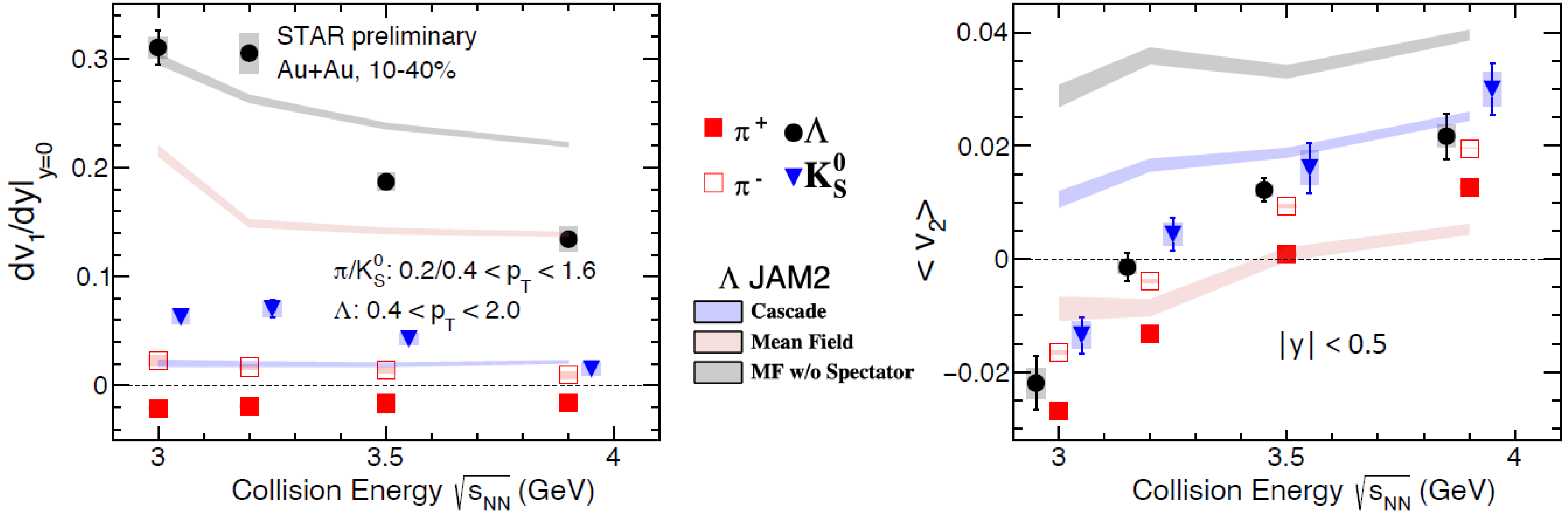

- v_1 slope decreases in the magnitude as collider energy increases. → Stronger tilted expansion.
- Negative v_2 turns to positive: Out-of-plane flow (spectator effect) → in-plane flow
- Better description for *Λ* v_1/v_2 with baryonic mean-field + spectator.

Note:
Soft EoS in JAM baryonic mean field:
the nuclear incompressibility K = 210 MeV

Yasushi Nara, Akira Ohnishi. Phys. Rev. C. 105, 014911(2022)

Flow (Au+Au)

- High precision measurement of Proton, Deuteron and Triton flow coefficients up to v_4
  Eur.Phys.J.A **59** (2023) 4, 80

- Important input to model calculations to constrain of EoS of compressed baryonic matter

- Correlations of flow coefficients can be studied event-wise

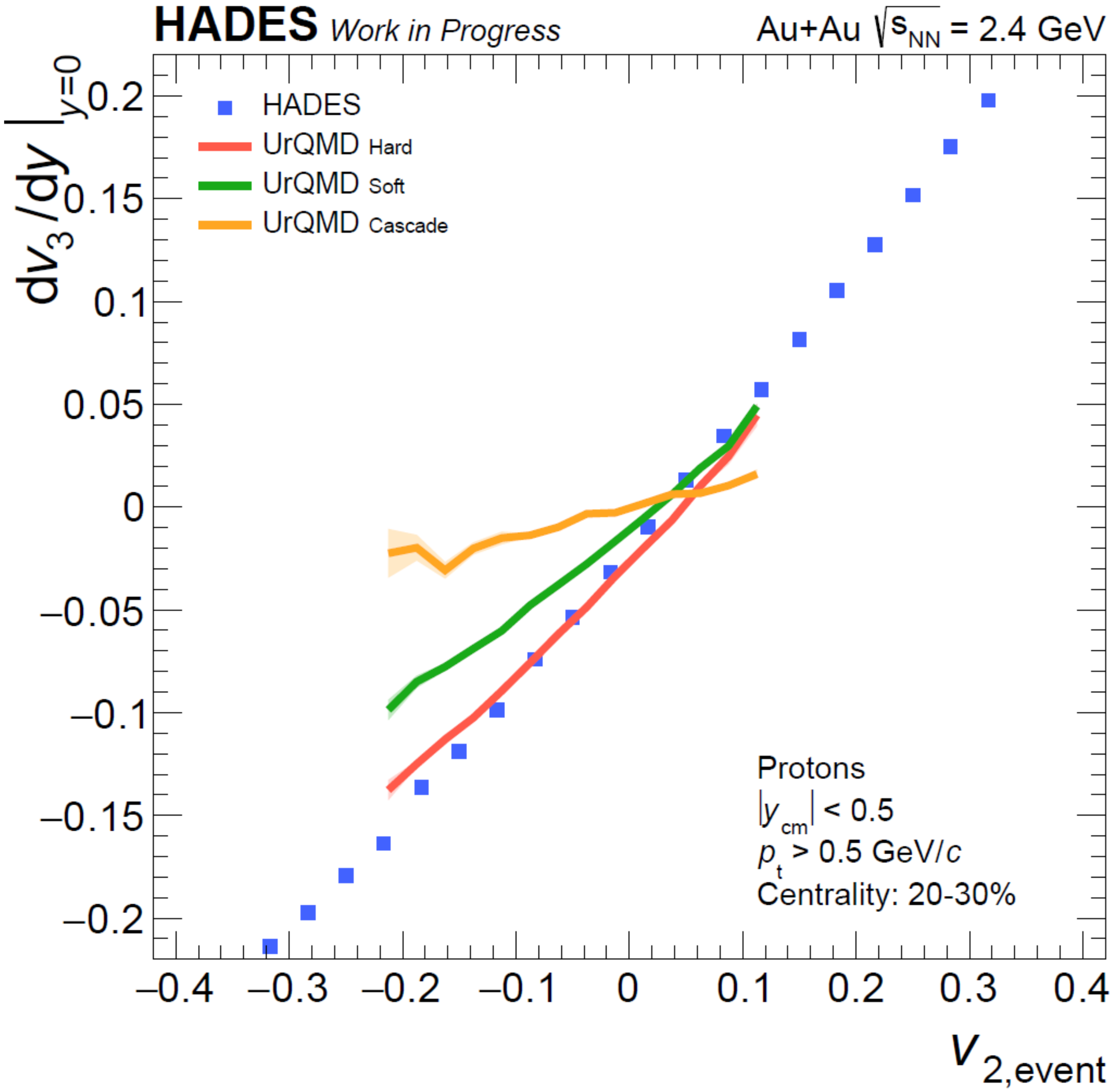

Proton $v_3\{\Psi_1\}$ @ FXT Energies

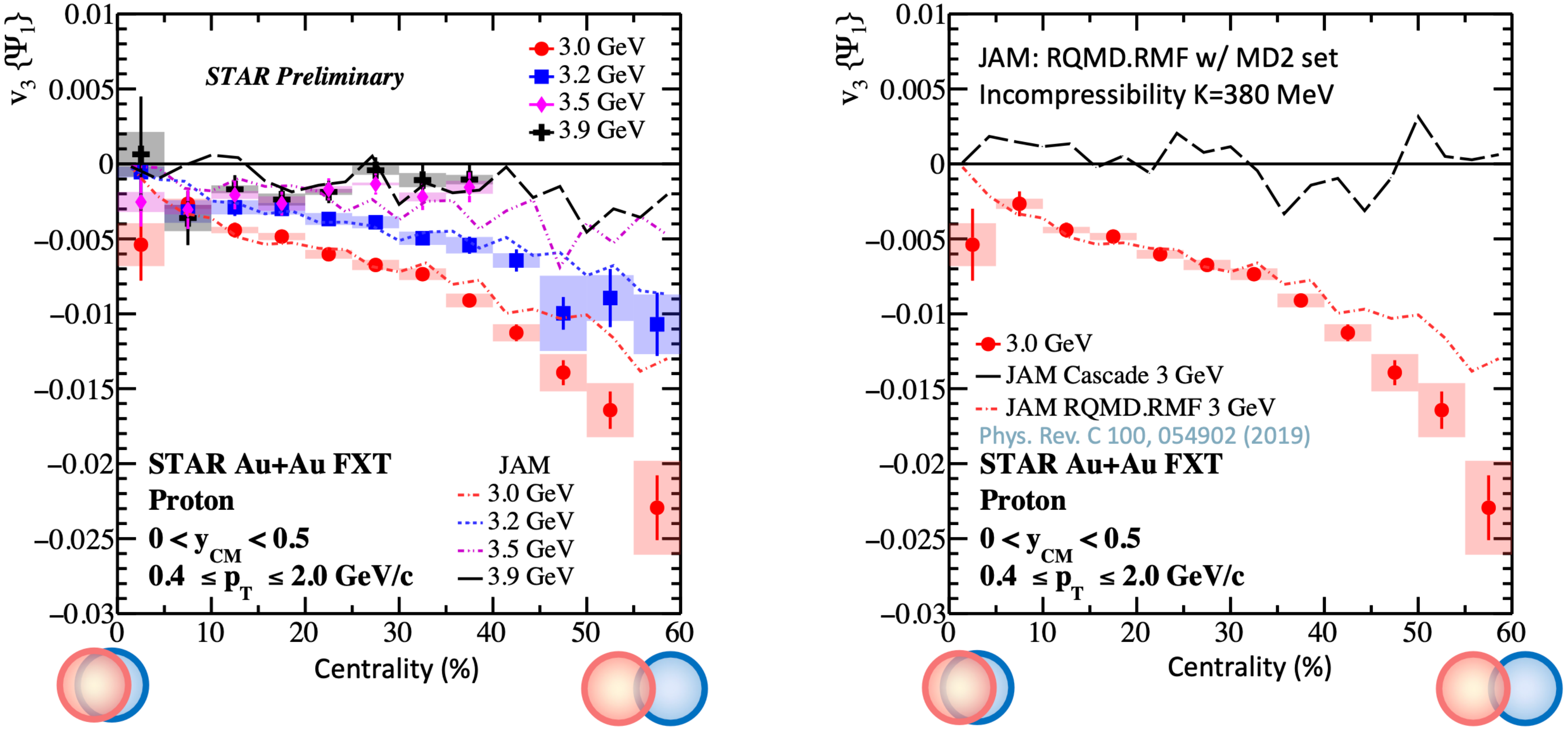

- $|v_3\{\Psi_1\}|$ increases towards peripheral collisions -> Geometry drives $v_3\{\Psi_1\}$.
- JAM describes the data -> Nuclear potential is essential for the development of $v_3\{\Psi_1\}$.

Limiting Fragmentation Of v_1

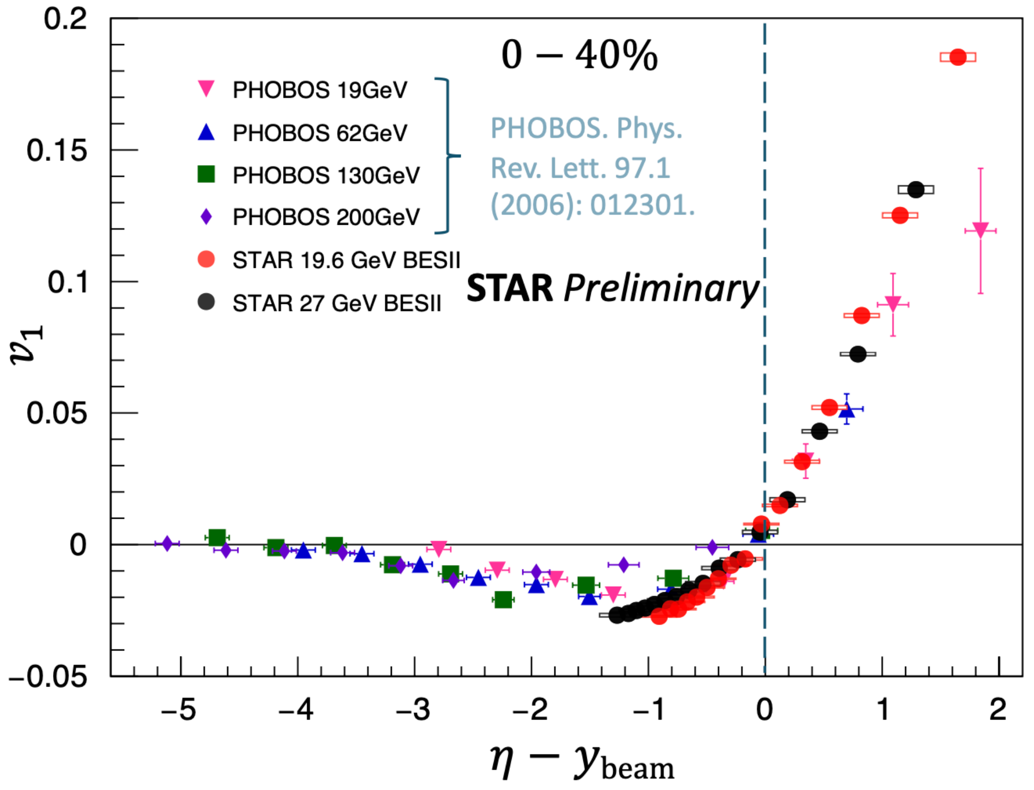

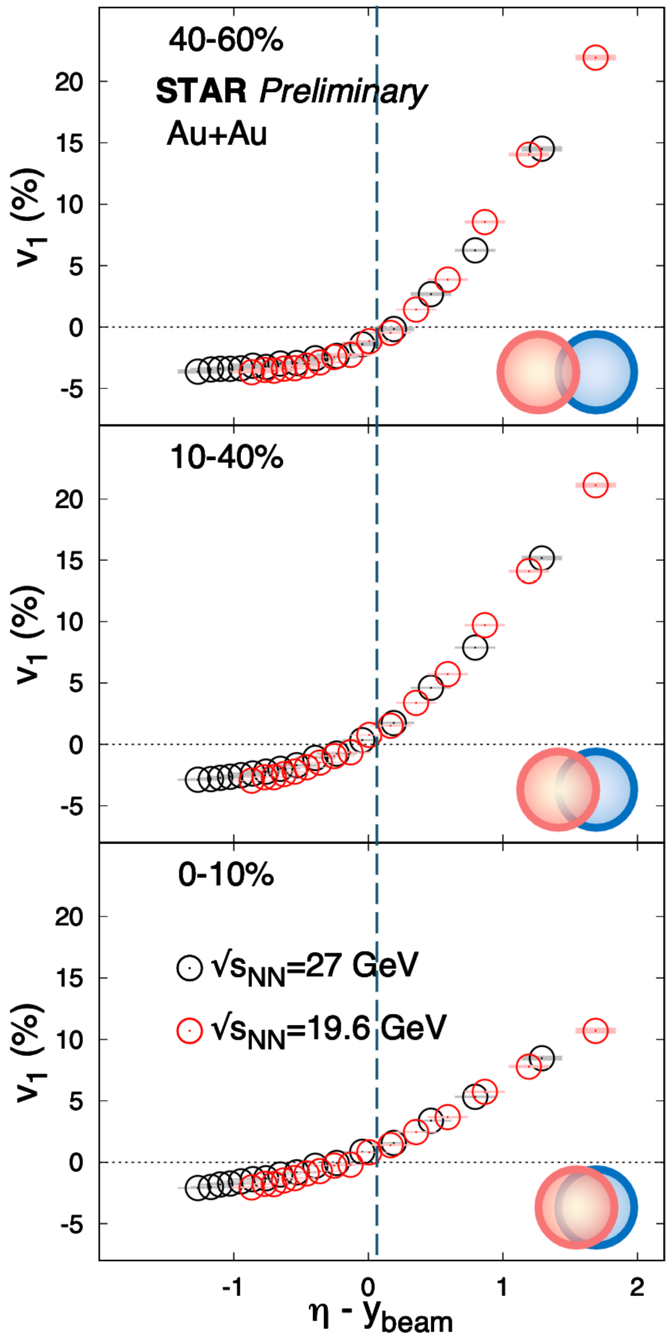

- "Limiting fragmentation" of v_1 observed for all the centralities.
- The phenomenon extends beyond yields to dynamics.

f₀(980) Quark Content

- $f_0(980)$ **structure unknown**
  - **Diquark**
  - **Tetraquark**
  - **K-K molecule**

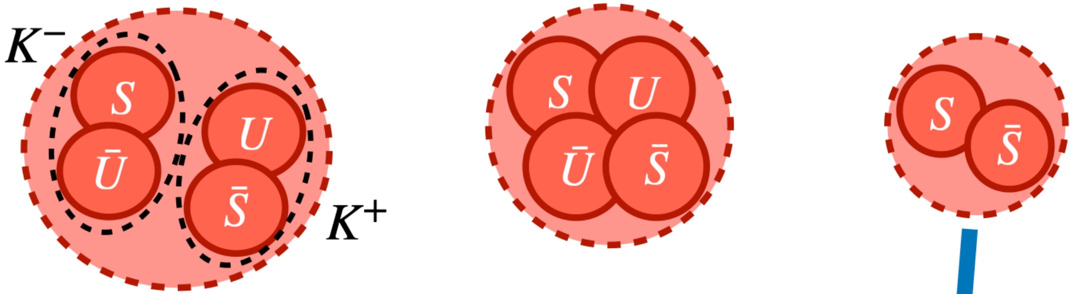

- **v₂ of $f_0(980)$ measured in pPb**

- **Use** **constituent quark scaling** **to extract number of quarks**

$$v_2(E_T)/n_q = v_{2,q}(E_T/n_q)$$

- **n_q = 4 excluded at $\geq 3.1\sigma$**
- **n_q = 2 favored**

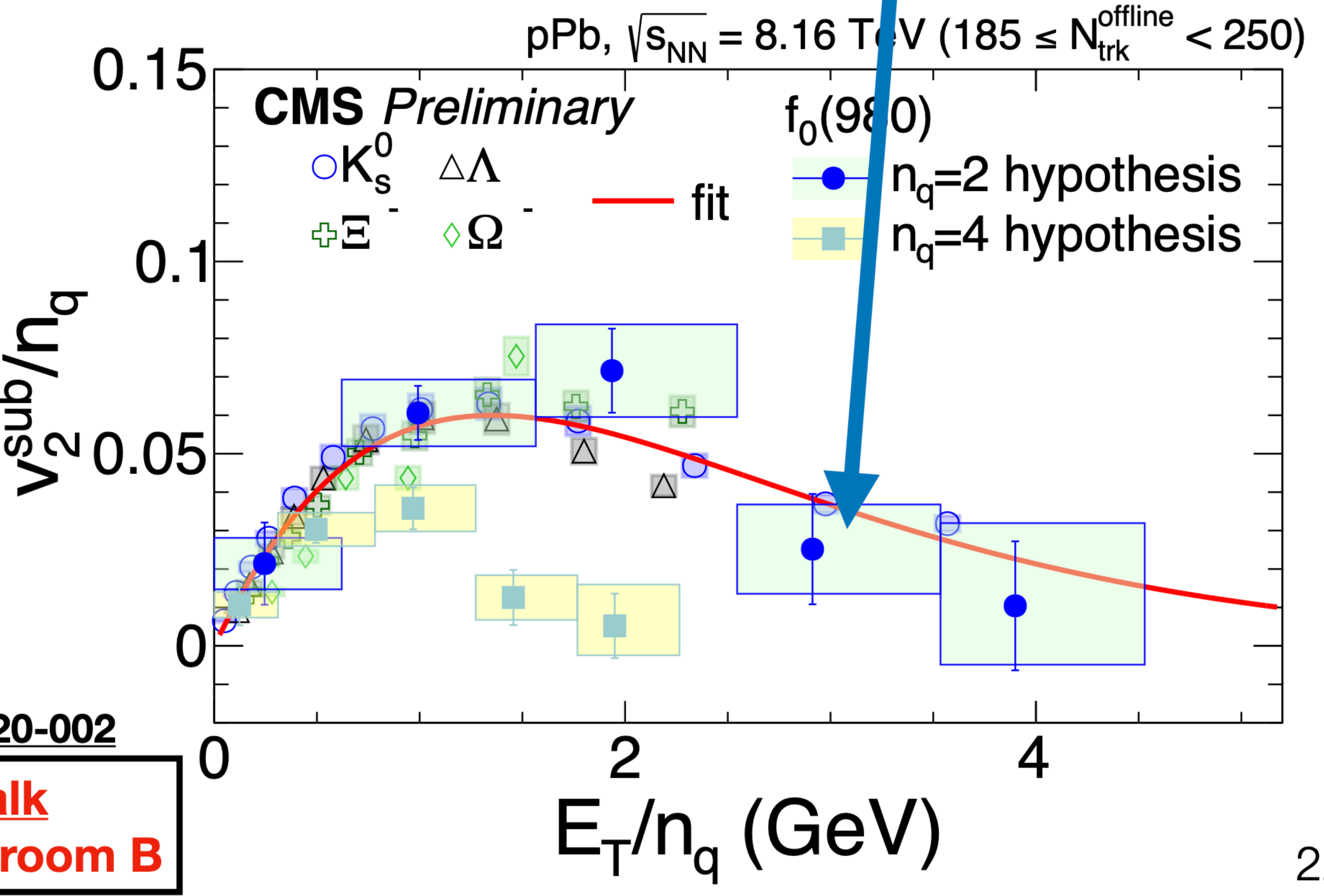

CMS NEW RESULT QM23

CMS PAS HIN-20-002

An Gu's talk
Tues. 9:30, Ballroom B

Fluctuations

Observables - Cumulants

N: Net-proton multiplicity

C_n: n^{th} order cumulant

$\delta N = N - \langle N \rangle$

$$C_1 = \langle N \rangle$$
$$C_2 = \langle (\delta N)^2 \rangle$$
$$C_3 = \langle (\delta N)^3 \rangle$$

$$C_4 = \langle (\delta N)^4 \rangle - 3\langle (\delta N)^2 \rangle^2$$
$$C_5 = \langle (\delta N)^5 \rangle - 10\langle (\delta N)^3 \rangle \langle (\delta N)^2 \rangle$$
$$C_6 = \langle (\delta N)^6 \rangle - 15\langle (\delta N)^4 \rangle \langle (\delta N)^2 \rangle - 10\langle (\delta N)^3 \rangle^2 + 30\langle (\delta N)^2 \rangle^3$$

Stephanov, Phys Rev Lett 107, 052301 (2011)

Higher-order cumulants are more sensitive to the correlation length

Cumulants ratios cancel trivial volume dependence

$$\frac{C_5}{C_1} = \frac{\chi_5}{\chi_1}$$
$$\frac{C_6}{C_2} = \frac{\chi_6}{\chi_2}$$

χ_n: n^{th} order cumulant

- Cumulant ratios are directly related to susceptibilities from theory
- Sensitive probes for the nature of the QCD phase transition

Critical fluctuations

CBM after 3 years – (improve STAR stat. errors by factor of 10):

- Measure excitation function (p) for $k\sigma^2 = \frac{\kappa_4}{\kappa_2}$
- First results on κ_6(p)
- Extension to strangeness?

STAR, PRL 128 (2022) 20, 202303
HADES, PRC 102 (2020) 2, 024914

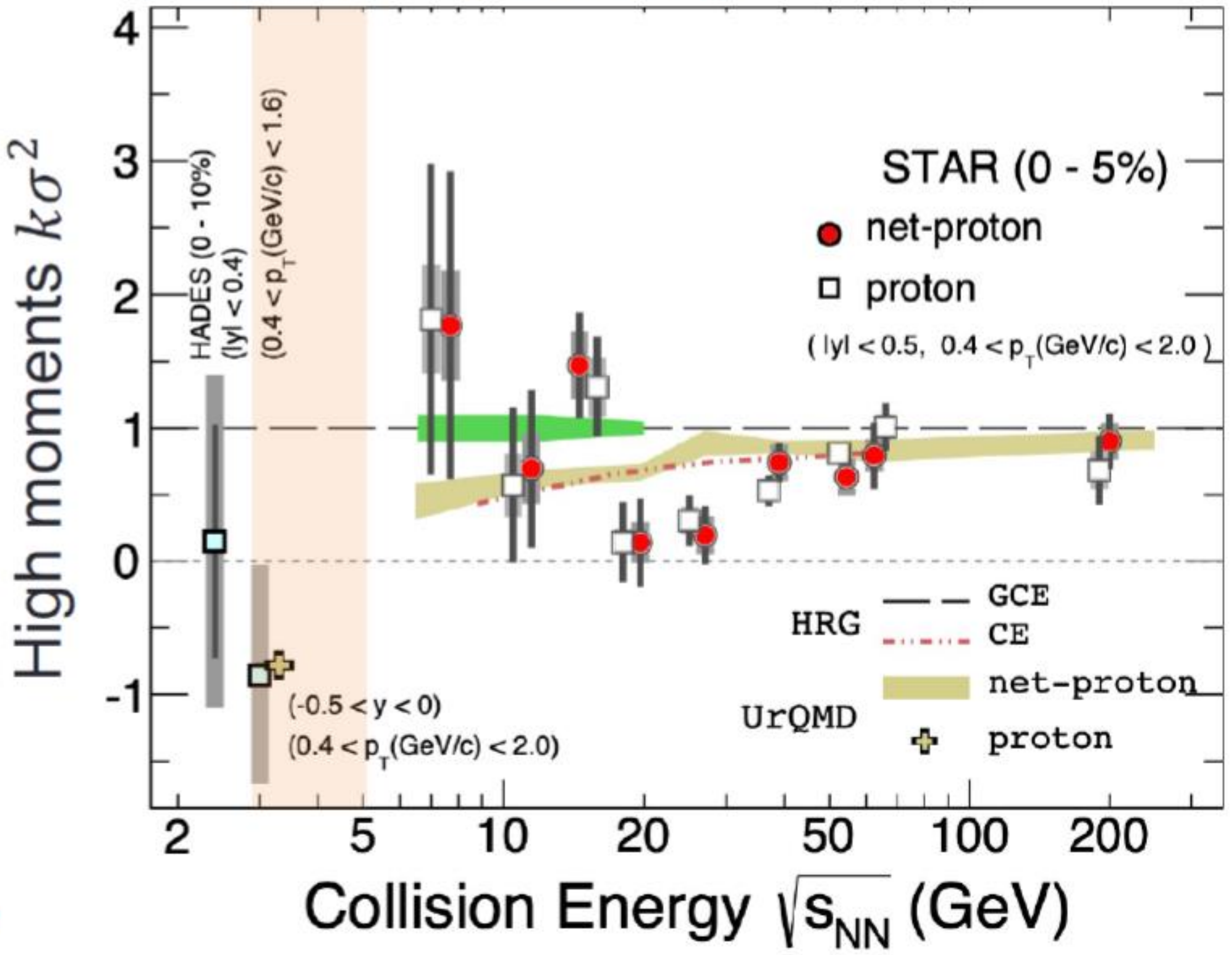

We hope to see:
Discontinuity?!
… that extends to even higher moments?!

Hyper-Order Cumulant Ratios

$C_4/C_2 \rightarrow$ Positive at 0-40%
$C_5/C_1 \rightarrow$ Weak trend with energy

C_6/C_2

- **Increasingly negative** with decreasing energy
  - ➪ Qualitatively matches trend of lattice calculations
- $\sqrt{s_{NN}}$ = 3 GeV positive and consistent with UrQMD

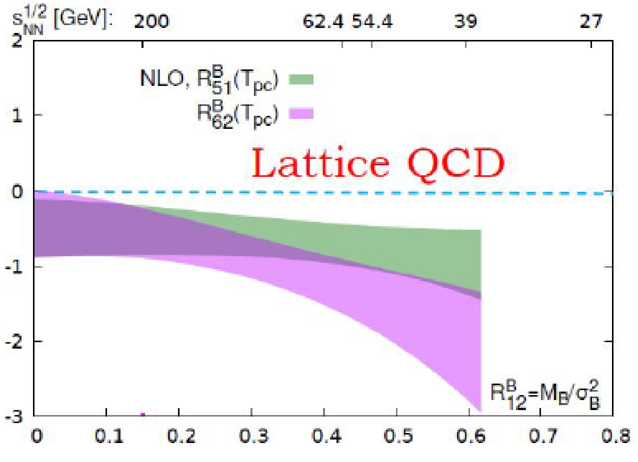

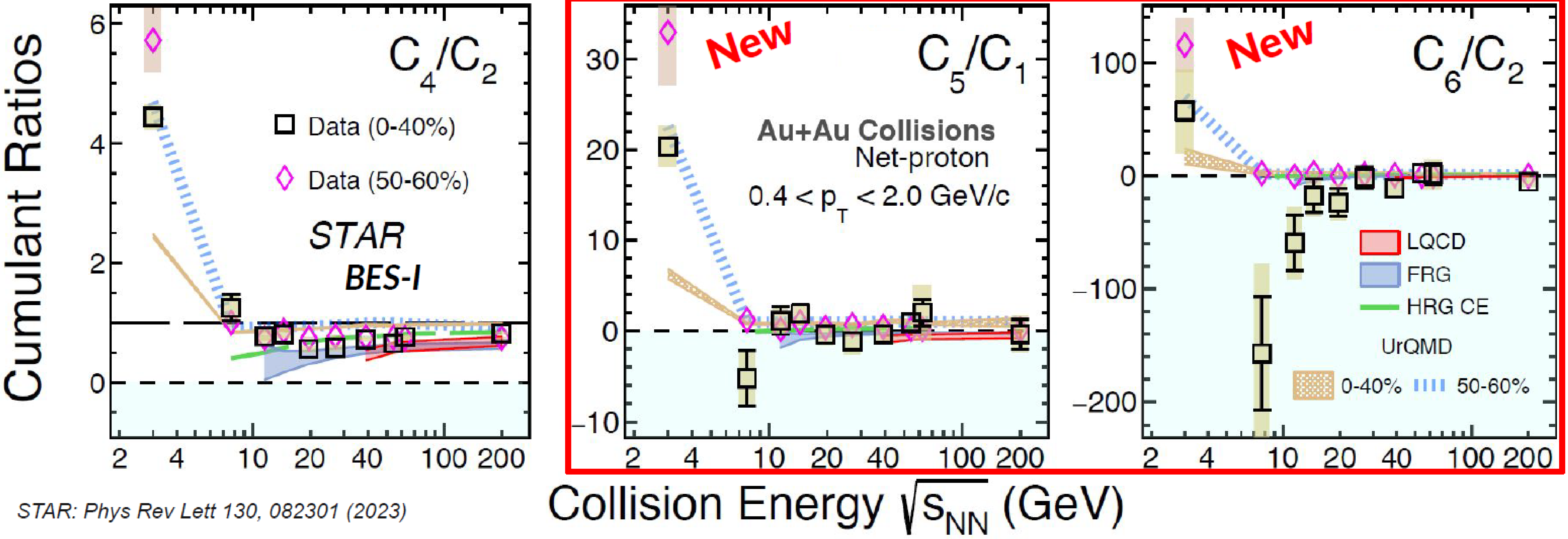

STAR: Phys Rev Lett 130, 082301 (2023)

Correlation Strength vs Energy

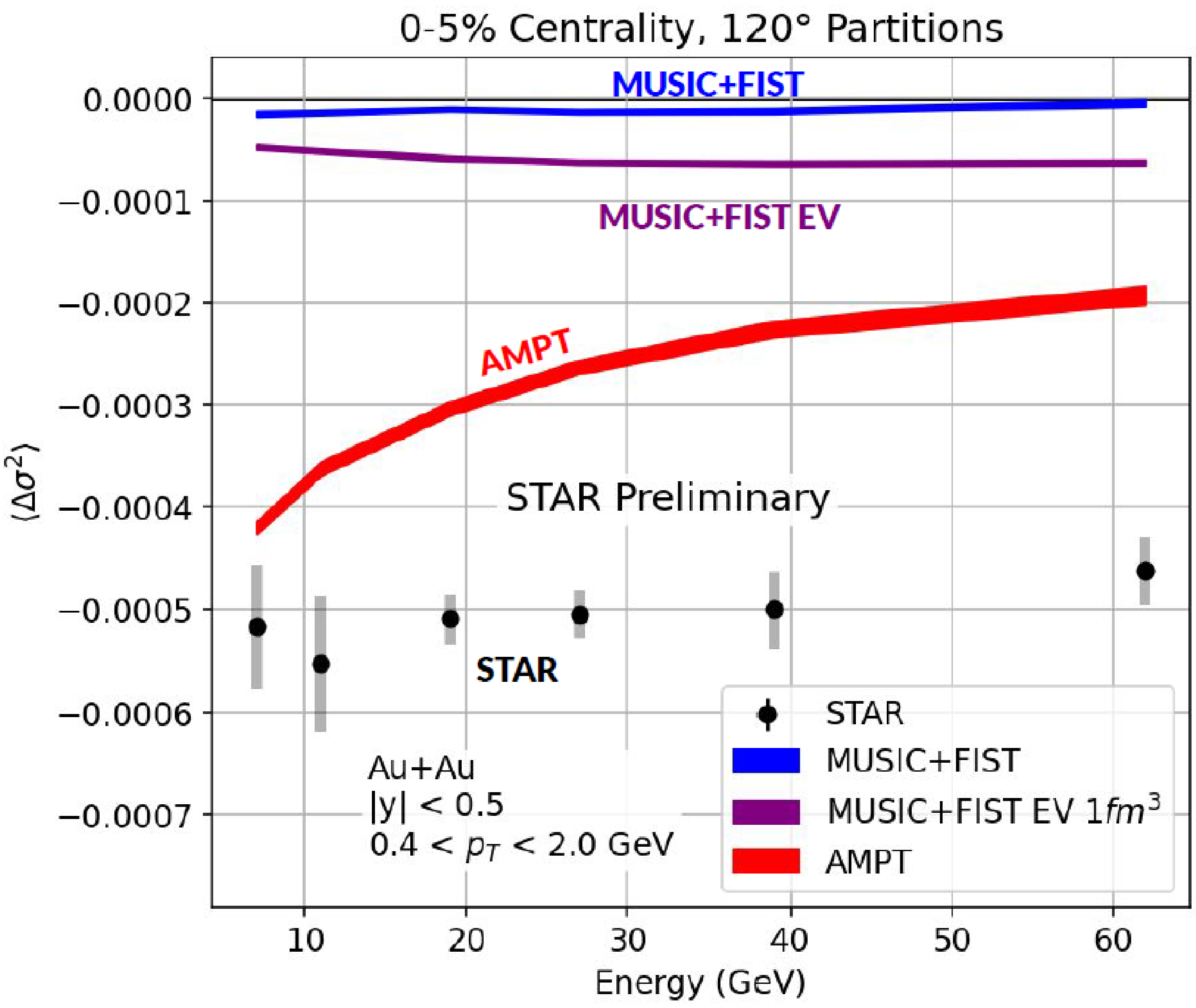

Negative $\Delta\sigma^2$ → Repulsion

- Repulsion observed between proton tracks in STAR data and all models
- STAR correlations from most central 0-5% centrality showed no significantly beam energy dependence and larger strength in correlation than AMPT. In addition, AMPT showed a moderate beam energy dependence.

⟨Δσ²⟩ vs Event Multiplicity

Magnitude of repulsive interaction increases with decreasing multiplicity per event

Multiplicity dependence likely dominated by global momentum conservation

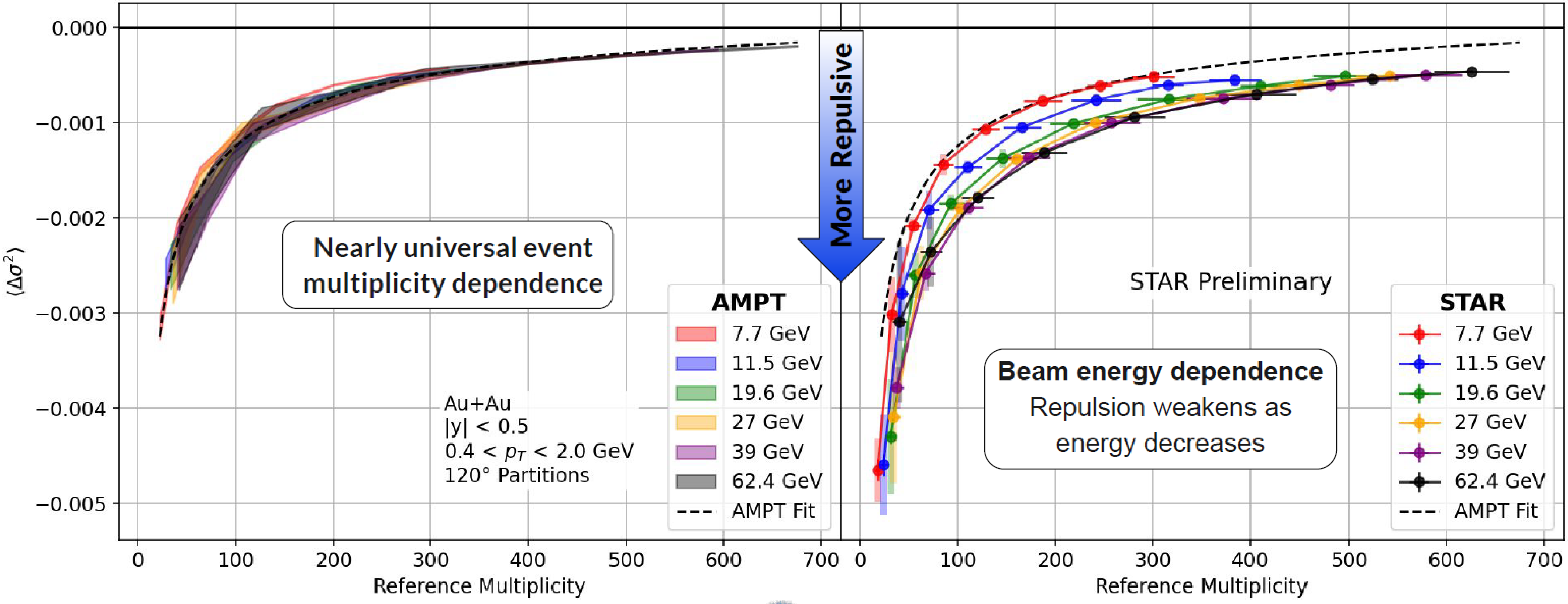

Probing the QCD Phase Diagram

Tues 830
D. Neff
ID 439

- Cumulants of net-particle distributions
  - **Cumulant ratios** directly related to **susceptibilities**
  - **Higher order moments** are sensitive probes for the nature of QCD phase transition

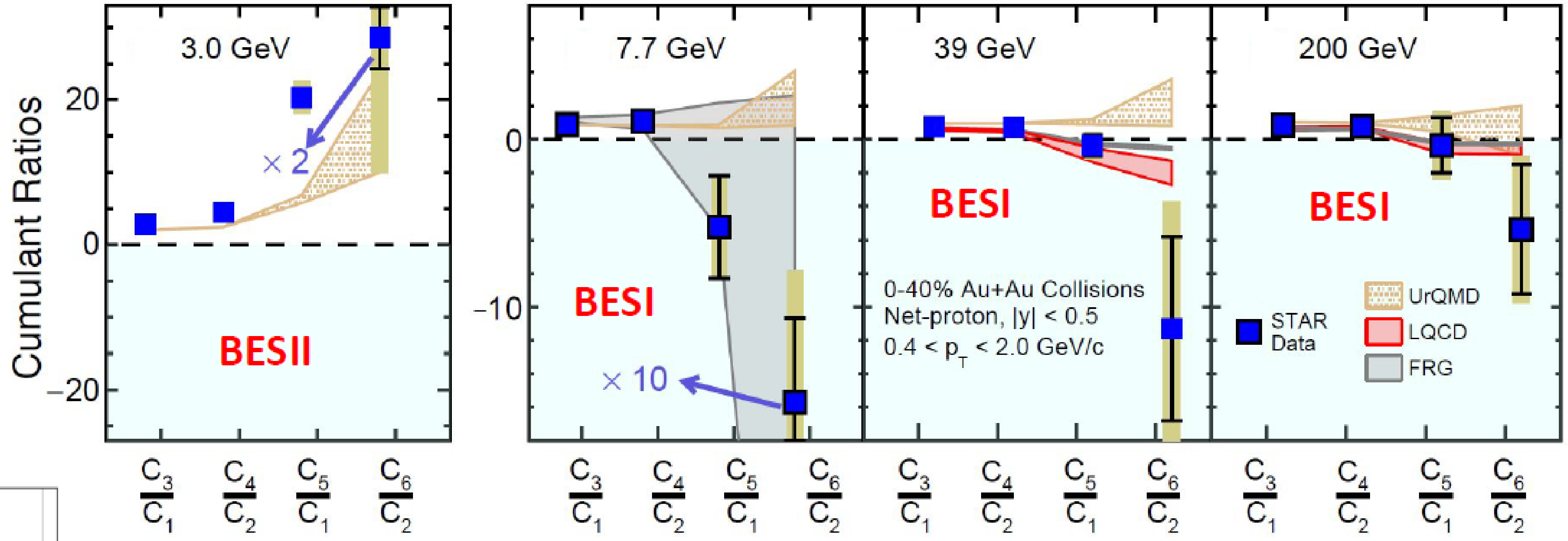

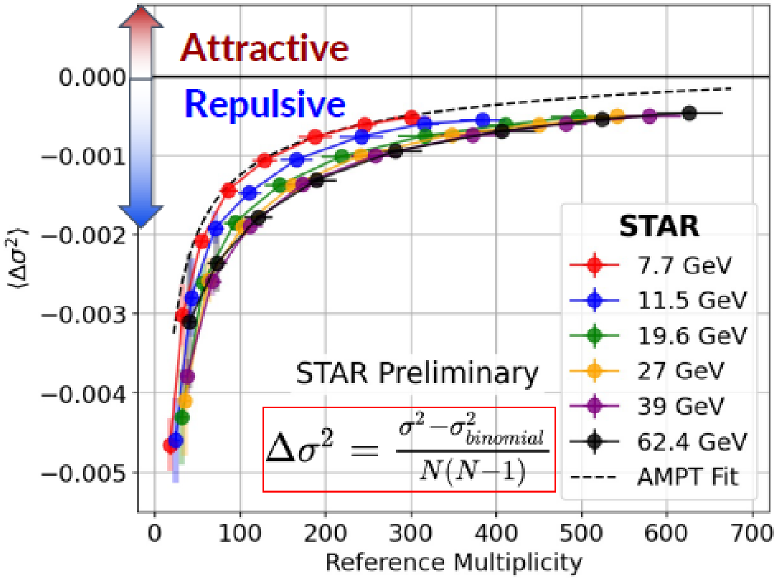

- Proton kurtosis results will be released directly to paper, work in progress
- Cumulant data consistent w/predicted hierarchy $\sqrt{S_{NN}}$= 7.7 to 200 GeV
  - Violation of ordering found at fixed target $\sqrt{S_{NN}}$ = 3 GeV
  - Reproduced by UrQMD → Suggests hadronic matter
- Magnitude of **repulsive** interaction **increases** with **decreasing multiplicity** per event → Multiplicity dependence likely due to global p conservation

Hypernuclei

Hypernuclei Lifetime Measurements

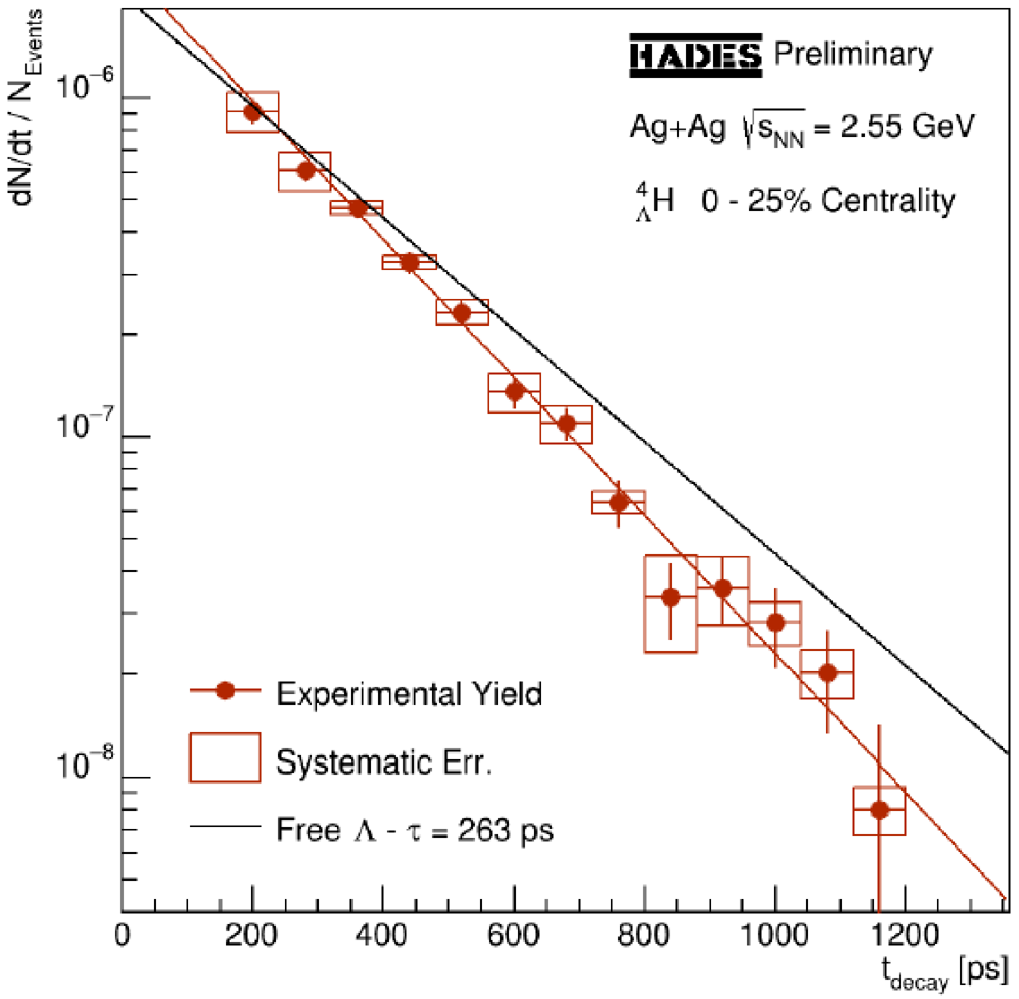

- $^{3}_{\Lambda}H$ lifetime of $(251 \pm 21_{stat} \pm 30_{sys})$ ps compatible with free Λ lifetime and earlier measurements measured
- $^{4}_{\Lambda}H$ lifetime of $(216 \pm 7_{stat} \pm 10_{sys})$ ps measured
  - 4.85σ deviation to free Λ lifetime
- Interaction cross-section within first 40cm of HADES detector material ≲ 0.5%

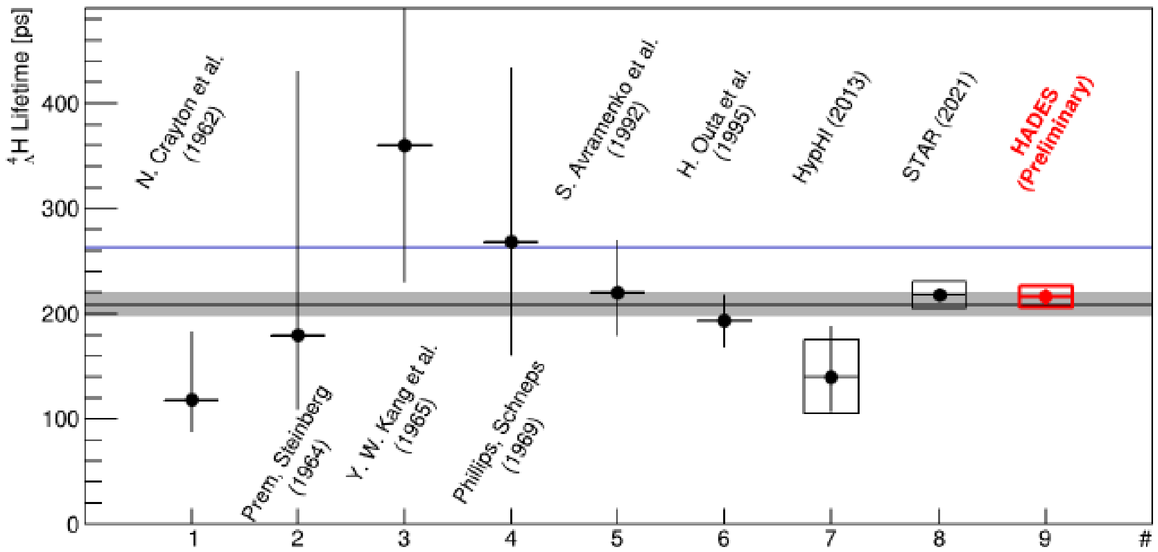

Hypernuclei p_T Spectra, $\langle p_T \rangle$, dN/dy

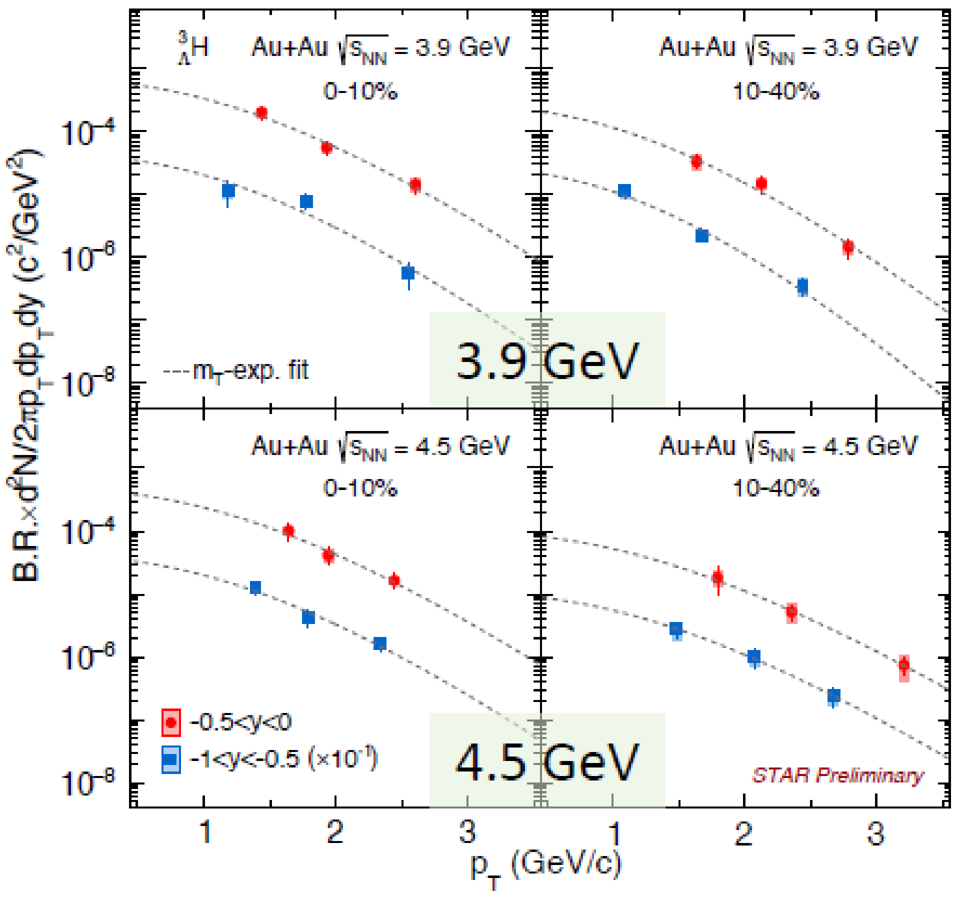

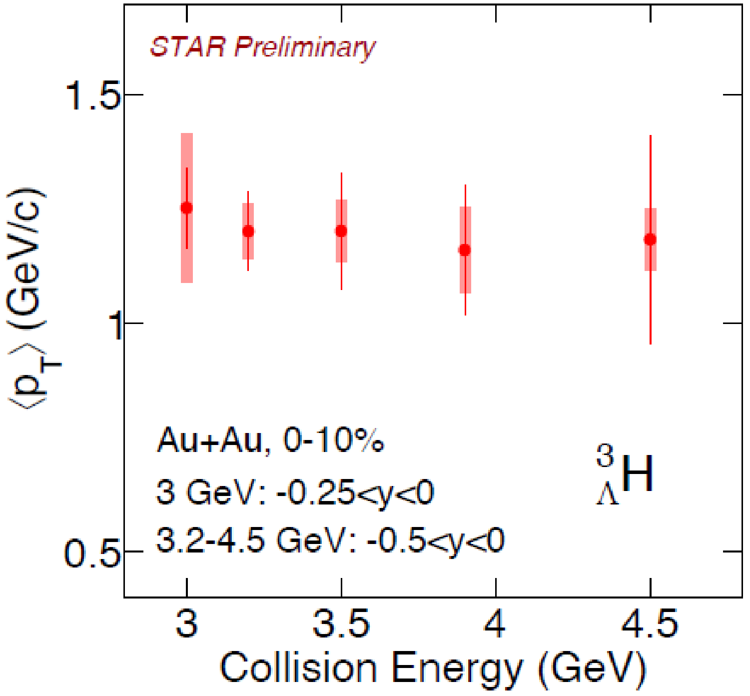

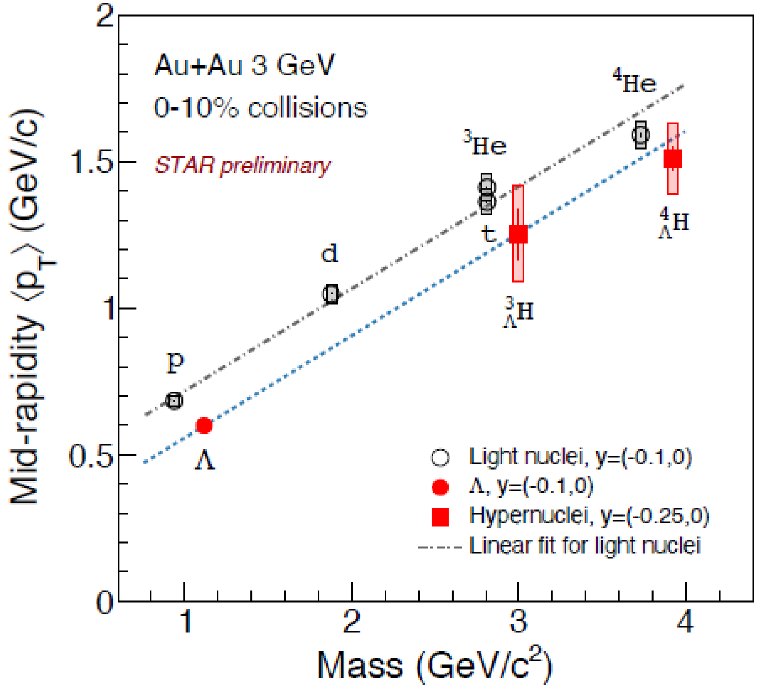

Au+Au central collisions

- Hypernuclei $\langle p_T \rangle$ follows the mass number scaling
- dN/dy vs. y qualitatively described by JAM + Coalescence

Energy dependence of hypernuclei production

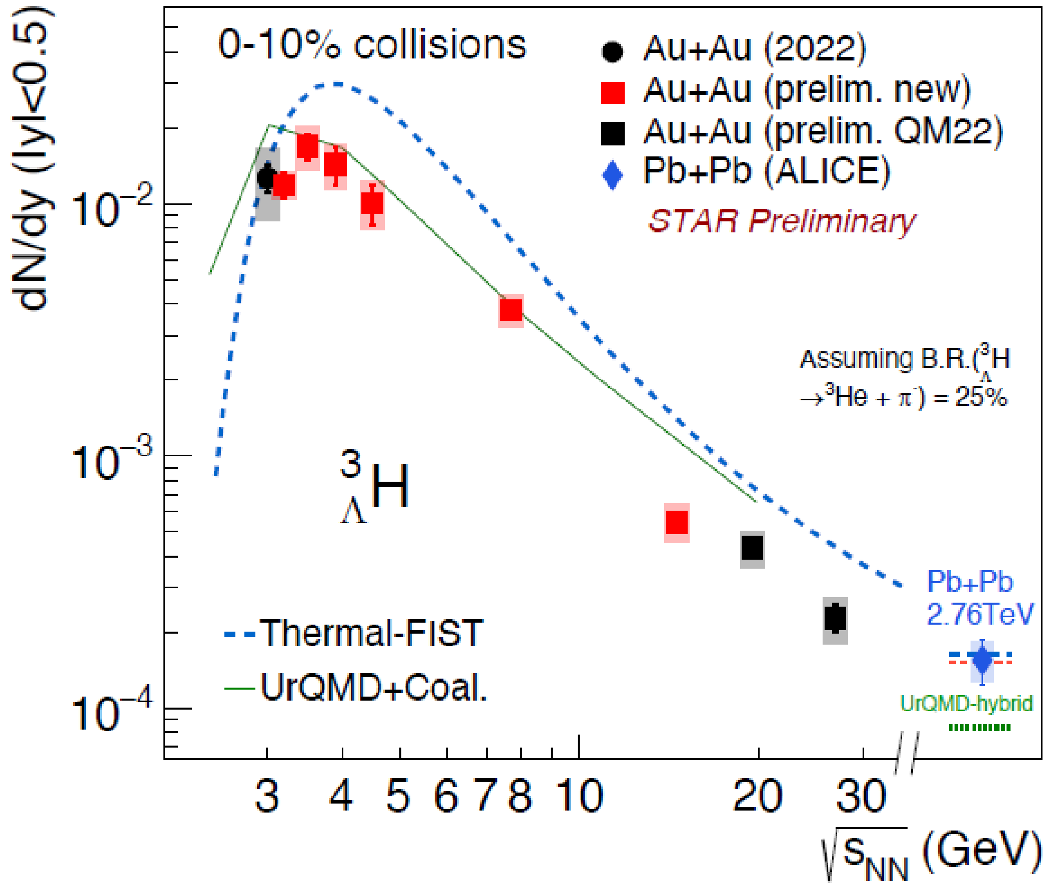

Thermal-FIST, Coal+UrQMD: Phys.Rev.C 107 (2023) 1, 014912
Pb+Pb: ALICE, PLB 754, 360 (2016)

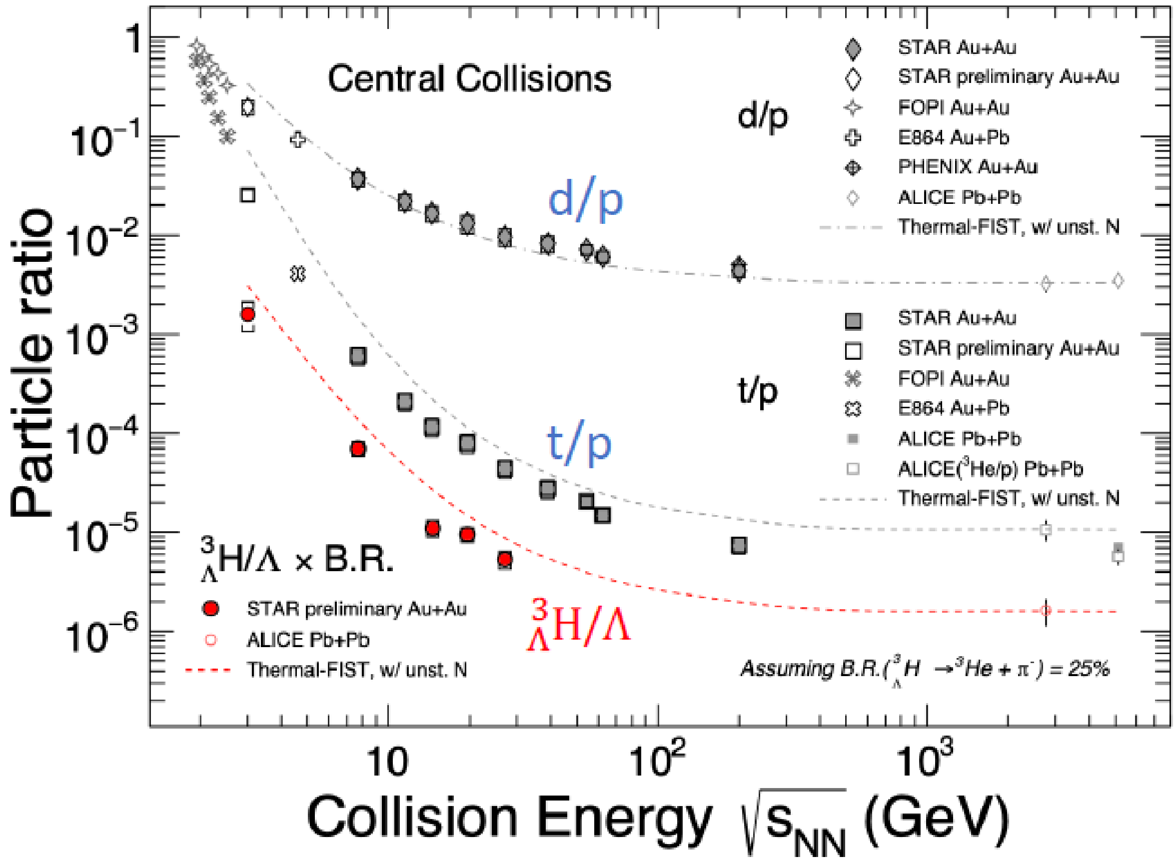

d/p and t/p: PRL 130 (2023) 202301

- Hadronic transport + coalescence models qualitatively describe the data
- Thermal model calculation ~2 times higher than data in BES-II energies

${}^{3}_{\Lambda}$H Binding Energy

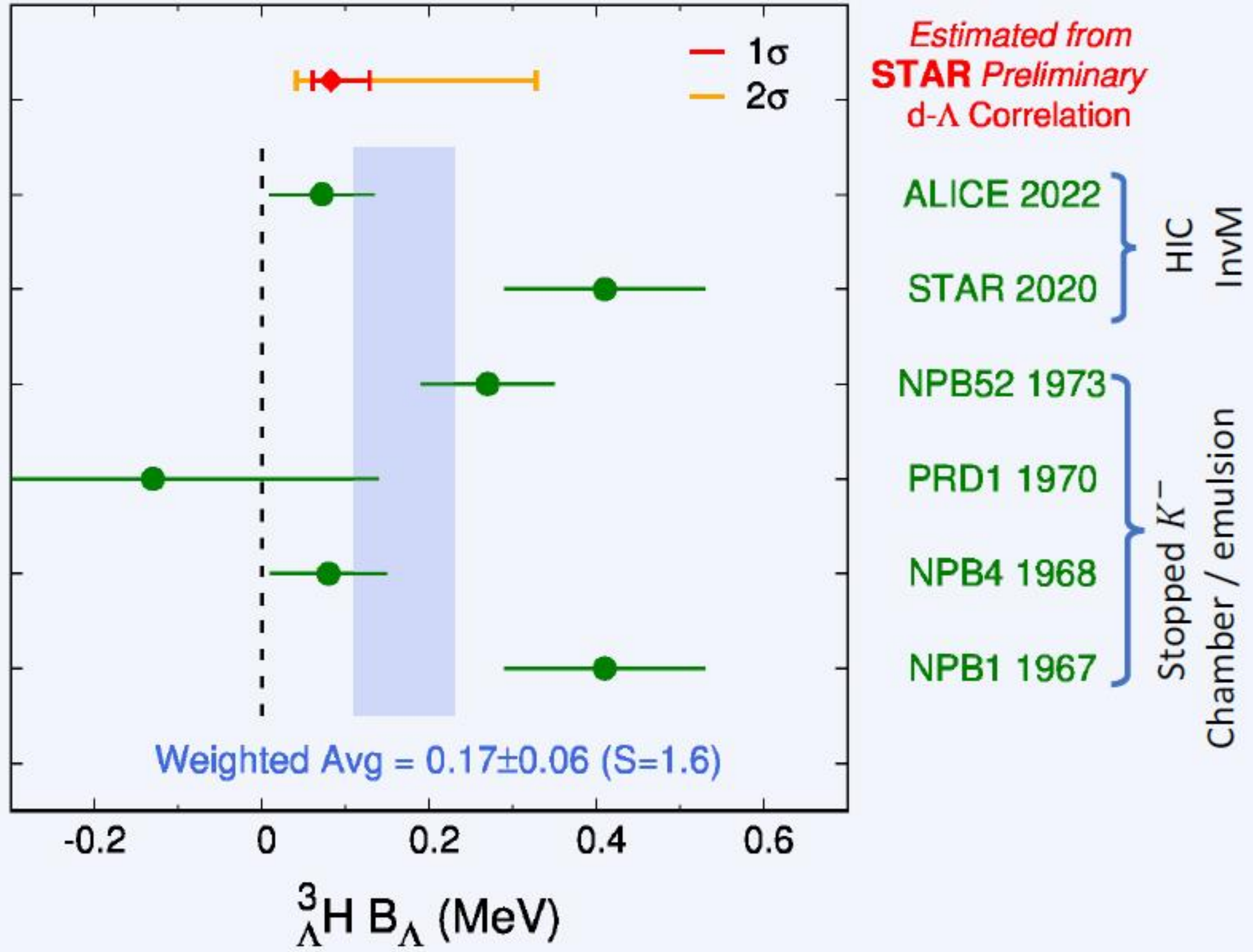

${}^{3}_{\Lambda}$H binding energy (B_Λ):

❖ Bethe formula from Effective Range Expansion (ERE) parameters $f_0(\mathrm{D})$ & $d_0(\mathrm{D})$

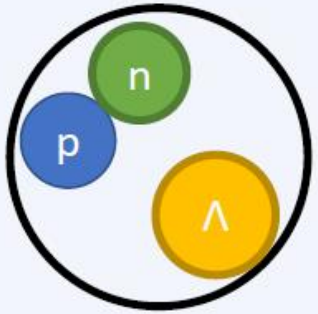

$$\frac{1}{-f_0} = \gamma - \frac{1}{2} d_0 \gamma^2$$

❖ $\mathrm{B}_\Lambda = \frac{\gamma^2}{2\mu_{d\Lambda}}$

❖ $\mu_{d\Lambda}$: reduced mass

❖ γ: binding momentum

❖ ${}^{3}_{\Lambda}$H $\mathrm{B}_\Lambda = [0.04, 0.33]$ (MeV) @ 95% CL

Consistent with the world average

❖ A new way to constrain the ${}^{3}_{\Lambda}$H structure

New facilities

The sPHENIX Experiment

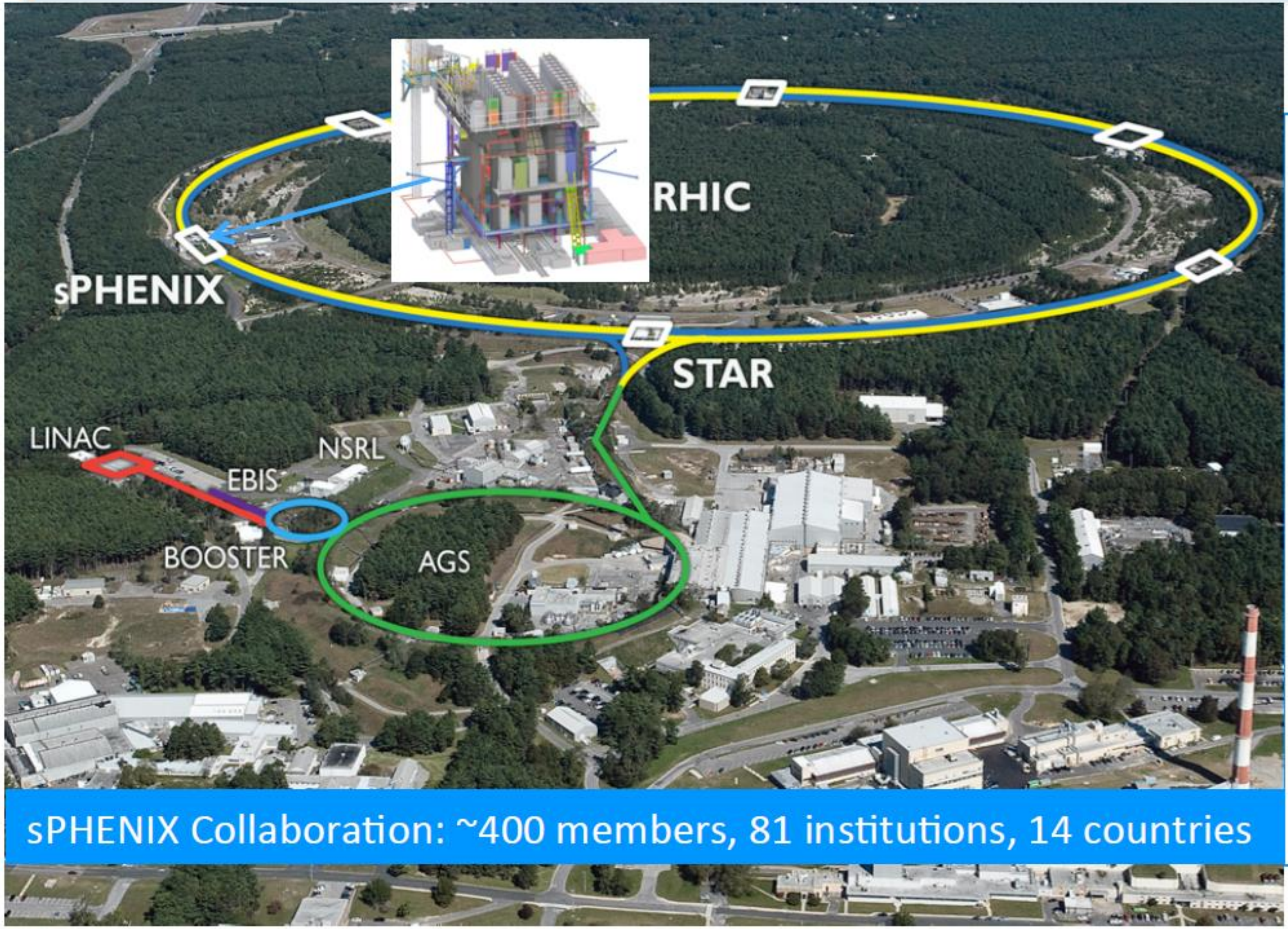

sPHENIX is the first new major detector at RHIC in over 20 years. It is a compete tear-down and rebuild of PHENIX reusing >$20M in existing PHENIX equipment and support facilities, plus brand new detector subsystems and a completely upgraded experiment complex.

sPHENIX Components: Vertical Slice and Actual

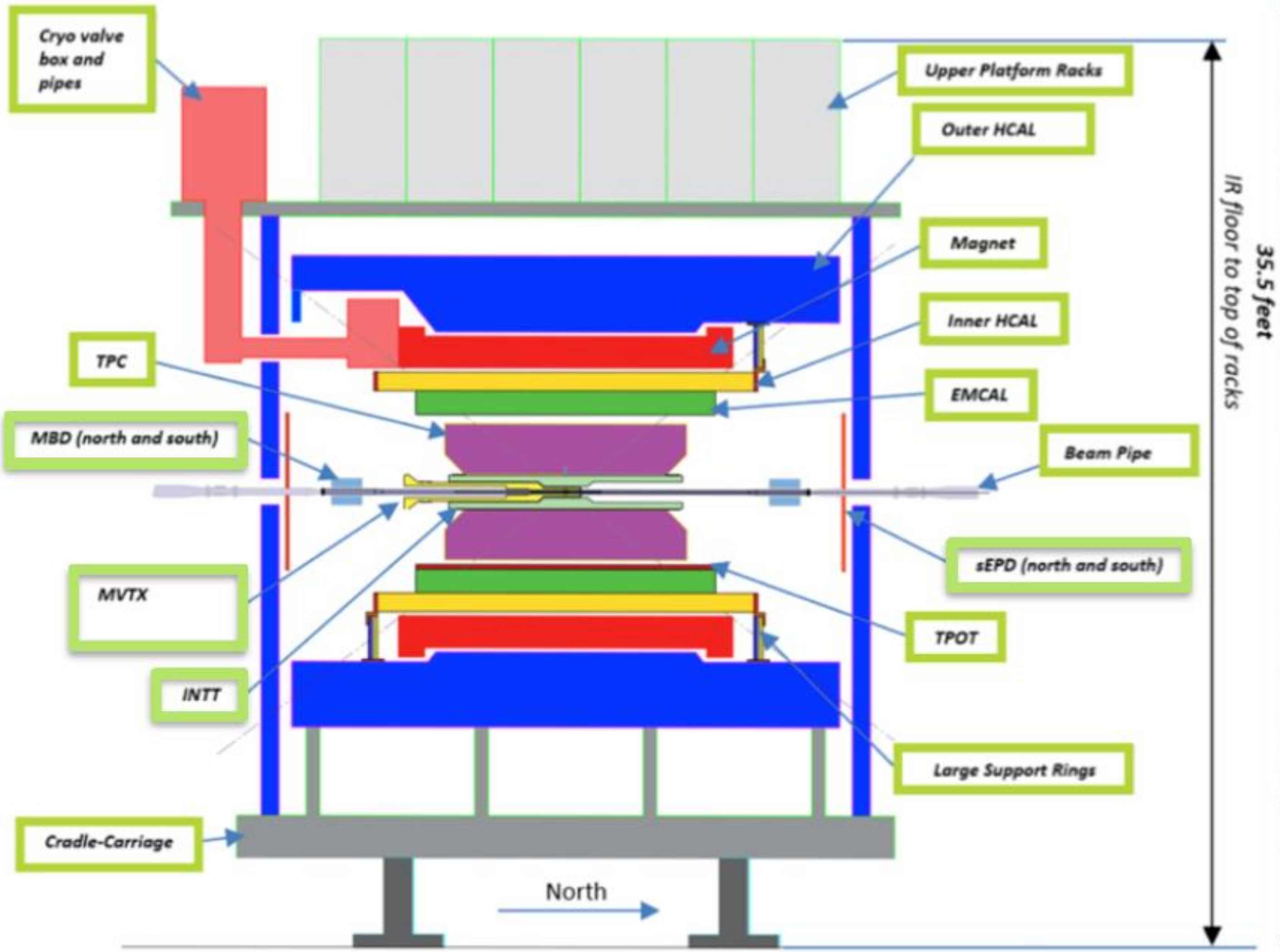

A Few Installation Highlights

1st OHCal Sector arrives at BNL, Aug 2017

Install of sPHENIX begins May 2021

OHCal Barrel complete Feb 2022

sPHENIX approved for routine operations, May 2023

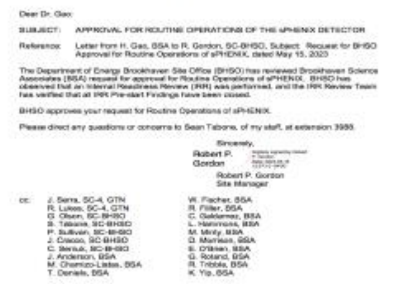

Dear Dr. Gao:

SUBJECT: APPROVAL FOR ROUTINE OPERATIONS OF THE sPHENIX DETECTOR

Reference: Letter from H. Gao, BSA to R. Gordon, SC-BHSO, Subject: Request for BHSO Approval for Routine Operations of sPHENIX, dated May 15, 2023

The Department of Energy Brookhaven Site Office (BHSO) has reviewed Brookhaven Science Associates (BSA) request for approval for Routine Operations of sPHENIX. BHSO has observed that an Internal Readiness Review (IRR) was performed, and the IRR Review Team has verified that all IRR Pre-start Findings have been closed.

BHSO approves your request for Routine Operations of sPHENIX.

Please direct any questions or concerns to Sean Tabone, of my staff, at extension 3998.

Sincerely,

Robert P. Gordon

Robert P. Gordon
Site Manager

cc: J. Serra, SC-4, GTN; R. Lukes, SC-4, GTN; G. Olson, SC-BHSO; S. Tabone, SC-BHSO; P. Sullivan, SC-BHSO; J. Cracco, SC-BHSO; C. Sersuk, SC-BHSO; J. Anderson, BSA; M. Chamizo-Llatas, BSA; T. Daniels, BSA; W. Fischer, BSA; R. Filler, BSA; C. Gaklarnez, BSA; L. Hammons, BSA; M. Minty, BSA; D. Morrison, BSA; S. O'Brien, BSA; G. Roland, BSA; R. Tribble, BSA; K. Yip, BSA

Roll into sPHENIX IR Aug 2022

DOE Ribbon Cutting ceremony w/ DOE-SC Director Asmeret Berhe, Jan 2023

RHIC AuAu and Cosmic Events in Tracking Detectors

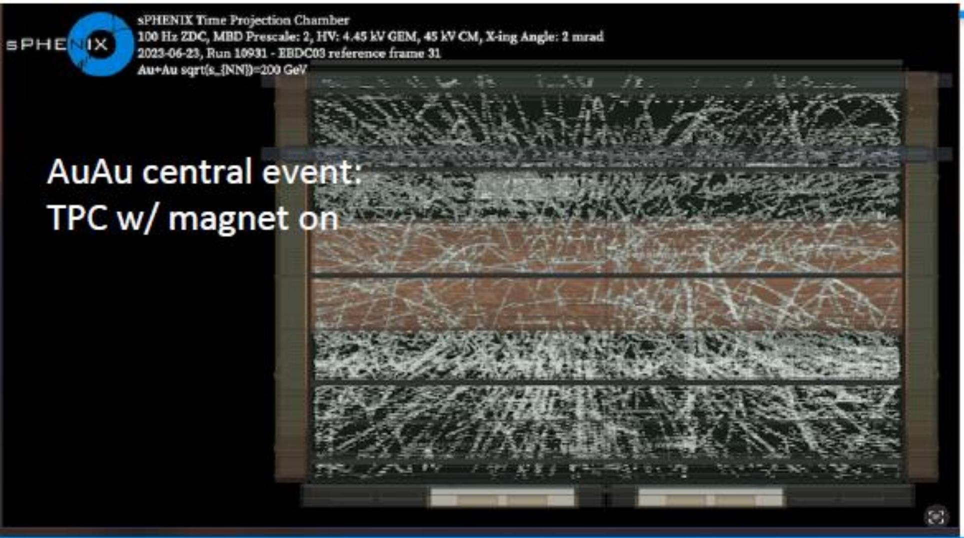

Plan to use track positions determined by the TPOT+INTT +MVTX to correct position distortions in the TPC.

Tracks seen through a combination of the sPHENIX Tracking detectors: Field on, field off, RHIC triggers and cosmic triggers

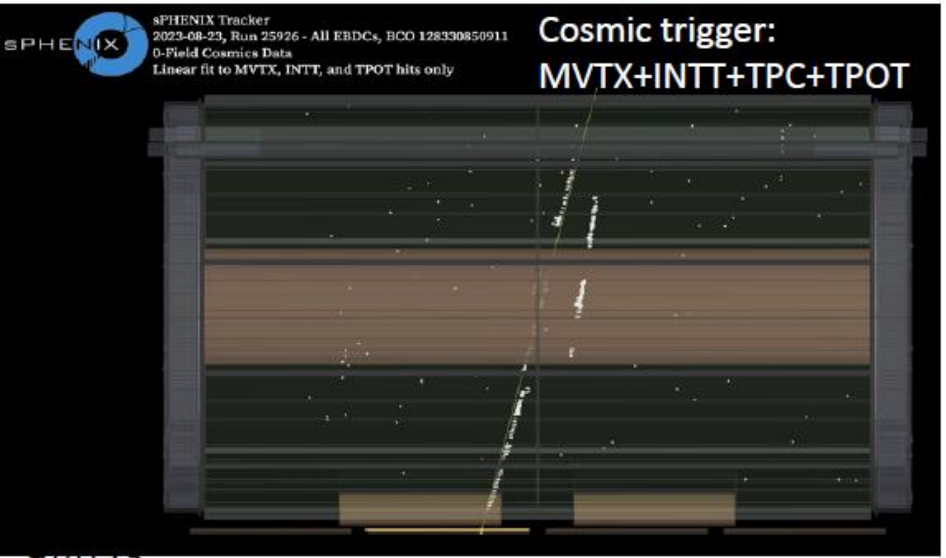

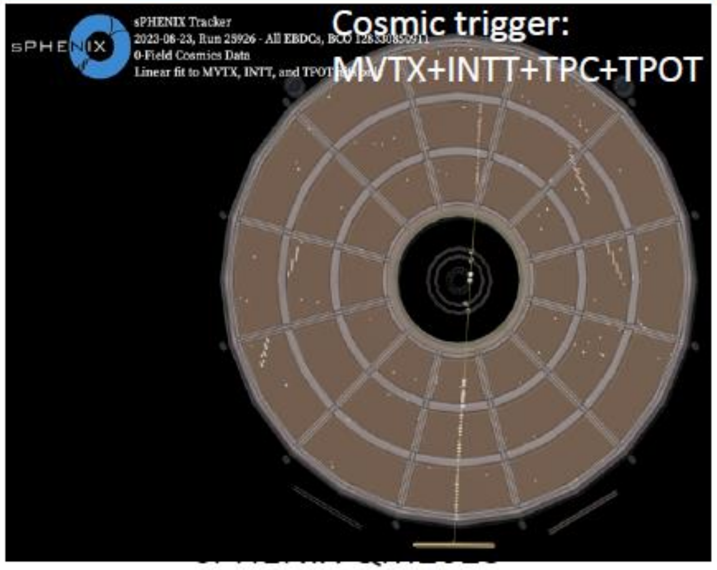

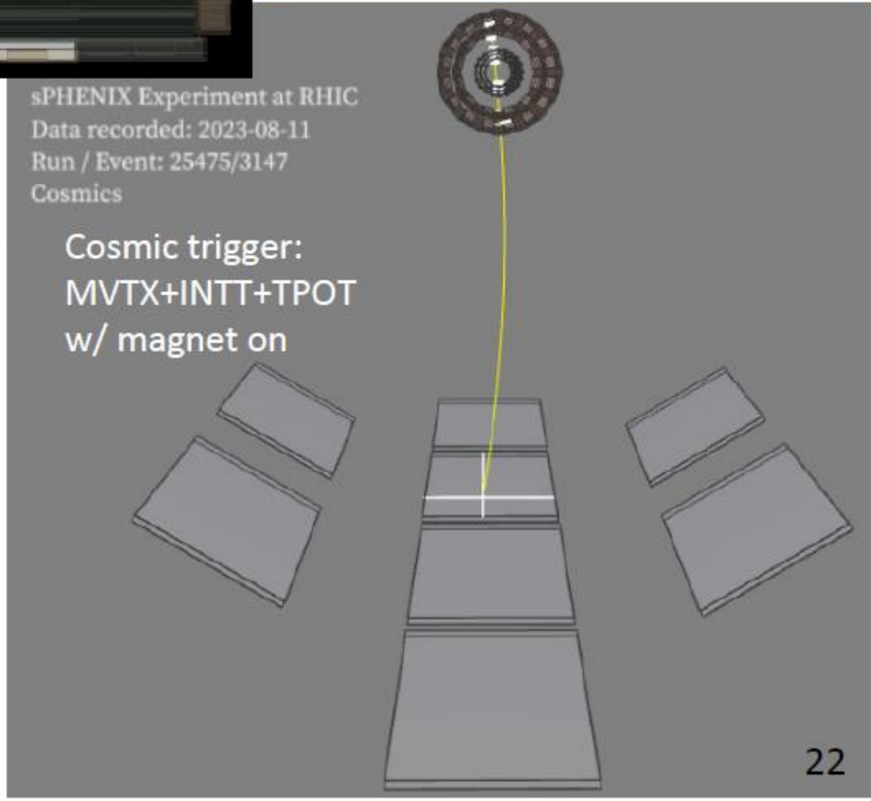

Status of FAIR & CBM

- FAIR construction progressing
  - ✓ SIS 100 tunnel ready, first installations ongoing
  - ✓ CBM cave ready
  - ✓ Upstream platform in CBM cave is installed – being the first user installations of FAIR!

Key observables – systematic measurements! :

- Dileptons
  → Emissivity of dense baryonic matter: lifetime, temperature, density, in-medium properties
- Fluctuations
  → System transition via 1st order PT line, CEP
- Hadrons/ Strangeness/ Charm
  → System in equilibrium, Hypernuclei, Vorticity, Flow, EOS
- Correlations
  → Flow, Vorticity, YN & YNN interactions

	$\sqrt{s_{NN}}$ [GeV]	μ_B [MeV]
SIS 18	2 – 2.5	830 – 760
SIS 100	2.3 – 5.3	785 – 520
SPS	5.1 – 17.3	530 – 220
STAR Collider	7.7 – 200	400 – 22
STAR FXT	3 – 13.7	700 – 265

$\mu_B(\sqrt{s_{NN}})$ from A. Andronic, P. Braun-Munzinger, K. Redlich and J. Stachel, Nature 561, no. 7723, 321 (2018)

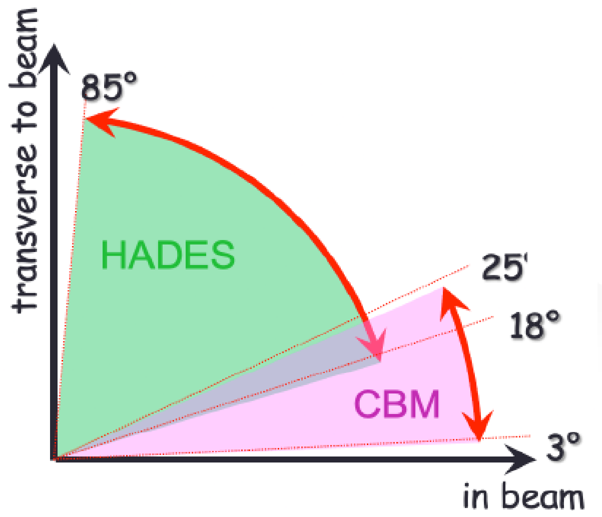

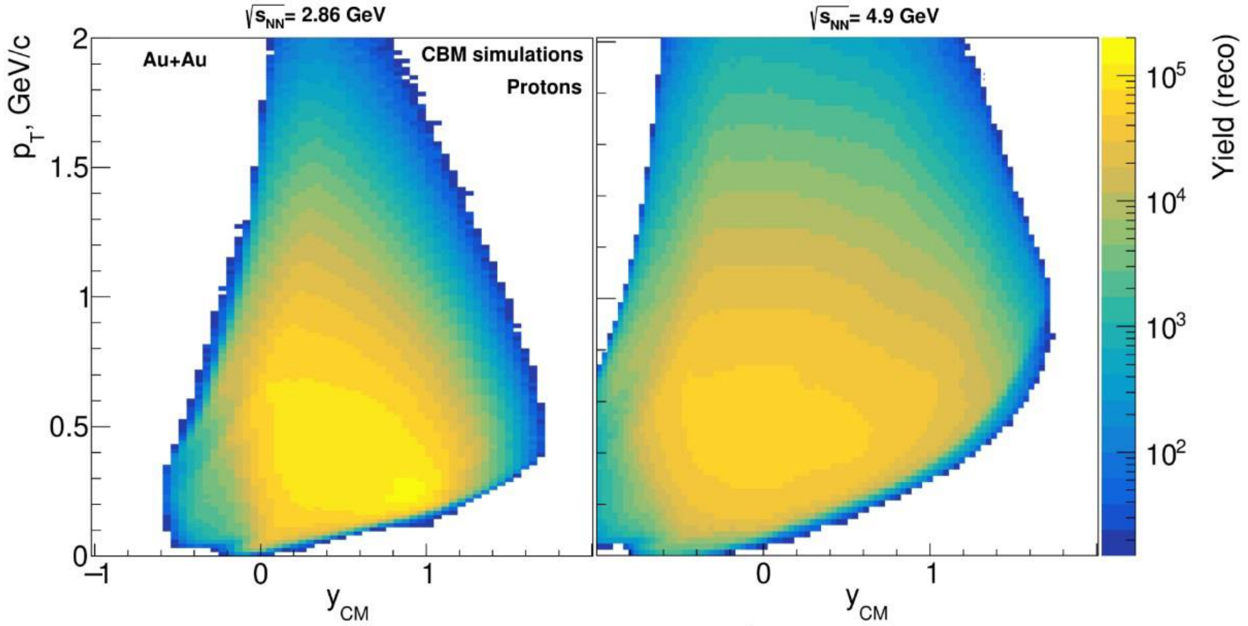

Thank you for the attention!

Хвала на пажњи!

Backup slides

A journey through QCD

- In 2022, ALICE published an overview of what we learned with the results from Run 1 and 2:
  1) Thermodynamic and global properties of the QGP
  2) Hydrodynamic and transport properties of the QGP
  3) Hadronization of the QGP
  4) Propagation of energetic hadrons in the QGP
  5) Deconfinement impact on the QCD force
  6) Limits of QGP formation
  7) Nature of the initial state of heavy-ion collisions
  8) Novel QCD effects
  9) Hadron-hadron interactions

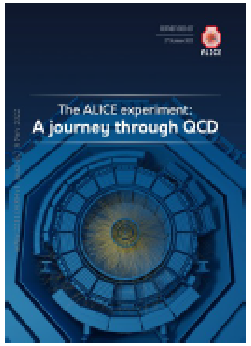

ALICE, arXiv:2211.04384

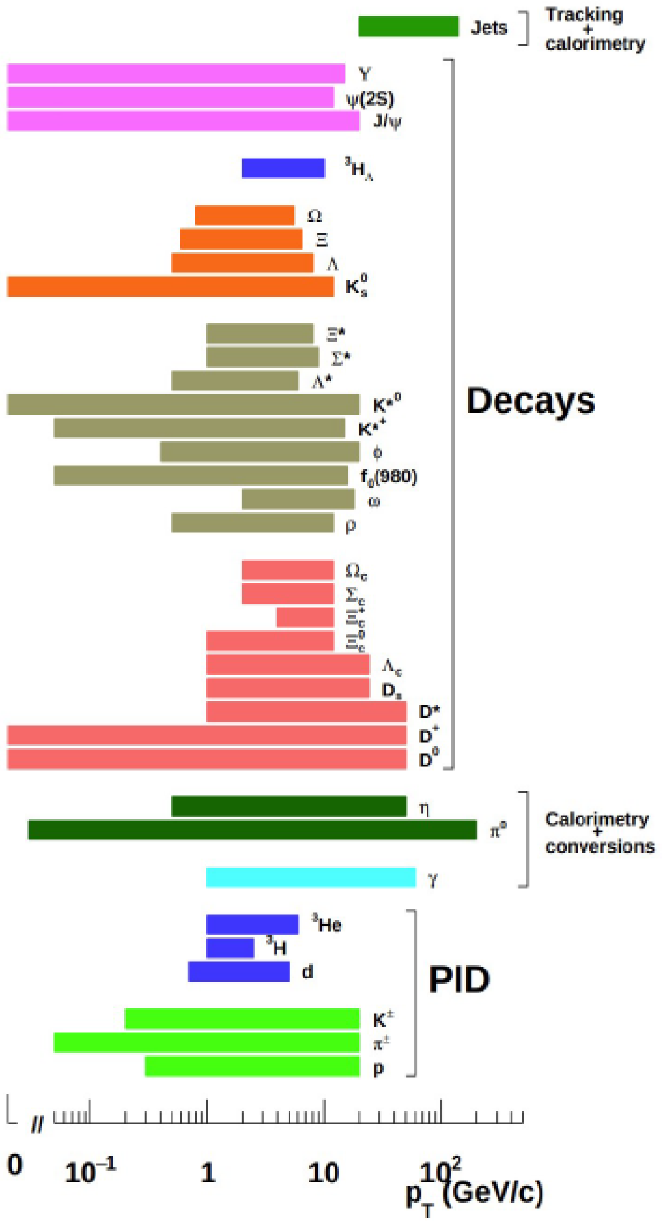

In this talk, highlights showing newer results from Run 3 and Run 2

Gluon polarization impact on proton spin

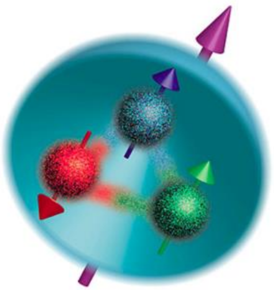

$$S = \frac{1}{2} = \frac{1}{2}\Delta\Sigma + \Delta G + L$$

quarks — gluons — orbital angular momentum

DSSV global fit including up-to-date jet, dijet, pion, W data

DSSV14 + RHIC (≤2022):

- $\Delta G = \int_{0.05}^{1} \Delta g(x)dx = 0.22 \pm 0.03$
- $\Delta G = \int_{0.001}^{0.05} \Delta g(x)dx = 0.17 \pm 0.20$

DSSV14:

- $\Delta G = \int_{0.05}^{1} \Delta g(x)dx = 0.20 \pm 0.06$
- $\Delta G = \int_{0.001}^{0.05} \Delta g(x)dx = 0.15 \pm 0.50$

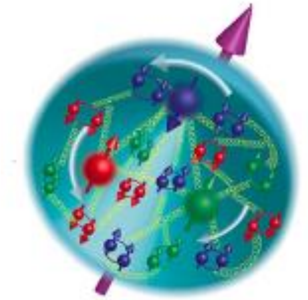

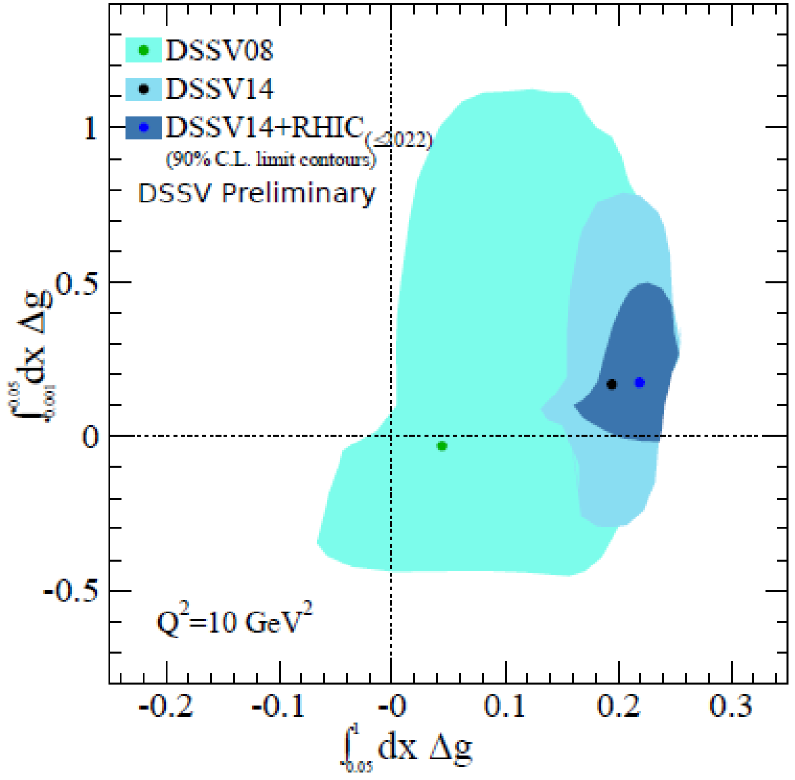

arXiv:2302.00605

Single spin asymmetry

W bosons production sensitive to flavor, spin, charge simultaneously
Powerful tool to probe sea quark polarization

First experimental observation of a flavor-asymmetry between anti-up and anti-down polarizations, opposite to the unpolarized distributions

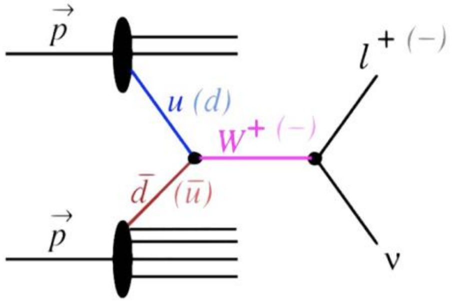

$$A_L = \frac{\sigma^+ - \sigma^-}{\sigma^+ + \sigma^-}$$

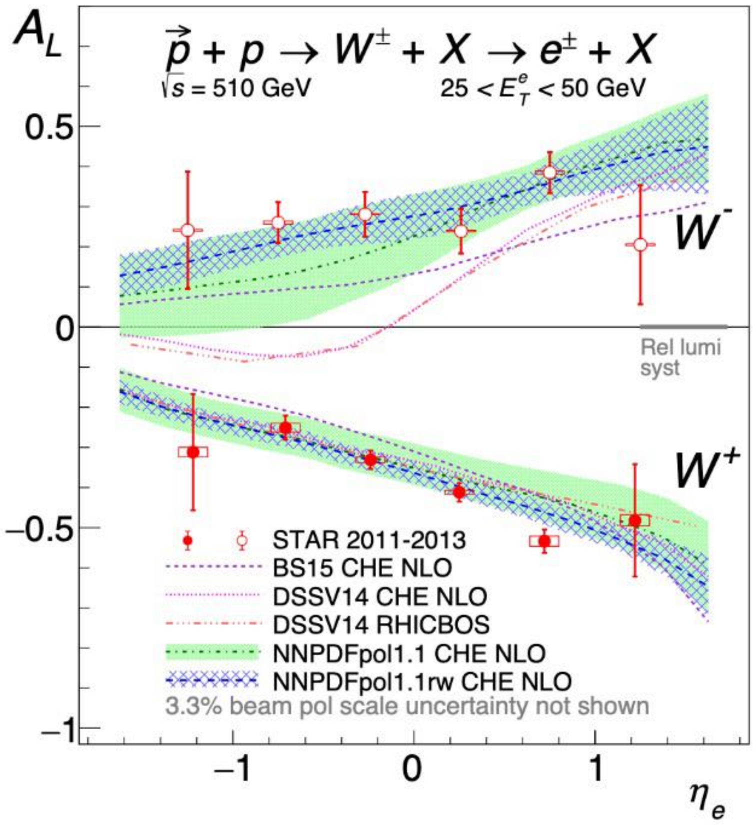

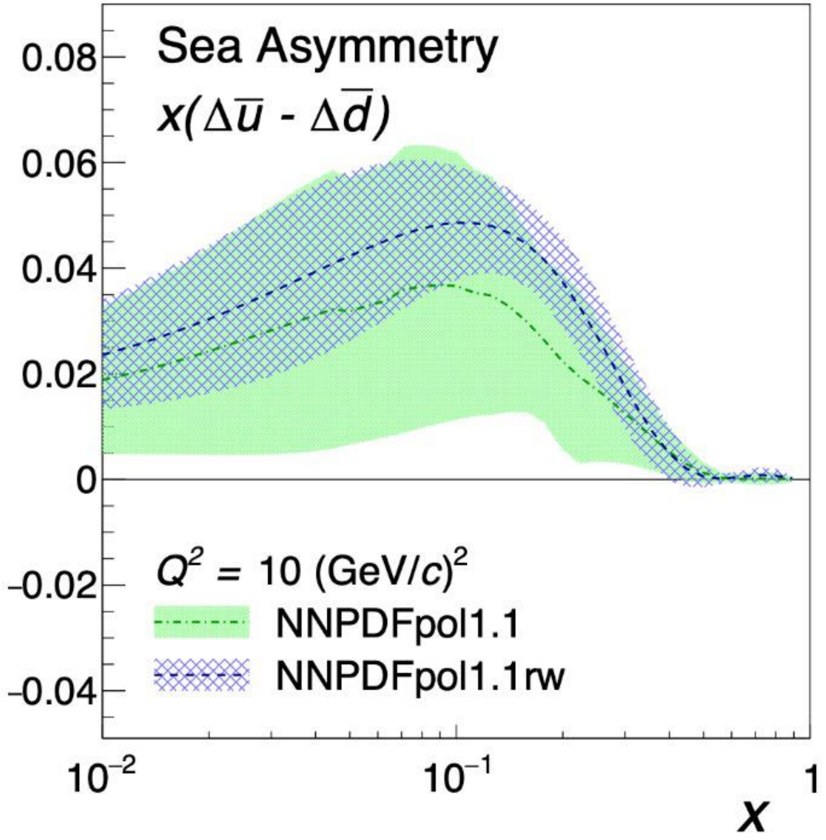

STAR, PRD 99, 051102(R) (2019)

Double spin asymmetry

Sub-processes directly sensitive to gluon
Constrain gluon helicity-dependent PDFs

$$A_{LL} = \frac{\sigma^{\uparrow\uparrow} - \sigma^{\uparrow\downarrow}}{\sigma^{\uparrow\uparrow} + \sigma^{\uparrow\downarrow}} \propto \overbrace{\frac{\Delta f_1}{f_1} \otimes \frac{\Delta f_2}{f_2}}^{\text{probed}} \otimes \overbrace{\hat{a}_{LL} \otimes D_f^h}^{\text{inputs}}$$

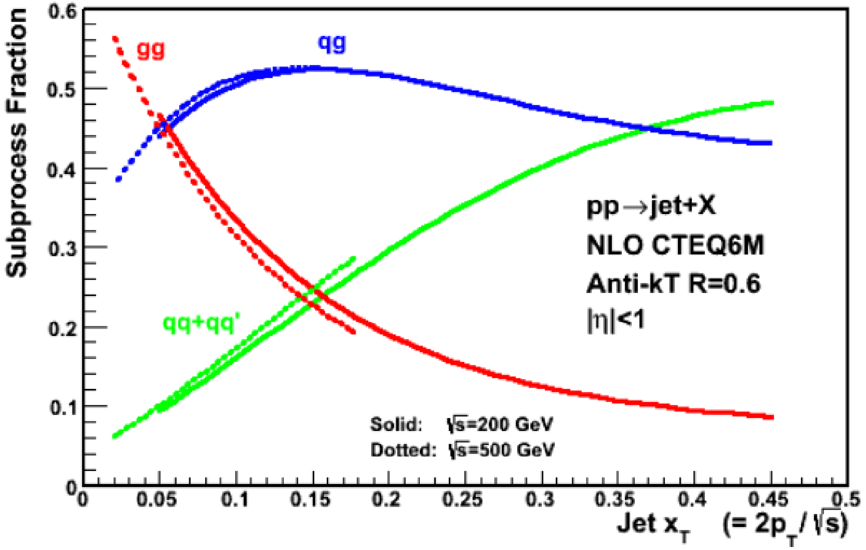

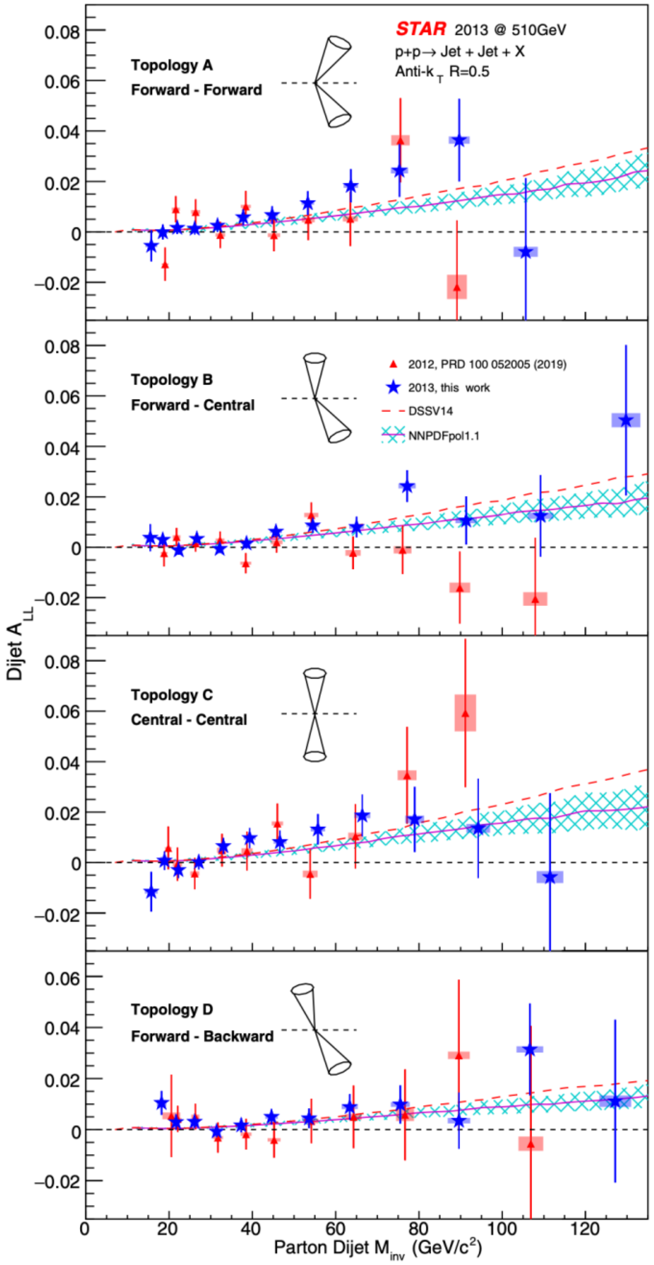

Di-jet measurements

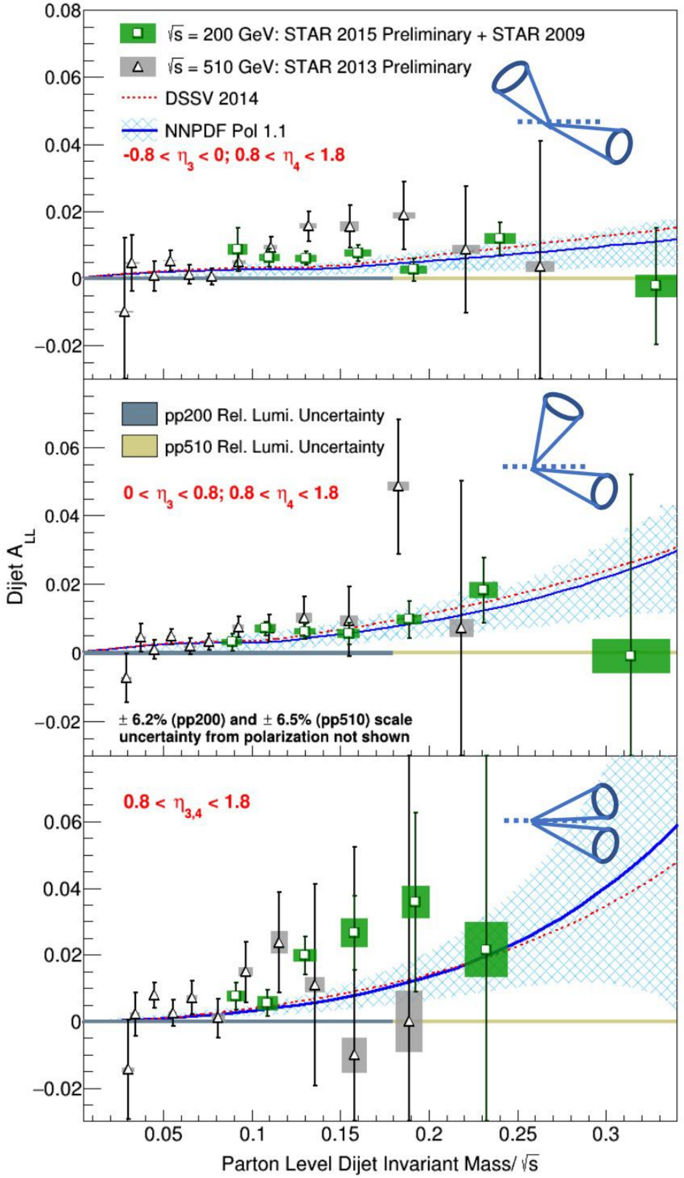

STAR Phys. Rev. D 105, 092011 (2022)
STAR Phys. Rev. D 103, L091103 (2021)

Heavy flavor production at STAR

$$R_{AA} = \frac{1}{N_{coll}} \times \frac{dN^2_{AA}/(dp_T dy)}{dN^2_{pp}/(dp_T dy)}$$

For the J/Ψ:
Low p_T: significant CNM effects. Consistent with model predictions
High p_T (> 3 GeV/c): R_{pAu} consistent with unity → suppression in AA due to QGP effects

STAR, Phys. Lett. B 797 (2019) 134917
STAR, Phys. Lett. B 825 (2022) 136865

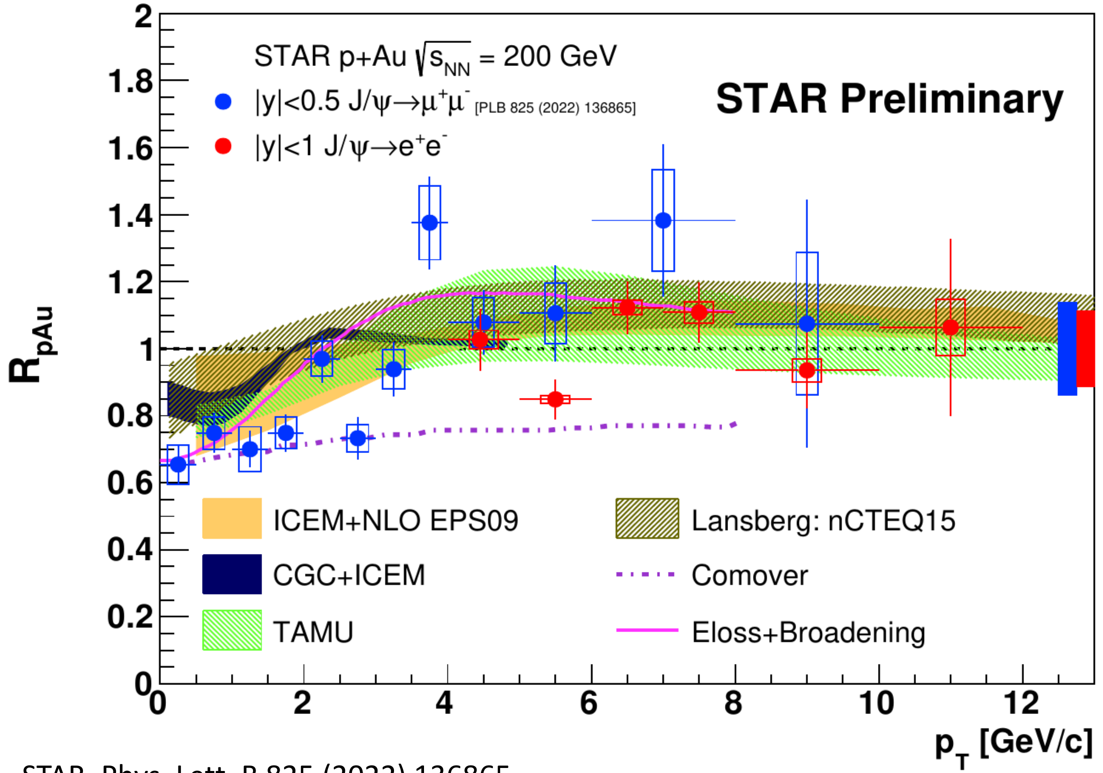

STAR, Phys. Lett. B 825 (2022) 136865

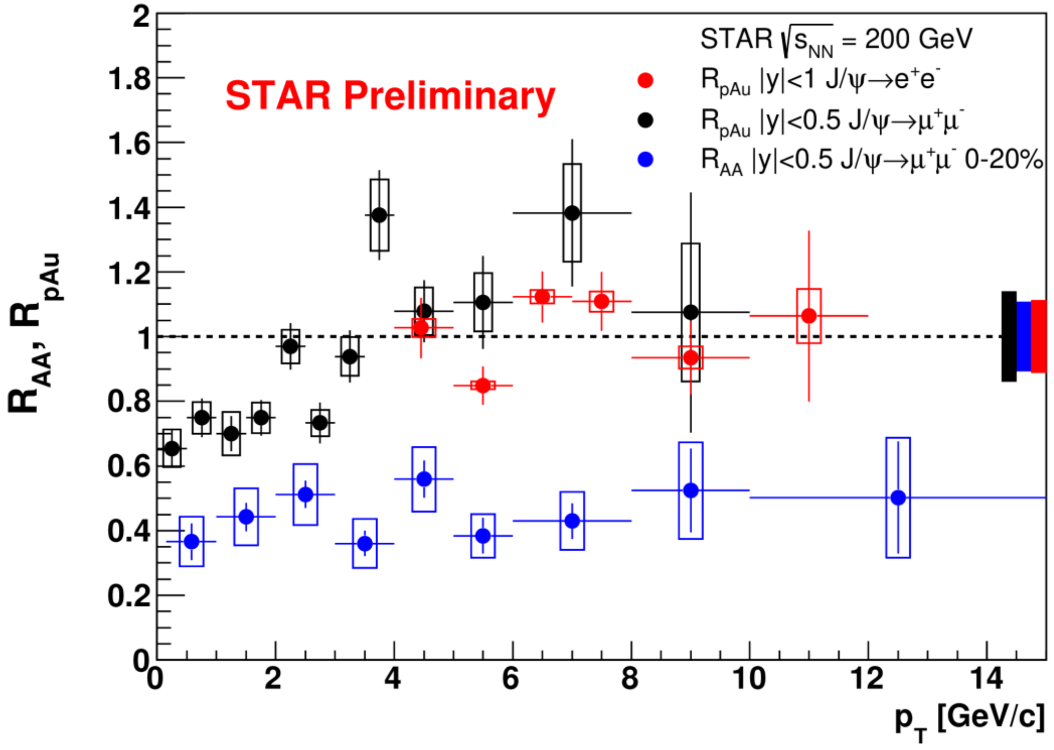

y-dependence of the coherent J/ψ photoproduction cross section

- A strong rapidity dependence is seen
- Models initially developed for VM photoproduction in UPC and modified for PC **are able to describe qualitatively the magnitude of the cross section, but fail at reproducing the *y*-dependence, similarly to UPC**.

NEW

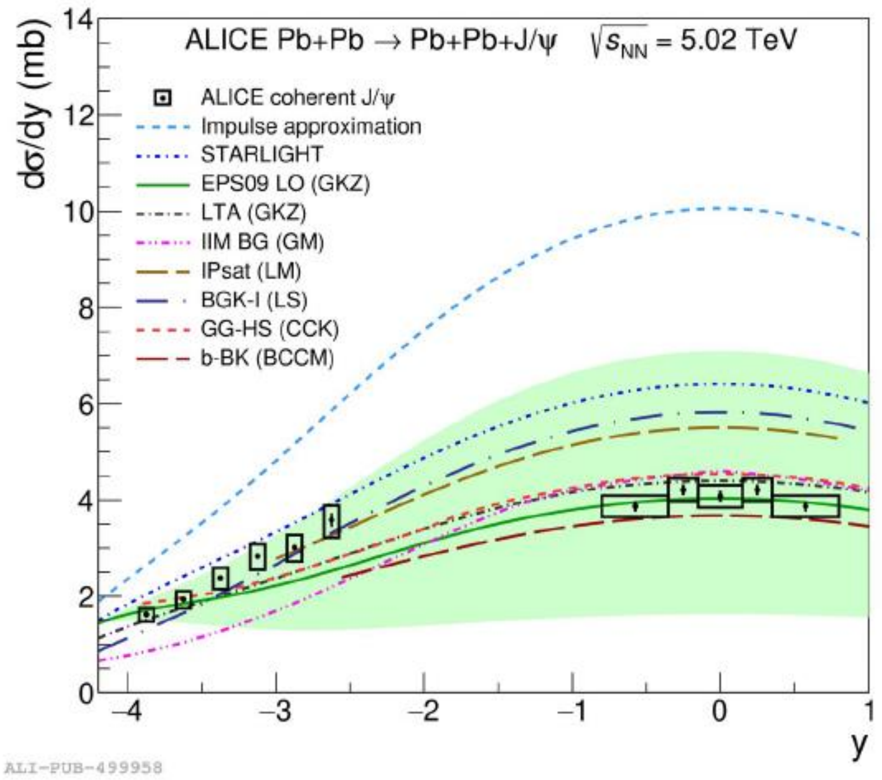

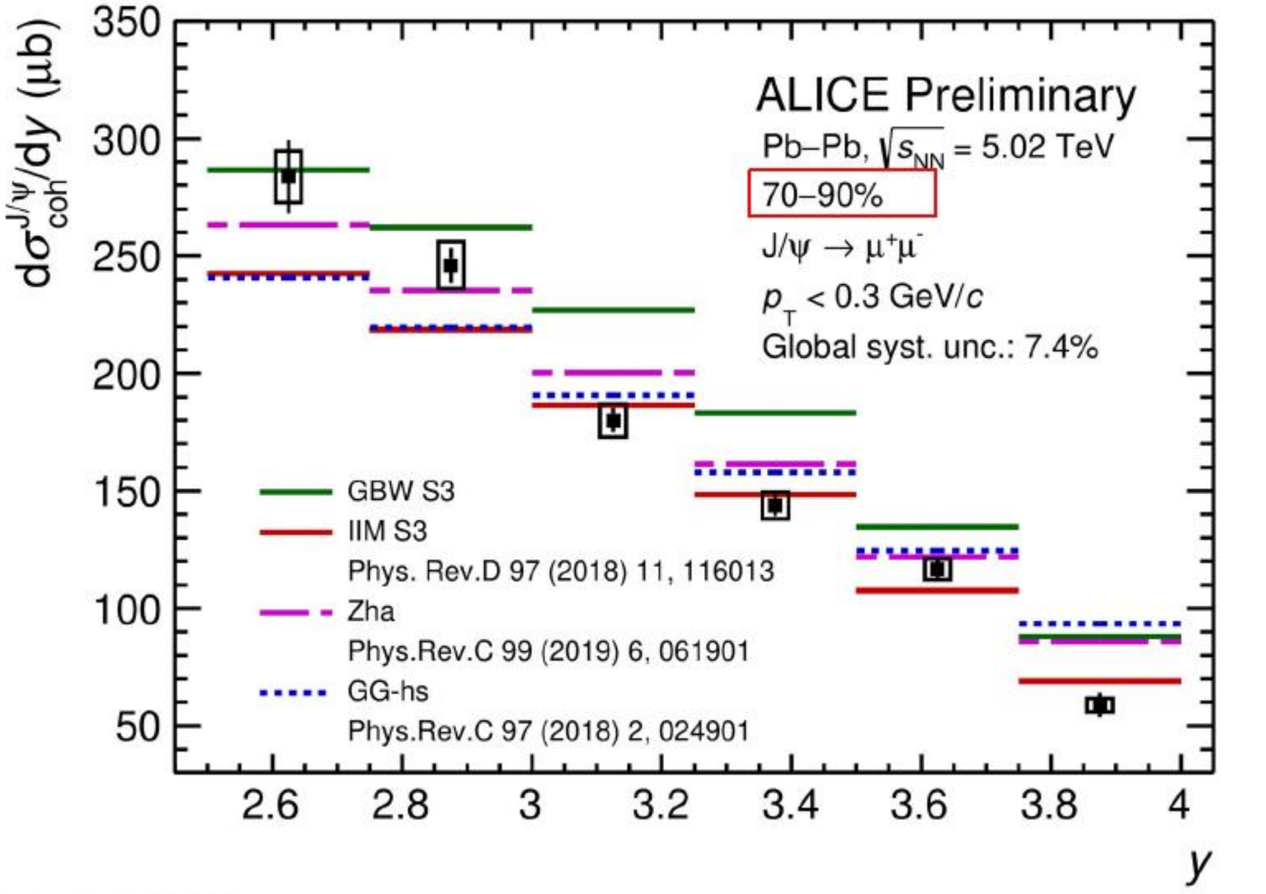

Search for evidence of the baryon junction

Wed 1440
ID 293
C. Tsang

What carries baryon number?

- Valence quark vs. baryon junction?

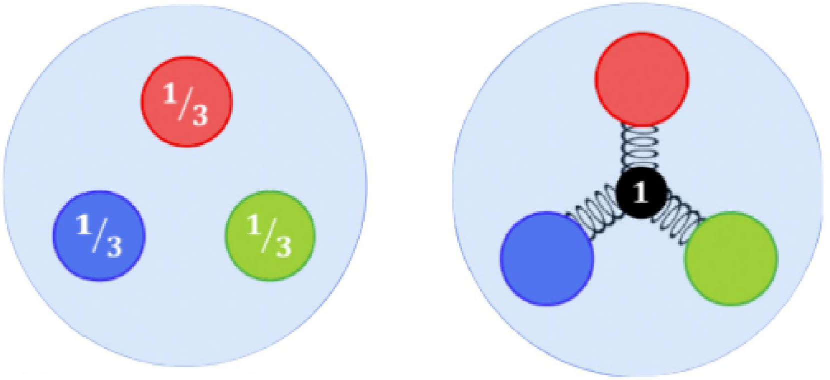

- Valence quarks carry most of the momentum
- Junction carries lower momentum → Enhanced baryon stopping at mid-rapidity

3 Tests:

1. Net-B vs. Net-Q in Isobar collisions
2. Net-Baryon in photonuclear collision
3. Net-proton yield as a function of rapidity in hadronic Au+Au collisions

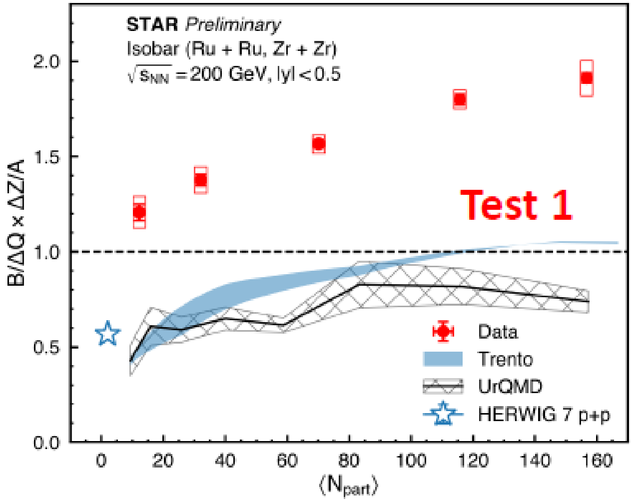

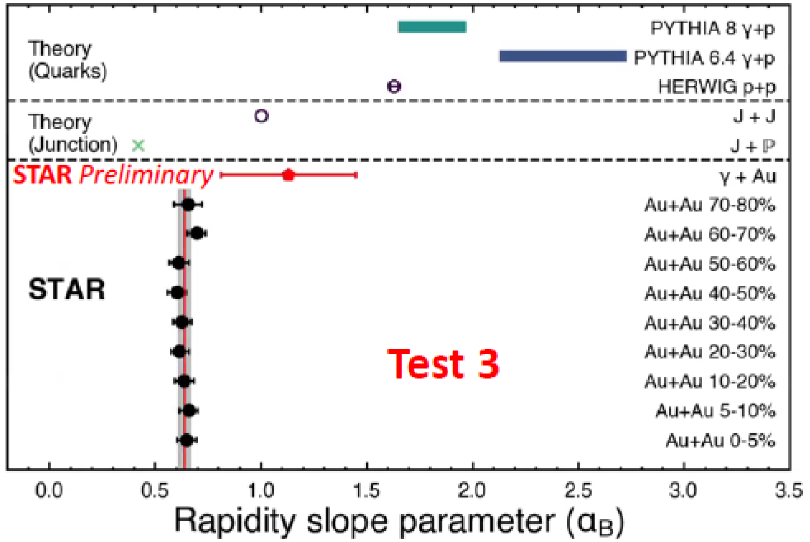

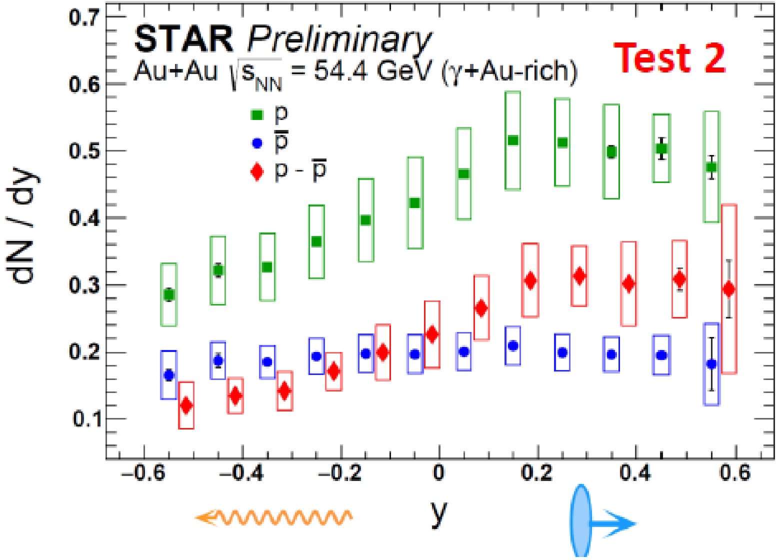

- Net p yield: $e^{-(1.32\pm0.32)\delta y}$
- PYTHIA yield: $e^{-(2.43)\delta y}$
- Model calculations cannot describe net-B vs net-Q
- Slope of net-p yield < PYTHIA/HERWIG
- **Simple valence q** picture is not compatible with data

Light nuclei acceptance at 3 GeV

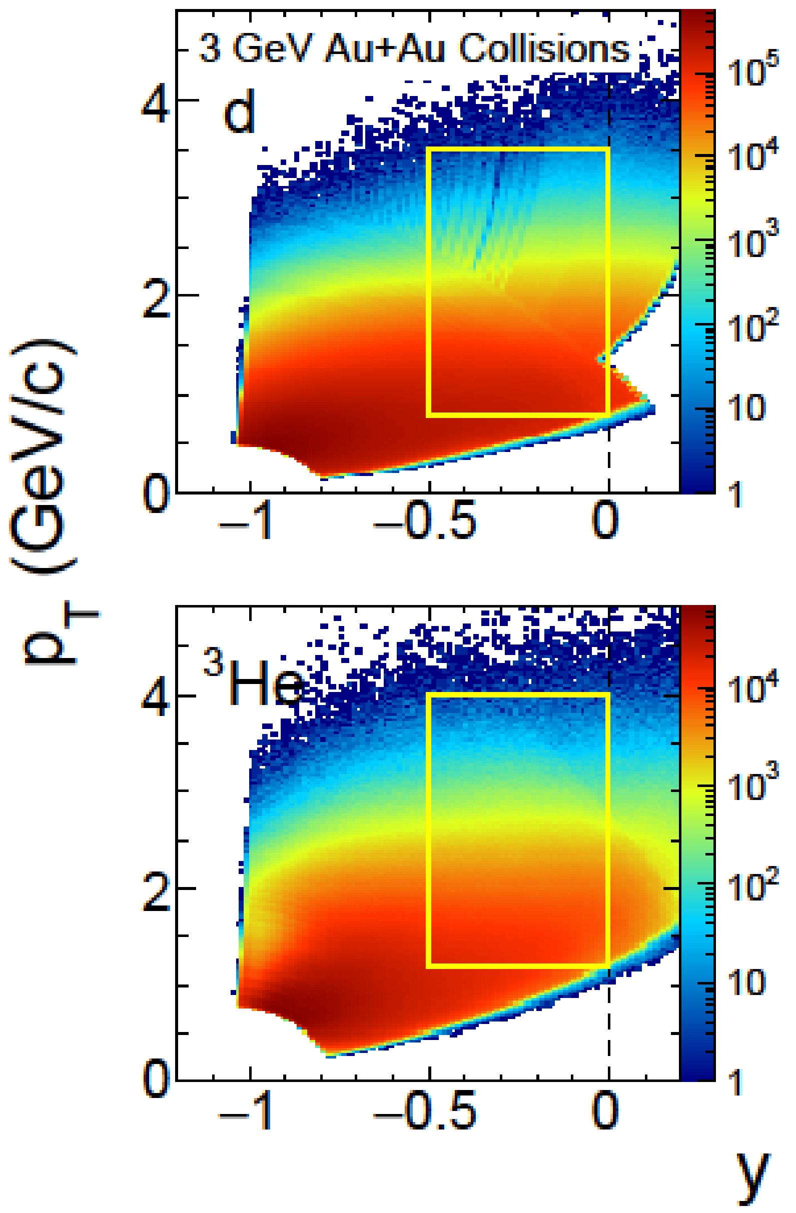

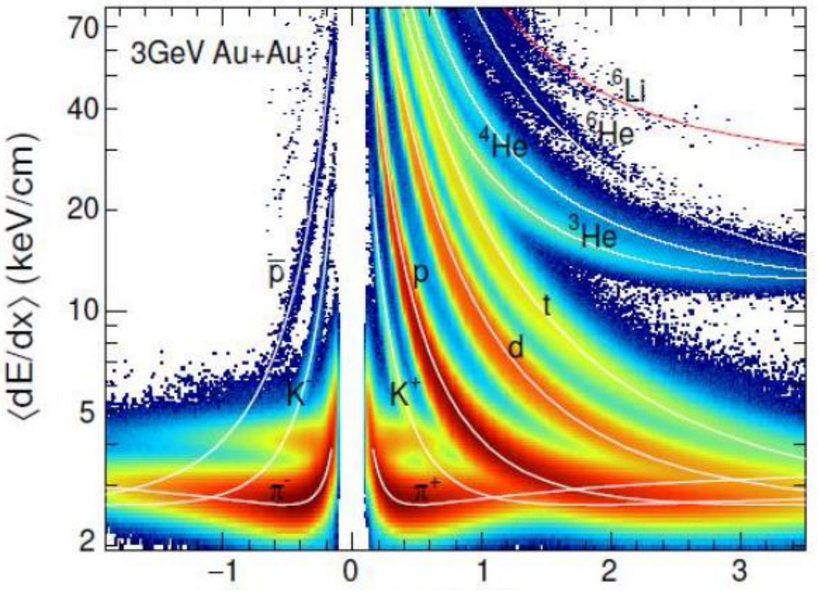

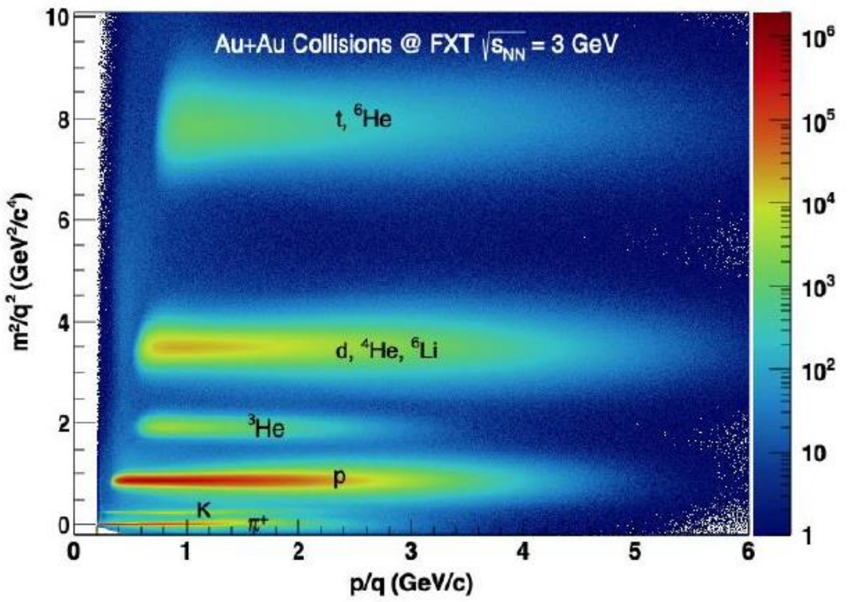

Future of NA61/SHINE

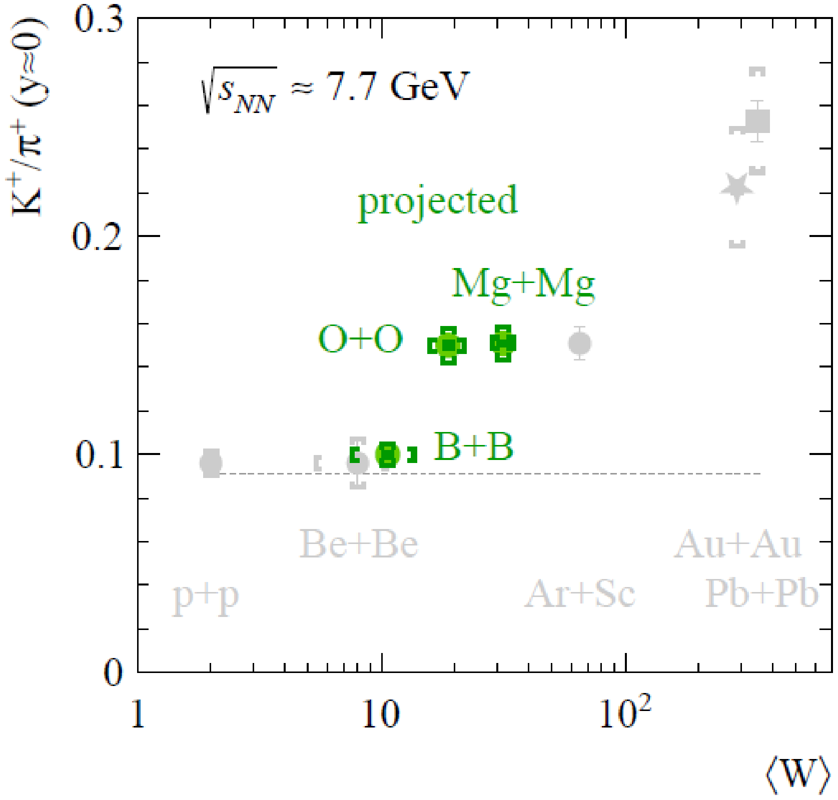

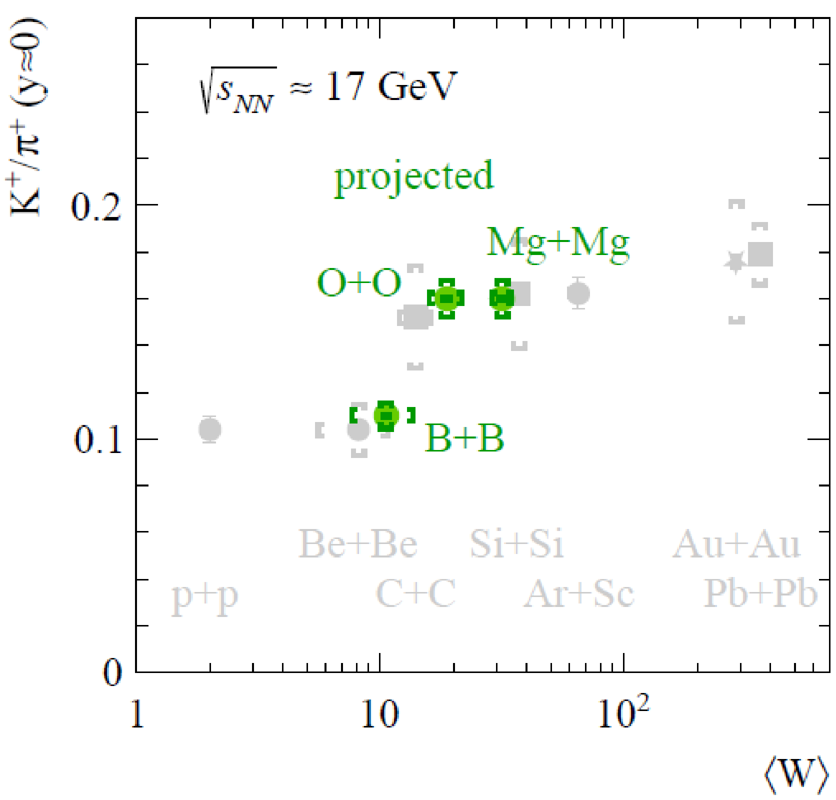

- Pb+Pb measurements for studies of open charm production at SPS energies ($\sqrt{s_{\mathrm{NN}}} = 7.7$ *and* 17 GeV) in 2022-2025
- Continuation of 2D scan with B+B, O+O and Mg+Mg collisions (latter two are $p - n$ symmetric) after CERN LS3 (2028+) - addendum SPSC-P-330-ADD-14 submitted last month